ARL-PROP-R-185

AR-006-147

(2)

AUSTRALIA

DEPARTMENT OF DEFENCE

DEFENCE SCIENCE AND TECHNOLOGY ORGANISATION

AERONAUTICAL RESEARCH LABORATORY

MELBOURNE, VICTORIA

Propulsion Report 185

AN INVESTIGATION OF VIBRATION SIGNAL AVERAGING OF INDIVIDUAL COMPONENTS IN AN EPICYCLIC GEARBOX

by

I.M. HOWARD

Approved for public release

JUNE 1991

AR-006-147

DEPARTMENT OF DEFENCE
DEFENCE SCIENCE AND TECHNOLOGY ORGANISATION
AERONAUTICAL RESEARCH LABORATORY

Propulsion Report 185

AN INVESTIGATION OF VIBRATION SIGNAL AVERAGING OF INDIVIDUAL COMPONENTS IN AN EPICYCLIC GEARBOX

by

I.M. HOWARD

SUMMARY

An investigation of vibration signal averaging for individual components in an epicyclic gearbox has been conducted. A new signal averaging technique was developed specifically for analysing planetary gears within epicyclic transmissions using the vibration measured on the annulus gear casing. It enables the acquisition of signal averages for individual planetary gears whereas previous methods gave a composite vibration pattern from all the planet gears. The new technique is outlined and its implementation is described. Results of tests on an epicyclic gearbox showed the advantages of separating individual planetary gear averages, compared with previous methods. Other conclusions include the effects of transducer location, number of tooth mesh cycles averaged, window width and the use and difficulties with the composite sun gear signal average.

POSTAL ADDRESS: **Director, Aeronautical Research Laboratory**
506 Lorimer Street, Fishermens Bend Victoria 3207
Australia

TABLE OF CONTENTS

PAGE

1. INTRODUCTION 1

2. EPICYCLIC COMPONENT SIGNAL AVERAGING 2
   - 2.1 Planet Pass Modulation
   - 2.2 Vibration Windowing
   - 2.3 Composite Averaging

3. EPICYCLIC GEARBOX TEST FACILITY 6
   - 3.1 Test Gearbox
   - 3.2 Instrumentation

4. SIGNAL AVERAGING IMPLEMENTATION 8
   - 4.1 Computer Hardware
   - 4.2 Software Operating System
   - 4.3 Signal Averaging and Enhancement

5. TEST PROGRAM 9
   - 5.1 Seeded Faults
   - 5.2 Planet Gear Seeded Faults
     - 5.2.1 Tooth Width Removal: Reduction Ratio 3.375
     - 5.2.2 Implanted Tooth Notch
   - 5.3 Sun Gear Seeded Faults
     - 5.3.1 Tooth Width Removal: Reduction Ratio 4.39
     - 5.3.2 Tooth Width Removal: Reduction Ratio 3.375

6. EXPERIMENTAL RESULTS AND DISCUSSION 11
   - 6.1 Planet Gear Seeded Faults
     - 6.1.1 Tooth Width Reduction
     - 6.1.2 Tooth Notching
     - 6.1.3 Effect of Load
     - 6.1.4 Number of Tooth Mesh Cycles
     - 6.1.5 Effect of Window Width
     - 6.1.6 Comparison With Composite Average
   - 6.2 Sun Gear Seeded Faults
     - 6.2.1 Progressive Damage
     - 6.2.2 Effect of Number of Tooth Mesh Cycles
     - 6.2.3 Effect of Window Width
     - 6.2.4 Comparison With Composite Average
   - 6.3 Recommendations for Further Work

7. CONCLUSIONS. 19

8. ACKNOWLEDGEMENTS. 20

9. REFERENCES. 21

10. FIGURES 1 - 48

DISTRIBUTION LIST

DOCUMENT CONTROL DATA

1. INTRODUCTION

The early detection of potentially serious faults in helicopter gear transmissions is required in order to prevent failure, which can result in serious or even catastrophic accidents [1]. Several techniques providing early fault detection of transmission components have been developed over the past decades and include wear debris analysis, oil analysis and vibration analysis. All of these techniques can form integral components of an overall condition monitoring program (Health and Usage Monitoring) for transmission systems [2, 3].

It is often desirable to use a number of monitoring techniques as some techniques may be unable to detect the early stages of failure for certain types of faults. The growth of a fatigue crack is one such example. A fatigue crack in a gear component may initiate and grow without the release of a detectable amount of metal particles. In this instance if only oil analysis or wear debris monitoring techniques are used, they may not detect any change in condition before catastrophic failure occurs. Vibration analysis on the other hand is able to detect the presence of fatigue cracks in gears as well as a number of other faults [4 - 26].

Vibration signals have been used for a number of years to detect changes in the condition of gear transmission components [14]. Initially, the monitoring was concerned only with the overall vibration levels. Any increase in the overall amplitude of the vibration was deemed to indicate a change in the mechanical condition of the transmission. While this may be true for simple components, it will not be true for more complex mechanical systems where changes in the total vibration due to a deterioration in a single element may be negligible. A more recent technique involved the use of frequency analysis, where the amplitude spectrum is calculated from the measured vibration. Frequency domain analysis is particularly useful when analysing mechanical system vibration. For rotating machinery, the various frequency components can often be associated with the rotational speeds of the different sub-elements, and changes in their amplitudes indicates which element in the system has altered its condition.

For complex mechanical systems, the use of frequency analysis alone may not be sufficient to detect a deterioration in the condition of single elements. A helicopter main rotor gearbox is a typical example, where there are a large number of rotating components. Interpreting the frequency content of such a system is complex and it is not always possible to separate out the contributions of individual components.

A more advanced diagnostic method which has been given wide attention over recent years has concentrated on the use of the signal average, [1, 3, 4, 6, 7]. The vibration signal is averaged in the time domain over a large number of cycles, synchronous with the rotational speed of a particular gear. Not only does this procedure help to remove background noise but it also eliminates any periodic vibration not exactly synchronous with the gear being monitored. The method has the advantage of giving a pictorial indication of the vibration produced by the mesh of the particular gear being analysed. It also enables a number of signal enhancement techniques to be used on the signal average to detect distributed and local faults in the gear as well as in the rotation of the associated shaft [1, 3, 4, 6, 7].

The two best known enhancement techniques for signal averages are those developed by Stewart [4] using the figures of merit on both frequency domain and reconstructed time domain data and those developed by McFadden [1, 6, 7] using the narrow band demodulated vibration. These techniques have been applied very successfully in the past to fixed axis gear systems, where the gears rotate on shafts mounted in bearings which are in fixed positions in the gearbox case. The problem area until recently has been the application of the signal averaging techniques to epicyclic gear systems, where a set of identical planet gears are mounted on a carrier arm which rotates around a central sun gear, all fitted inside an annulus or ring gear.

Epicyclic transmissions enable high torques to be transmitted due to the load sharing of the planet gears. They are used in the last stage in the main rotor gearbox of almost all helicopters, and in large marine and industrial gearboxes. Epicyclic gears have not been monitored successfully in the past, using signal averaging techniques, because of the motion of the planet gears and the sun gear, relative to one another and to the annulus gear, and the multiplicity of mesh points. A helicopter main rotor gearbox typically contains five moving planetary gears, giving ten regions of contact, all producing vibration at the same tooth meshing frequency.

If a vibration transducer such as an accelerometer is mounted on the gearbox casing at a fixed location, then the moving planetary gears give rise to a varying transmission path from the mesh points to the fixed transducer. If conventional signal averaging techniques for fixed axis gears are applied to the moving axis planetary gears, then the individual planetary gear components cannot be separated, rather a composite planet signal average will be produced [27]. The composite signal average consists of the instantaneous sum of the vibration of all of the planet gears, detected at the transducer location. However, the vibration signal from a damaged planet gear will, in this instance, be combined with the vibration from the undamaged planet gears. Any change due to the damaged planet gear will be reduced in relative magnitude and as a consequence the damage must be far more severe before it can be detected. The differential mesh phasing of the planet gears causes another difficulty, by attenuating the tooth mesh harmonics and many of the modulated sidebands, which carry the information revealing the damage [28-31].

To overcome the limitations which arise when using composite epicyclic component signal averages, a new signal averaging technique was developed at ARL for calculating the separate signal averages of the individual planet gears, and the sun gear, using a single vibration transducer fixed to the annulus gear.

This report outlines the principles of the new epicyclic signal averaging technique and presents results from tests using industrial standard epicyclic speed reducers with a range of seeded planet and sun gear faults. Comparison is also made with the previous composite signal averaging technique, showing the superior sensitivity of the new signal averaging procedure.

2. EPICYCLIC COMPONENT SIGNAL AVERAGING

In epicyclic gear systems, the sidebands in the vibration frequency spectrum are associated with the movement of the planets and occur at the planetary mesh frequency

plus or minus the planet pass frequency [28]. Their presence is due simply to the dynamics of the planetary reduction where the planets physically pass any point on the fixed annulus gear. This may make narrow band analysis [1], where the modulation content in a narrow frequency band about the mesh harmonic is analysed for the presence of localised tooth defects, of little use. If the tooth mesh harmonic is suppressed or the sidebands are of large amplitude, the narrow band envelope and polar plot of the complex rotating vector may not be interpretable.

2.1 Planet Pass Modulation

A detailed explanation of the planet pass induced vibration was undertaken by McFadden and Smith [31] who developed a theoretical model to show that the planets passing a fixed point of the annulus gear often cause asymmetry of the modulation sidebands. Complete suppression of the tooth mesh frequency and harmonics can even occur. The factors which control the resultant vibration are the number of teeth on the gears and the angles between the planets.

The vibration produced by each planet gear is modulated at the planet pass frequency. This can be readily observed by computing the signal average at the carrier rotation frequency for an epicyclic gearbox. Figure 1 shows the carrier arm signal average calculated from vibration recordings of the main rotor gearbox of a Sea King helicopter. Amplitude modulation of the signal can be seen as each of the five planets moves past the accelerometer mounted on the annulus gear. The transmission path between the transducer and the meshing of the planet with the annulus will vary as the carrier arm rotates.

If it assumed that the annulus gear behaves as an elastic ring, it can be shown [28] that the transfer function between the planet gear and the transducer consists of symmetric harmonic series as shown in Figure 2. When the planet gear is remote from the transducer, its contribution to the total instantaneous vibration will be small. The dominant contribution will be from the meshing of the teeth of the planet gear nearest to the transducer. This fact gives rise to the possibility of using the proximity of the planet gear to the transducer as a means of separating out the vibration from individual planets.

The modulation of the vibration signal due to each planet pass can be observed by demodulating the carrier arm signal average shown in Figure 1 and computing the amplitude modulation component, shown in Figure 3. The demodulation is calculated by first computing the analytic signal of a bandpass filtered component of the carrier signal average. It is known [1] that the signal average generated by a gear after bandpass filtering about a dominant mesh harmonic can be given by,

$$Z_m(t) = X_m(1+a_m(t))\,\mathrm{Cos}(2\pi m T f_s t + \Phi_m + b_m(t)) \qquad (1)$$

where $a_m(t)$ represents the amplitude modulation component and $b_m(t)$ represents the phase modulation term. f_s is the carrier arm rotation frequency, T the number of teeth on the annulus gear and X_m is the amplitude of vibration of the mth mesh harmonic. The equation for $Z_m(t)$ can be considered to be the real part of a complex function $C_m(t)$ known as the analytic signal and defined as,

$$C_m(t) = Z_m(t) - j\,H(Z_m(t)), \quad (2)$$

where $H(Z_m(t))$ is the Hilbert transform of $Z_m(t)$. The analytic function is illustrated in Figure 4, as a complex rotating vector where the real part $Z_m(t)$ is defined as the projection of the complex vector onto the real plane.

The Hilbert transform of $\cos\omega t$ is $-\sin\omega t$, so substituting equation (1) into equation (2) allows the analytic function to be expressed as,

$$C_m(t) = X_m(1+a_m(t))\, e^{j(2\pi m T f_s t + \Phi_m + b_m(t))}, \quad (3)$$

and it can be seen that the length of the rotating vector is subject to amplitude variations $X_m\, a_m(t)$ and the uniform rotation of the vector is subject to phase variations $b_m(t)$. The amplitude modulation of the carrier arm signal average is shown in Figure 3. If it is assumed that the amplitude modulation is greatest at the moment when the planet is directly opposite the transducer then the orientation of the planet carrier can be found with respect to the transducer at any time.

2.2 Vibration Windowing

The rotation and meshing frequencies of an epicyclic gear system with a fixed annulus gear, shown in Figure 5, can be defined with respect to the sun gear, planet gears and carrier arm rotation frequencies f_s, f_p and f_c respectively. By superimposing a whole-body counter-rotation of f_c, as shown in Figure 6, the carrier arm is brought to rest and the rotation frequencies of the planet gears and sun gear relative to the carrier arm become f_p+f_c and f_s-f_c respectively. Note that the planet, sun and annulus gears now rotate about fixed axes and so may be analysed very simply. With the teeth numbers being represented by N_r, N_s and N_p for the annulus, sun and planet gears respectively, the tooth mesh frequency f_m will be given by

$$f_m = N_r\, f_c = N_p(f_p+f_c) = N_s(f_s-f_c). \quad (4)$$

From equation (4), the rotation frequencies of the planet gears and the sun gear are given by,

$$f_p = f_c\,(N_r - N_p)/\,N_p \quad (5)$$

$$f_s = f_c\,(N_r + N_s)/\,N_s \quad (6)$$

and the relative rotation frequencies of the planet and sun gears with respect to the planet carrier are given by,

$$f_p + f_c = f_c\,(N_r/N_p) \quad (7)$$

$$f_s - f_c = f_c\,(N_r/N_s) = f_s\,N_r/(N_r+N_s) \quad (8)$$

The frequencies f_p+f_c and f_s-f_c are important as they define the relative motion of the epicyclic gear components for use in the individual planetary and sun gear signal averages.

The technique developed at ARL to obtain the individual epicyclic component signal averages, involves windowing the vibration signal as each planet passes the transducer. If the physical path between the mesh point and the transducer is nearly constant, the transfer function between the region of tooth contact and the transducer can be considered constant. The time period of the window width must be small in relation to the carrier rotation period.

Consider the epicyclic gearbox illustrated in Figure 5 containing three planetary gears, with a transducer attached to the ring gear. Planet gear A is at the angular position closest to the transducer and so a window of vibration data can be captured. One revolution of the planet carrier later, different teeth of the same planet gear A will again be in mesh near the transducer, so that another window of vibration data can be captured. From the numbers of teeth on the gears, it can be determined which teeth on the planet gear are now in mesh, relative to the meshing teeth in the first window. Each window of vibration data is stored in an accumulator in the correct planet gear tooth position. This process is repeated for each revolution of the planet carrier until a window of data has been captured for every tooth on the planet gear. The process is illustrated in Figure 7. When there are N_p teeth on the planet gear, N_p revolutions of the planet carrier are required to obtain windows of vibration data for each planet gear tooth to complete the signal average. The process is identical for the remaining planetary gears B and C.

By repeating the process for $N_a N_p$ revolutions of the planet carrier, N_a windows of vibration will have been captured for every tooth on the planet gear and N_a planetary tooth mesh cycles will be averaged. It can be shown that the smallest viable width of the vibration window is a single tooth mesh period. Broader windows, spanning a number of tooth mesh periods, can also be used, providing the total window width is an integral number of tooth mesh cycles. By using a wider window width more samples of data are used for the same number of carrier revolutions, increasing the effective number of tooth mesh cycles which are obtained in the signal average and making more efficient use of the data. It is desirable that the window width is narrow enough that the transfer function between the region of tooth contact and the transducer remains approximately constant within each window.

The same technique can also be used to calculate the signal average for the sun gear. When a planet gear is closest to the transducer then the transmission path between the mesh of that planet gear with the sun gear, through the planet gear, is shortest. By synchronizing with the rotation of the sun gear relative to the planet carrier, instead of the planet gear with respect to the carrier, the signal average of the vibration of the sun gear can be produced. For the planet gear, only one window can be captured per revolution of the planet carrier, whereas for the sun gear, a window can be captured each time one of the planet gears moves past the transducer. This enables the sun gear signal average to be accumulated more quickly.

2.3 Composite Signal Averaging

Conventional signal averaging techniques can be applied to epicyclic gear transmission systems to obtain composite planetary and sun gear signal averages. The composite signal

averages must be calculated using the relative rotation frequencies outlined in equations (7) and (8) to synchronize the meshing vibration with the planet carrier rotation.

The composite signal average consists of the instantaneous sum of the vibration of all of the planet-sun and planet-annulus mesh points, detected at the transducer location. In this instance, the individual planetary gears cannot be separated and the vibration from a damaged gear will be combined with the vibration from the undamaged gears. Consequently any change in the vibration modulation due to the damaged gear will be reduced in relative magnitude and must be far more severe before it can be detected. It is also found, [28-31] that the differential mesh phasing of the planet gears can attenuate the tooth mesh harmonics and some of the modulated sidebands which carry the information revealing the tooth damage. The equations for predicting the dominant tooth mesh frequency components given in [31] were found to hold for both the planet and sun gear composite signal averages. This was found to affect interpretation of the narrow band modulation envelope and Polar plots [1] which are used to diagnose localised changes in the meshing behaviour of gear teeth. When the transducer is located on the annulus gear, the planet pass modulation was observed to affect the planetary and sun gear composite signal averages, due to the non-uniform amplitude of the meshing vibration as the planets rotate past the transducer. This does not occur when the transducer is located near the centre line of the gearbox.

3.0 EPICYCLIC GEARBOX TEST FACILITY

An epicyclic gearbox test facility was constructed at ARL using an industrial quality, single stage, Brevini epicyclic spur gear speed reducer, model EM1010-MN, powered by a 40kW three phase motor and loaded by a conventional dynamometer. The test rig is illustrated schematically in Figure 8. The input shaft was belt driven from the electric motor and was supported by two angular contact bearing mounts, and contained a flexible coupling to facilitate alignment. The output shaft was flexibly coupled to the splined carrier arm, through a large journal bearing to a pulley, which in turn rotated a smaller pulley connected to the input side of the dynamometer. Figure 8 also shows the cooling system used in the experimental investigation, where the oil temperature within the gearbox was maintained close to 50°C.

3.1 Test Gearbox

The epicyclic speed reducer, Brevini model EM1010-MN contained three planetary gears, shown in an exploded view in Figure 9. Two gearbox models were used in the investigation, having reduction ratios of 4.39 and 3.375. The tooth facewidth was 15.5mm and the tooth root thickness was 3.5mm for both reduction ratios. Other details are given in Table 1. The sun gear and carrier arm were splined onto the input and output shafts respectively. A synchronising signal was taken initially from a photoelectric transducer on the input shaft to the gearbox at a nominally constant rotational speed of 19 Hz, although a signal from the output shaft was also used. The two reduction ratios had rated loads of 18kW and 25kW respectively.

Table 1

Epicyclic Gear Components

INPUT SHAFT SPEED		1140rpm	
GEARBOX NUMBER		1	2
REDUCTION RATIO		4.39	3.375
OUTPUT SHAFT SPEED		259rpm	338rpm
RATED LOAD		18kW	25kW
TEETH NUMBERS:	PLANET	32	26
	SUN	28	40
	ANNULUS	95	95

The planet gears ran on needle bearings, while ball bearings were used for the input and output shafts. The gearbox design contained a floating sun gear, facilitating equal load sharing among the three planet gears.

3.2 Instrumentation

The transducers used in the investigation were Kistler Model 818 low impedance accelerometers, with a sensitivity of 10mV/g and a mounted resonance of 32 kHz. These were mounted on a set of small steel blocks bonded to the gearbox casing at various positions.

A six channel PCB charge amplifying power unit, model F483B08, was used to amplify the low impedance transducers prior to recording. This unit contained a continuous gain adjustment from 0 to 100.

A Bruel and Kjaer photoelectric tachometer probe, model MM0012 was used, containing an infra-red light source and photo sensor. A strip of white reflective tape was attached to the shaft giving a tachometer pulse once per revolution.
The vibration and tachometer signals were recorded on a portable instrumentation recorder, Bruel and Kjaer model 7006. This included four IRIG Standard Wideband 1 FM channels, running at 381 mm/sec with an upper frequency limit of 12.5 kHz at -1 dB. Instrumentation grade magnetic tape, with 180mm diameter spools was used to record the vibration data, giving 30 minutes of recording on each tape. Prior to digitisation, a Wavetek low pass anti-aliasing brickwall filter model 752A was used for signal conditioning. This two channel analogue device, with gain adjustment, had low pass filters adjustable from 1Hz to 99kHz.

4.0 SIGNAL AVERAGING IMPLEMENTATION

The epicyclic component signal averaging technique was originally developed on a DEC LSI11/73 computer system having four megabytes of memory, hard disc of 20Mb, floppy disc drive and a Sinetrac analogue to digital converter running under the DEC RT-11 operating system [32].

4.1 Computer Hardware

In the present investigation, an IBM compatible AMSTRAD PC2386/65 personal computer system was used, having four megabytes of memory, hard disc drive of 65Mb, and a 1.44Mb floppy disc drive. This contained a 20MHz 80386 processor with a 80387 math co-processor, an enhanced VGA adaptor and a 14inch VGA graphics display. Standard serial and parallel ports were also attached.

A Data Translation DT2821-F-8DI data acquisition card was used to digitise the vibration signature, having eight differential channels. This provided a maximum sampling rate of 160kHz of 12 bit data to be obtained in pc memory, or a continuous sampling rate of 80kHz to be obtained on hard disc, where a 20Mb logical drive D was set aside for this purpose.

4.2 Software Operating System

A DOS 4.01 operating system was used along with a Microsoft Fortran compiler version 4.1 to post process the digitised data. A Fortran callable library of routines, ATLAB, available with the data acquisition card was used to acquire the digitised data into Fortran 2-byte integer arrays. A graphics interface was developed using a Metawindow Fortran graphics library and device driver for the VGA screen. Standard Fortran FFT algorithms were then used to analyse and post process the vibration data.

Graphics output was obtained using a Brother HL-8e laser printer under the HP-GL emulation mode. HP-GL compatible software was written using Microsoft Fortran to drive the laser printer and produce hard copy output of all the signal averages, frequency spectra and enhancement techniques contained in this report. The complete computer hardware system is illustrated in Figure 10.

4.3 Signal averaging and enhancement

The process of signal averaging typically required over 5Mbytes of digitised data to be stored on hard disc for analysis. For the two gearboxes tested the mesh frequencies were 410 Hz and 535 Hz. To include at least the first three mesh harmonics in the signal averages, the anti-aliasing filter was set to 2kHz and a sample rate of 5kHz for each of two channels was used, giving a total sample rate of 10kHz. This enabled 270 seconds of continuous 12 bit vibration and tachometer data to be captured and stored in a 2-byte integer file on the hard disc.

The vibration and tachometer data were then read from the hard disc, scaled in terms of acceleration units (g) and rotation units of the tachometer shaft and written back to the hard disc in separate files. The photoelectric tachometer probe produced a positive pulse

above a nominally zero voltage level. During the scaling of the tachometer data, a number of tachometer cycles were scanned to determine the maximum and minimum excursions of the signal, then a specified fraction was used to determine the actual threshold from which to determine the shaft rotation period.

From the scaled vibration and tachometer data files resident on the hard disc, a signal average was calculated, synchronised by the rotation of the carrier arm. With the tachometer signal taken from the input sun gear shaft, equation (6) can be rearranged to determine the required carrier arm rotation, given the sun gear rotation. This was not required when the tachometer signal was taken from the output shaft as the carrier arm rotation was given directly. 2048 or 1024 points were normally used in the calculation of the carrier arm signal average, cubic interpolation being used to calculate the value of the vibration signal at each position [33].

The carrier arm signal average was demodulated as described in section 2.1 to determine the amplitude modulation caused by the passing of the planets. The angular position of the peaks in the modulation are used to locate the planets with respect to the transducer. In this way, the actual position of the planet gears at any moment of time can be related to the original tachometer signal. This angular position was used in the calculation of the planet and sun gear signal averages.

Having determined the position of the planetary gears with respect to the tachometer signal, a window of the vibration signal can be captured each time a planetary gear passes the transducer, the window width being a multiple of tooth width. The windows are located according to which teeth of the respective planet or sun gears are in mesh until a window of vibration has been obtained for every tooth. Equations (7) and (8) must be used to relate the position of the planet and sun gears respectively, to the tachometer signal. By repeating this process N_a times, N_a complete tooth mesh cycles are averaged as described in section 2.2. The complete signal averaging process is shown in Figure 11.

A range of signal averaging enhancement techniques can be used to determine the presence of local and distributed gear damage [1, 4, 27]. In this investigation five enhancement techniques were used, three based upon narrow band demodulation and two based upon Figures of Merit. Kurtosis was used as the condition index in each case, the normalised fourth statistical moment. The three narrow band demodulation enhancements comprised the narrow band envelope, amplitude modulation and phase modulation and these are referred to as K_{env}, K_{amp} and K_{phase} respectively. The two Figure of Merit enhancements, FM4 and FM5, [4, 27], were used for the detection of local tooth damage.

5.0 TEST PROGRAM

5.1 Seeded Faults

A previous investigation into the detection of epicyclic gear faults was undertaken in the U.K. [27] where progressively larger portions of the length of one tooth was removed. The same procedure was used in the present investigation, where spark erosion was used to remove progressively larger portions of the teeth on the planet and sun gears. A further investigation involved the implantation of a notch at the root of a gear tooth, whose depth

was progressively increased until it was detected. Four series of tests were conducted in this investigation, two involving implanted planet gear faults and two involving implanted sun gear faults.

The implanted faults were initially so small that they were not detected using the demodulation enhancement techniques. To obtain information on the sensitivity of techniques, these faults were then increased until they were detected. The investigation included the effects of progressive damage, load, number of tooth mesh cycles, window width and a comparison with the composite average.

5.2 Planet Gear Seeded Faults

5.2.1 Tooth Width Removal

With the epicyclic gearbox having the reduction ratio of 3.375 as detailed in Table 1, a test sequence was undertaken which involved the progressive removal of the width of one of the planet gear teeth. The series of five tests were a) undamaged, b) 20% removed, c) 40% removed, d) 60% removed and e) 80% removed. Figure 12 shows a photo of the planet gear with 26 teeth where 60% of a single tooth has been removed, stage d) of the test series.

At each stage in the test series, at least five minutes of vibration and tachometer data were recorded on the .FM tape recorder for further analysis, the epicyclic gear rig being operated at the rated load of the transmission. For this test sequence, the tachometer probe was located on the output shaft rotating at a nominal speed of 338 rpm. Three channels of vibration data were recorded, corresponding to three transducer locations on the gear casing. The three locations, shown in Figure 13, were on the input shaft side of the gear casing, axial direction close to the input shaft bearing, on the annulus gear in the radial direction and on the output shaft side of the gear casing in the axial direction.

These transducer positions enabled a comparison to be made between the individual epicyclic component signal averages and the composite signal averages. For the final test where 80% of the planet tooth was removed, three loading conditions were recorded, corresponding to 50%, 100% and 133% of the rated load of 25kW.

5.2.2 Implanted Tooth Notch

With the epicyclic gearbox having the reduction ratio of 3.375 and the tachometer probe located on the input shaft, a test sequence was undertaken which involved the progressive implantation of a notch at the root of one of the planet gear teeth.

The notch was cut across the full facewidth of the planet gear, tangentially from the root of one tooth towards the root of the adjoining tooth. The notch was cut by spark erosion using a copper wire electrode of diameter 0.2mm. Figure 14 shows a photo of the test planet gear with an implanted notch of depth 1.2mm, the tooth root thickness being 3.5mm. A series of five tests were conducted with the notch depth going from a) undamaged, b) 1.2mm, c) 1.3mm, d) 1.4mm and e) tooth completely removed.

Various transducer positions were used throughout the test series. Initially three transducers were equally spaced at 120 degrees around the circumference of the annulus gear in the radial direction. Towards the end of the test series, the transducer locations shown in Figure 13 were used in order to compare the composite signal averages with the individual epicyclic component signal averages. The tests were conducted at the rated load of 25kW, although additional loadings of 50% and 133% of rated were also used for the last two tests.

5.3 Sun Gear Seeded Faults

Two test series using epicyclic gearboxes of differing reduction ratios were conducted with the sun gear, seeding progressively larger faults into a localised portion of one tooth. The test procedures were identical and consisted of the progressive reduction of face width of the sun gear tooth in steps of 20%, similar to the planet gear test described in section 5.2.1. The epicyclic gearboxes had reduction ratios given in Table 1.

5.3.1 Tooth Width Removal: Reduction Ratio 4.39

Five tests were conducted at the rated load of 18kW. The three transducer positions used were those shown in Figure 13, providing a comparison between the two signal averaging approaches. The tachometer probe was located on the output shaft rotating at a nominal speed of 262 rpm. Five minutes of the vibration and tachometer data was recorded at each stage of the test series. Figure 15 shows a photo of the sun gear with 28 teeth having 80% of one tooth removed, corresponding to the last stage of the first test.

5.3.2 Tooth Width Removal: Reduction Ratio 3.375

The five tests for the second sun gear implanted fault were similar to the first although a combination of transducer positions was used. For the sun gear removal of 40%, 60% and 80% of the tooth, the transducer positions shown in Figure 13 were used. The tachometer signal was also taken from the input shaft rotating at a nominal speed of 1140 rpm, and the rated load of 25kW was used throughout.

6.0 EXPERIMENTAL RESULTS AND DISCUSSION

Figure 16a shows a typical carrier arm signal average from the test series, taken with a damaged planet gear with 80% of one tooth removed. The amplitude modulation from the three planet passes can be observed in the signal average and Figure 16b shows the amplitude modulation component obtained from demodulation of the first mesh harmonic.

The first planet pass occurs at 73.5 degrees with respect to the carrier arm trigger position and this value is used by the planet and sun gear signal averaging programs in calculating the individual signal averages. Although the signal average shown in Figure 16a was obtained with a large planet tooth defect, no unusual vibration can be observed as the damaged planet gear rotation is not synchronous with the carrier arm rotation. The load sharing of the three planet gears can be seen in the modulation function of Figure 16b where the first planet gear generates a larger vibration modulation than the other two

planet gears. Figure 16c shows the amplitude spectrum of the carrier arm signal average. As expected [31], heavy suppression of the first two mesh harmonics is observed, due to the mesh phasing of the three planet gears and the location of the transducer on the annulus gear.

6.1 Planet Gear Seeded Faults

6.1.1 Tooth Width Reduction

The first investigation involving the progressive removal of 20% portions of the planet tooth was conducted with the tachometer signal taken from the carrier arm output shaft. In this way the damaged planet gear was always positioned so as to be the third planet gear seen in the carrier arm signal average as shown in Figure 16. Figure 17 shows the five signal averages for the progressively damaged planet gear taken at identical operating conditions at the rated load of 25 kW. Each signal average included data from fifty passes of each tooth, using a sampling window of one tooth.

The angular datum/reference of the planet gear signal averages is arbitrary, so they must be shifted in phase to compare them directly with each other. Although similarities can be seen among the five signal averages, even the first three, where the planet damage is not visible in the raw signal average, do not appear to have identical mesh patterns. The reason for this rests with the experimental procedure which was followed to implant the faults in the planet gear. At each stage in the program, the epicyclic gearbox had to be stripped and the planet gear removed from the planet carrier. Although the planet, sun and annulus gear teeth were reinserted in the epicyclic gearbox in the identical mesh pattern at each stage, the alignment and setup conditions could have differed slightly after reassembly.

The amplitude spectra for the above mentioned five signal averages are shown in Figure 18, where the first four mesh harmonics of 26 shaft orders can be seen. The common factor of two in the tooth numbers of the planet and sun gears produces components of 13 shaft orders. As expected, for the undamaged planet gear signal average, low level modulation sidebands were observed, whereas for the signal average for the planet gear with 80% of one tooth removed, significant modulation is apparent around all the mesh harmonics. The fundamental mesh frequency of 26 shaft orders was dominant for the above tests, followed by the second harmonic. The second mesh harmonic was chosen for the narrow band time domain demodulation techniques as it was found to show an earlier indication of the implanted defect.

Enhancements of the planet gear signal averages were calculated, and Figures 19 and 20 show the narrow band envelope and Polar plots from the five planet gear signal averages. In both the envelope and Polar diagrams the change in the modulation behaviour about the second mesh harmonic becomes apparent when 40% of the planet tooth is removed. The kurtosis of the narrow band envelope exceeds 4.0 at this stage. From the Polar plot, a significant amount of amplitude modulation can be seen, even when 40% of the planet tooth is removed. The amplitude and phase modulation functions of the damaged planet gear signal averages are shown separately in Figures 21 and 22 respectively. The amplitude modulation appears to be more sensitive than the phase modulation in indicating damage.

A significant change can be observed in the amplitude modulation at the 40% tooth removed, whereas the phase modulation does not alter significantly until 60% of the tooth has been removed. The kurtoses of the modulation functions are also shown on the Figures 21 and 22.

The kurtoses of the three modulation functions and two of the Figures of Merit condition indices are shown in Figure 23 for the series of five tests. The Figures of Merit used in the present investigation included the FM4 and FM5 kurtosis values [4]. The other three functions are the kurtosis values obtained from the narrow band envelope (kenv), amplitude modulation (kamp) and phase modulation (kphase). From the comparison shown in Figure 23, all of the indices are within the undamaged levels (<3.5) initially and exceed the danger levels (>4.5) for 60% of the planet tooth removed. The first index to indicate a significant change was the amplitude modulation, as shown in Figure 21, with a kurtosis of 5.14 after 40% of the planet tooth had been removed.

6.1.2 Tooth Notching

The second progressive damage sequence involved the introduction of a notch at the root of one of the planet gear teeth. Figure 24 shows the signal averages of the damaged planet gear when the notch was 1.4mm deep (a), and when the planet tooth was completely removed (b), 1.4mm corresponding to 40% of overall tooth thickness. The mesh pattern in Figure 24b has high amplitude disturbances at 160 and 340 degrees as the missing tooth rotates through the sun gear mesh and the annulus gear mesh respectively.

The five condition indices are shown in Figure 25 as a function of the notch depth. Two of the condition indices, Kenv and FM4 show danger levels, 5.33 and 4.89 respectively, when the implanted notch was 1.2mm deep. Four of the indices increased substantially as the notch was deepened to 1.3mm and 1.4mm, however the amplitude modulation decreased slightly.

When the damaged tooth was completely removed, all the indicators increased except for the narrow band envelope and phase kurtoses which decreased slightly. The phase modulation became very irregular at this stage and was not considered further.

6.1.3 Effect of Load

Two planet gear tests also provided an assessment of the effect of load upon the various condition indices. Figure 26a and 26b show the five condition indices as a function of load with 80% of one planet tooth removed, and with a notch depth of 1.4mm respectively. Recordings of the vibration signal were taken at 50%, 100% and 133% of the rated load. In both tests, the load had a major impact on all of the condition indices. These results show that for relatively minor damage such as that which applied in Figure 26b, the condition indices will give no indication of change in the condition of the gear teeth mesh behaviour unless the applied load is close to the rated load. This is to be expected, as the increased deflection due to damage, and hence changed meshing action, is greatest at heavy tooth load.

6.1.4 Number of Tooth Mesh Cycles

For the epicyclic component signal averaging, the number of tooth mesh cycles included in the signal average is limited by the time record length which may reasonably be recorded and captured by computer. For the gearbox test facility, computer storage of the digitised data was initially set to a maximum of 5.4Mbyte. This provided 270 seconds of data digitised at 10KHz. In the present investigation, this translated to 50 and 32 tooth mesh cycles per average for the reduction ratios 3.375 and 4.39 respectively.

With the damaged planet gear having 80% of one tooth removed, the effect of the number of tooth mesh cycles in the average was determined. Planet records were obtained for 1, 2, 3, 4, 5, 10, 15, 20, 25, 30, 35, 40, 45 and 50 tooth mesh cycles and the five condition indices were computed. The results are shown in Figure 27a, where the recordings were taken at the rated load. In all of the indices, the kurtosis values can be seen to stabilise after five or more tooth mesh cycles are averaged.

The amplitude modulation kurtosis was lower than the other condition indices. Although the damage due to the tooth removal could be seen in the modulation, the modulation was very irregular over a significant portion of the planet gear revolution resulting in a lower index.

Similar analysis was conducted for the case of 40% of the planet tooth removed. In this situation the kurtosis values of the various enhancement methods stabilised after 20 tooth mesh cycles were averaged, as shown in Figure 27b. The number of tooth mesh cycles which are averaged can be seen to be crucial to the early detection of localised planet gear faults. In general, the smaller the localised tooth damage, the more tooth mesh cycles required.

6.1.5 Effect of Window Width

The previously described results have been based upon the capture of vibration data at each planet pass, using a window width of one tooth. To determine the sensitivity of the results to the window width, planet averages were calculated using window widths up to +/- 30 degrees of planet gear mesh. This corresponds to a data capture width of up to 15 teeth. The effect of the five condition indices when 80% of one tooth was removed is shown in Figure 28. In this case the data capture window width appears to have had little influence on the fault detection for the large tooth damage.

The test was repeated with only 40% of one planet tooth removed. In this situation, the majority of the five condition indices gave warning levels for a window width of a single tooth only. For larger window widths, no indication of damage could be found. This suggests, as might be expected, that narrow window widths are more effective for the early detection of tooth damage.

6.1.6 Comparison with Composite Average

The vibration of individual planet gears combines to produce a composite vibration, [27], from which planet gear signal averages can be calculated. The relative rotation frequency given in Equation 7 is used to synchronise the meshing vibration of the planet gears with

the planet carrier rotation. Three transducer positions shown in Figure 13 were used to generate such composite planet gear averages. In each test case, the transducer location on the output side of the epicyclic gearbox gave a better indication of the implanted fault than the other transducer positions.

Figure 29a shows the composite planet gear average taken at the rated load with 80% of one planet gear tooth removed, after 200 synchronous averages. This can be compared with Figure 17e for the individual epicyclic component signal average at the identical load setting and with the same implanted fault.

Figure 29b shows the amplitude spectrum of the composite signal average shown in Figure 29a. The second mesh harmonic (52 shaft orders) has been almost completely suppressed due to the differential mesh phasing of the planet gears. The first upper sideband of the fundamental mesh frequency is enhanced for the same reason [31]. Significant modulation is present in the signal average as evidenced by the magnitudes of the sidebands. As the second mesh harmonic has been suppressed, the narrow band envelope enhancement about the second mesh harmonic, which was found to be sensitive to the fault detection using the individual epicyclic component signal averages, gave no indication of damage. For this reason, the envelope and demodulation analysis about the first mesh harmonic was used.

The Figures of Merit indicators of damage were found to be more sensitive than the narrow band envelope and demodulation analysis for the composite signal averages. Figure 30a shows the narrow band envelope of the composite planet average about the first mesh harmonic with a bandwidth of 24 shaft orders. The resultant kurtosis gave a damage indicator of 4.92. Figure 30b shows the Figure of Merit residual FM4, where the impulsive vibration can be readily seen, and had a residual kurtosis of 7.48.

Figure 31 compares the five condition indices taken from the composite planet average as a function of the percentage of rated load, for 80% of one planet gear tooth removed. In the analysis the narrow band was centered about the first mesh harmonic. It is evident that the Figure of Merit indices FM4 and FM5 were able to detect the damage before the narrow band analysis. This situation was more pronounced at the high load conditions.

Comparison with the individual epicyclic component signal averages shown in Figure 26a, obtained for the identical test conditions, shows that the composite planet average is far less sensitive than the new planet gear signal averaging technique. This is more pronounced for the less severe planet tooth damage. For the test case where 60% of the planet gear tooth was removed, the Figure of Merit indices of the composite average gave a warning level only (<4.5), whereas the individual planet gear average gave kurtosis kevels >4.5 as shown in Figure 23.

6.2 Sun Gear Seeded Faults

Two series of sun gear tests with different transmission reduction ratios, similar to the planet gear tests, were conducted to further investigate the sensitivity of the new epicyclic component signal averaging technique. The investigation again included the effects of progressive damage, number of tooth mesh cycles, tooth window width and a comparison with the composite averaging technique.

6.2.1 Progressive Damage

The signal average of the sun gear (28 teeth, reduction ratio 4.39) in the initial undamaged condition, is shown in Figure 32a. Figure 32b shows the corresponding sun gear signal average with 80% of the sun gear tooth removed. The averages appear to be very similar and the damage is not observable in the time representation. The corresponding amplitude spectrum for the initial and damaged tests are shown in Figures 33a and 33b respectively. A slight increase in modulation sideband level can be seen in the damaged sun gear average in Figure 33b.

The narrow band envelopes for the undamaged sun gear and for the sun gear with 80% of one tooth removed are shown in Figure 34a and 34b respectively. Corresponding kurtosis values were calculated to be 2.67 and 4.62. Two peaks in the envelope can be observed in Figure 34b, corresponding to the mesh of the damaged sun gear tooth with two of the planet gears. The reason that three peaks are not observed in the envelope, corresponding to each planet gear mesh, is assumed to be due to a slight eccentricity of the sun gear with respect to the planet gears, so that planet loading is not equal. The Polar plots for the initial and damaged sun gears are shown in Figure 35a and 35b respectively. Two significant changes in the modulation can be observed in Figure 35b corresponding to the damaged sun gear tooth meshing with two of the planet gears.

The signal averages of the sun gear with 40 teeth, (reduction ratio 3.375) in the undamaged state and with 80% tooth removed are shown in Figure 36a and Figure 36b respectively. The signal averages were obtained by capturing vibration data with a window width of 5 teeth, as there is a common factor of 5 in the sun and annulus gear teeth numbers. The sun and planet gear teeth effectively mesh in groups of 5; only one sun gear tooth of each group meshes with any specific annulus gear tooth, such as the tooth closest to the transducer. This pattern of 5 can be observed in the signal average obtained with the undamaged sun gear shown in Figure 36a.

Meshing of the damaged sun gear tooth can be observed in the signal average shown in Figure 36b at 100 degrees, 220 degrees and 340 degrees. The corresponding amplitude spectra are shown in Figure 37a and 37b and a significant increase in the modulation sideband levels can be seen for the damaged sun gear.

The narrow band envelopes are shown in Figures 38a and 38b for the undamaged and damaged sun gear respectively, obtained with a pass band of +/-19 about the first mesh harmonic. The three peaks at each planet pass can be seen in the envelope at 100 degrees, 220 degrees and 340 degrees. The change in envelope kurtosis is from 2.09 to 9.54. Figure 39a and 39b show the undamaged and damaged Polar plots for the sun gear with 40 teeth and a large modulation change can be observed corresponding to the removal of 80% of a sun gear tooth.

Condition indices calculated for the 28 and 40 tooth sun gears, Figures 40a and 40b, show the change in the various kurtosis values as a function of percentage of the tooth removed. The change in gear condition was only detectable using the new epicyclic signal averaging technique after 80% of the tooth was removed.

The phase modulation gave the greatest indication of damage in both cases, with the amplitude modulation giving the least. For the sun gear with 40 teeth, the damage was observed in the amplitude modulation after only 60% of the sun gear tooth had been removed. For the sun gear with 28 teeth, the FM4 and FM5 kurtosis values did not give a warning level even with 80% of the tooth removed.

6.2.2 Effect of the Number of Tooth Mesh Cycles

The sun gear signal averages calculated above were obtained after 100 tooth mesh cycles were averaged. Figure 41 shows the various kurtosis values for the damaged gear with 40 teeth, where 80% of one tooth was removed, as a function of the number of tooth mesh cycles. With only one mesh cycle, all the kurtosis values were above the warning level of 4.5. After 5 mesh cycles the various modulation functions were found to be very repeatable. This result is important as it demonstrates that for large localised tooth damage, a large number of sun gear tooth mesh cycles is not required.

6.2.3 Effect of Window Width

The sun gear with 40 teeth and 80% of one tooth removed was used to investigate the effect of altering the vibration window width. Due to the common factor of 5 between the sun and annulus gears, only multiples of 5 teeth can be considered for the window width. Figure 42 shows the resultant kurtosis values for the various narrow band enhancement and Figure of Merit functions, with a vibration window width of 5, 10 and 15 teeth. In general, it was found that the Figure of Merit kurtosis values increased slightly and the modulation function kurtosis values decreased slightly, but these changes were barely significant and no significant improvement can be gained by increasing the window width. A similar result was observed for the sun gear test with 28 teeth.

6.2.4 Comparison with Composite Average

The two sun gear test sequences provided an opportunity to compare the sensitivity of the new signal averaging technique with the classical composite signal averaging approach. Composite sun gear signal averages were calculated at various stages in the damage for both sun gear tests. A number of transducer positions were used to calculate the composite sun gear signal average as shown in Figure 13. Preliminary analysis showed that the best position for detecting the sun gear faults was the output shaft gear casing in the longitudinal direction, shown in Figure 13. This position was used for the calculation of all subsequent sun gear composite averages.

Figure 43a shows the composite average calculated from the undamaged sun gear with 28 teeth, reduction ratio 4.39, after 200 sun gear revolutions with respect to the carrier arm. The mesh pattern is nonuniform throughout the sun gear rotation. The corresponding composite sun gear average for 80% of one tooth removed is shown in Figure 43b and the three changes in mesh pattern as the planet gears mesh with the damaged sun gear tooth can be clearly seen at 90 degrees, 210 degrees and 330 degrees.

Figures 44a and 44b show the corresponding amplitude spectra of the composite averages for the undamaged and damaged sun gears respectively. The effect of the differential planet mesh phasing can be observed in the undamaged spectrum shown in Figure 44a.

The first upper sideband of the second mesh harmonic is significantly higher than the first lower sideband, while the reverse is true about the first and third mesh harmonics. This situation is more pronounced in Figure 44b for the sun gear with 80% of one tooth removed. The dominant spectral component is now the first upper sideband about the second mesh harmonic and the first lower sideband about the third mesh harmonic has significantly increased. The modulation level in the spectrum of the damaged sun gear has increased dramatically, particularly about the second mesh harmonic.

The composite averages for the damaged sun gear with 40 teeth, reduction ratio 3.375 are shown in Figures 45a and 45b corresponding to 40% and 80% of tooth removal. The 80% tooth damage can be seen in the composite sun gear average at an angular position of 65 degrees, 185 degrees and 305 degrees as each planet meshes with the damaged sun gear tooth. Corresponding amplitude spectra are shown in Figures 46a and 46b. The differential mesh phasing shows up dramatically in both the amplitude spectra, where the mesh components for the first two harmonics are suppressed and the sidebands become dominant. As predicted this does not occur for the third mesh harmonic, but does for the fourth. A significant increase in modulation information can also be observed about the mesh harmonics as the damage increases.

The condition indices of the composite average for the test series with 28 sun gear teeth are shown in Figure 47 as a function of percentage of tooth width removal. The damage is detected by the kurtosis values when 80% of the tooth is removed. Of note is that the kurtosis of the phase modulation does not reveal any change in gear condition. This is likely to be due to the mesh phasing problem and the corresponding suppression of the mesh harmonics. Figure 48 shows the kurtosis values of the composite average with 40 teeth as the implanted tooth damage increases. The Figure of Merit kurtosis values were found to be the most sensitive, the damage being detected at 60% tooth removal.

Once again, the sideband cancellation causing asymmetry in the spectrum is thought to be the reason that the narrow band enhancement techniques could not detect the tooth damage before 80% of the tooth was removed. The kurtosis values as a function of tooth removal for the composite sun gear averages shown in Figures 47 and 48 should be compared to Figures 40a and 40b, the sun gear signal averages calculated with the new epicyclic component signal averaging technique. The narrow band enhancement techniques were found to provide the best indication of damage in both instances.

Altnough the sun gear damage was only detected after 80% of one tooth had been removed, the composite sun gear average was found to be just as sensitive as the new sun gear signal averaging technique.The results obtained for the 40 tooth sun gear tests, Figures 40b and 48, showed that the composite average gave the earliest indication of sun gear damage, the Figure of Merit indices having kurtosis values above 4.5 after 60% of the sun gear tooth was removed. The earliest indication of damage with the new signal averaging technique was after 80% of the sun gear tooth was removed.

The reason why the new sun gear signal averaging technique is not as sensitive as the composite signal average, is thought to be the placing of the transducer. By placing the transducer close to the centreline of the gearbox, the transmission path from the sun gear tooth mesh through the planet gear and carrier arm to the transducer may be more direct than the transmission path through the planet and annulus gear mesh. The vibration signal

measured near the centre line of the transmission should also have less interference from the planet pass modulation detected on the annulus gear. These factors should enhance the sun gear teeth meshing vibration over the planet gear teeth meshing vibration as measured near the gearbox centreline.

6.3 Recommendations for Further Work

As a result of the current investigation, a number of suggestions for further work can be made. These include;

1. Speed up the averaging procedure by collecting additional data. One option would be to use multiple transducers located either around the circumference of the annulus gear or in a sector corresponding to a planet gear revolution. The time period of the vibration record required for the planet gear averaging process can be related to the number of planet/annulus gear teeth and the rotational speed of typical helicopter transmissions. Assuming at least twenty planet tooth mesh cycles are required, at least 20Np revolutions of the planet carrier are necessary.

2. Investigate alternative narrow band enhancement techniques for use with composite sun gear signal averages. The composite sun gear signal averages have phase information from the meshing of the different planet gears, which could possibly be used as a further diagnostic tool.

3. Experimental verification of the new technique should be expanded to establish its effectiveness and sensitivity in relation to other forms of tooth damage such as surface spalling. The results of the present experiments give little guide to the sensitivity of the technique for these different types of faults.

7.0 CONCLUSIONS

The principles of a new epicyclic signal averaging technique have been outlined in this report, and results from four test sequences reported and discussed. Conclusions of the investigation are :

1. The planet pass modulation provides a means of detecting the location of the planetary gears with respect to a transducer mounted on the annulus gear. By demodulating the vibration synchronous with the carrier arm revolution, the planet pass can be readily seen.

2. The new epicyclic component signal averaging technique is superior to previous methods for the calculation of individual planet gear signal averages. An implanted defect in the planet gear of 40% tooth width removal was detectable using the new technique. Using the composite planet signal average the earliest detectable fault was when 60% of tooth width was removed.

3. The composite sun gear average was shown to be more sensitive than the new signal averaging technique for sun gears when optimum transducer placement is used. Tests showed that using the composite signal average, the implanted sun gear fault was detected when 60% of the tooth width was removed compared with 80% of the tooth width when using the new signal averaging technique.

4. The artificial faults implanted in the planet and sun gears described in this report effectively represent a reduction in tooth stiffness. The new signal averaging technique would be expected also to be useful for detecting a range of other planet and sun gear mesh faults, including localised and distributed defects such as spalling, wear and fatigue cracks.

5. The transducer location is an important factor in providing the earliest indication of sun gear damage using composite averaging. The best indication was obtained when the transducer was positioned close to the output shaft bearing.

6. The running load has a significant effect upon the detection capability of the signal averaging enhancement techniques. Enhancement techniques detect localised tooth damage best where a significant amount of tooth bending occurs.

7. The actual number of tooth mesh cycles averaged in the new technique is less critical than at first thought. However, at least 20 tooth mesh cycles are recommended for both planet and sun gear averaging.

8. The effect of the width of the window of vibration captured at every planet pass is less sensitive than first anticipated. A window width of a single tooth is recommended, as no significant advantage was gained by using multiple tooth widths. However, the window width must at least equal any common factors existing between tooth numbers.

9. Composite averages cause difficulties when using the narrow band demodulation and enhancement techniques, due to the differential planet gear mesh phases which occur in epicyclic transmissions. Often the upper and lower sidebands are of greater magnitude than the mesh harmonic, rendering the narrow band envelope and Polar plot unusable.

8.0 ACKNOWLEDGEMENTS

The author wishes to acknowledge the many members of the Propulsion Mechanics Group of ARL who contributed to the investigation. Particular thanks go to those involved in the initial construction of the epicyclic gearbox test facility, Mr Robert Edgar for supervising the many hours of gearbox run time and the assembly and disassembly of the gearboxes, and to Dr. P.D. McFadden for the initial software development.

9.0 REFERENCES

1. McFadden, P. D., "Analysis of The Vibration of The Input Bevel Pinion in RAN Wessex Helicopter Main Rotor Gearbox WAK143 Prior to Failure", Department of Defence, Aeronautical Research Laboratory, Aero Propulsion Report 169, 1985.

2. Lambert, M., "Helicopters Need Health and Usage Monitoring", Interavia 2, 1988, 127-129.

3. Swansson, N.S., Howard, I.M. and Forrester B.D., "Fault Detection and Location in Helicopter Transmissions: Trends in Health and Usage Monitoring", The Australian Aeronautical Conference, Melbourne 9-11, Oct., 1989, pp 288-294.

4. Stewart, R. M., "Some Useful Data Analysis Techniques For Gearbox Diagnostics", Machinery Health Monitoring Group, Institute of Sound and Vibration Research, University of Southampton, Report MHM/R/10/77, 1977.

5. Randall, R. B., "A New Method of Modelling Gear Faults", Transactions of The ASME, Journal of Mechanical Design, Vol. 104, 259-267, 1982.

6. McFadden, P. D. and Smith, J. D., "A Signal Processing Technique For Detecting Local Defects in a Gear From the Signal Average of The Vibration", Proceedings of The Institute of Mechanical Engineers 199(C4), 287-292, 1985.

7. McFadden, P. D., "Detecting Fatigue Cracks in Gears by Amplitude and Phase Demodulation of The Meshing Vibration", Transactions of The ASME, Journal of Vibration, Acoustics, Stress, and Reliability in Design, Vol. 108, 165-170, 1986.

8. Astridge, D., "Application of Vibration Analysis to Health Monitoring of High Duty Gearboxes", PEMEC. Design Engineering Conference, Birmingham, Session 2b, paper 2, Oct. 1981.

9. Lewis, D. C. and Powell, G. A., "Monitoring The Quality of Repaired Gearboxes With Vibration Analysis", Condition Monitoring Proceedings 1987, 2nd International Conference on Condition Monitoring, 1987, 672-684.

10. Stewart, R. M., "The Specification And Development of a Standard For Gearbox Monitoring", Institute of Mechanical Engineers, 2nd International Conference on Vibrations in Rotating Machinery, 1980, C303, 353-358.

11. Furley, A. J. D., Jefferis, J. A. and Smith, J. D., "Drive Trains in Printing Machines", Institute of Mechanical Engineers, 2nd International Conference on Vibrations in Rotating Machinery, 1980, C286, 239-245.

12. Taylor, J. I., "Fault Diagnosis of Gears Using Spectrum Analysis", Institute of Mechanical Engineers, 2nd International Conference on Vibrations in Rotating Machinery, 1980, C275, 163-168.

13. Lees, A. W., "Vibration Spectra From Gear Drives", Institute of Mechanical Engineers, 2nd International Conference on Vibrations in Rotating Machinery, 1980, C265, 103-108.

14. Houser, D. R. and Drosjack, M. J., "Vibration Signal Analysis Techniques", USAAMRDL Technical Report 73-101, Dec. 1973.

15. Navy General Air Staff Target (NGAST) 6638 Feasibility Study, "Gearbox Monitoring Using Vibration Analysis Techniques", 1987.

16. McFadden, P. D., "Advances in the Vibration Monitoring of Gears and Rolling Element Bearings", Paper presented at the I.E.Aust / R.Ae.S. Joint National Symposium, Melbourne, Australia, August 1985.

17. McFadden, P. D., "Examination of a Technique for the Early Detection of Failure in Gears by Signal Processing of the Time Domain Average of the Meshing Vibration", Mechanical Systems and Signal Processing, Vol. 1 (2), 1987, 173-183.

18. Gu, A. L. and Badgley, R. H., "Prediction of Gear Mesh Induced High Frequency Vibration Spectra in Geared Power Trains", USAAMRDL Technical Report 74-5, January 1974.

19. Gu, A. L. and Badgley, R. H., "Prediction of Vibration Sidebands in Gear Meshes", ASME Design Engineering Technical Conference, Oct., 1974, paper 74-DET-95.

20. Astridge, D. G. and Roe, J. D., "The Health and Usage Monitoring System of the Westland 30 Series 300 Helicopter", presented at the Tenth European Rotorcraft Forum, The Hague, The Netherlands, August 1984,

21. Astridge D. G., "Advanced Gearbox Health Monitoring Techniques", The International Journal of Aviation Safety, September 1984, 165-169.

22. Dale, A. K., "Gear noise and the Sideband Phenomenon", ASME Design Engineering Technical Conference, Oct., 1984, paper 84-DET-174.

23. Pratt, J., "Engine and Transmission Monitoring - A Summary of Promising Approaches", 41ST Mechanical Failures Prevention Group Meeting, NATC, Patuxent River, Maryland, Oct., 1986.

24. Astridge, D. G., "Vibration Health Monitoring of the Westland 30 Helicopter Transmission - Development and Service Experience -", 41ST Mechanical Failures Prevention Group Meeting, NATC, Patuxent River, Maryland, Oct., 1986.

25. Stewart, R. M., Cheeseman, I.C., Bonfield, D. G., "How to Get the Designer into the Box", Stewart Hughes Limited, 1986.

26. Baines, N. C., "Incorporation of Modern Vibration Analysis Techniques in Condition Monitoring Systems", Stewart Hughes Limited, 1987.

27. Legge, P.J., "Vibration health monitoring of epicyclic gearboxes", Royal Aircraft Establishment, Technical Report 84064, 1984.

28. Gu, A.L., Badgley, R.H., and Chiang, T., "Planet Pass Induced Vibration in Planetary Reduction Gears", ASME paper 74-DET-93, 1975.

29. Seager, D.L., "Conditions for the Neutralization of Excitation by the Teeth in Epicyclic Gearing", Journal of Mechanical Engineering Science, Vol. 17, No 5, 1975, pp 293-298.

30. Stockton, R.J., "Sun Gear Traveling Wave Vibration in a Sequential Planetary Gearbox", ASME paper 85-DET-167, 1985.

31. McFadden, P.D. and Smith, J.D., "An explanation for the asymmetry of the modulation sidebands about the tooth meshing frequency in epicyclic gear vibration", Proceedings of the Institution of Mechanical Engineers, 1985, 199(C1), pp 65-70.

32. McFadden, P.D. and Howard, I.M., "The detection of seeded faults in an epicyclic gearbox by signal averaging of the vibration", Department of Defence, Aeronautical Research Laboratory, Propulsion Report 183, October 1990.

33. McFadden, P.D., "Interpolation techniques for the time domain averaging of vibration data with application to helicopter gearbox monitoring". Department of Defence, Aeronautical Research Laboratory, Aero Propulsion Technical Memorandum 437, September 1986.

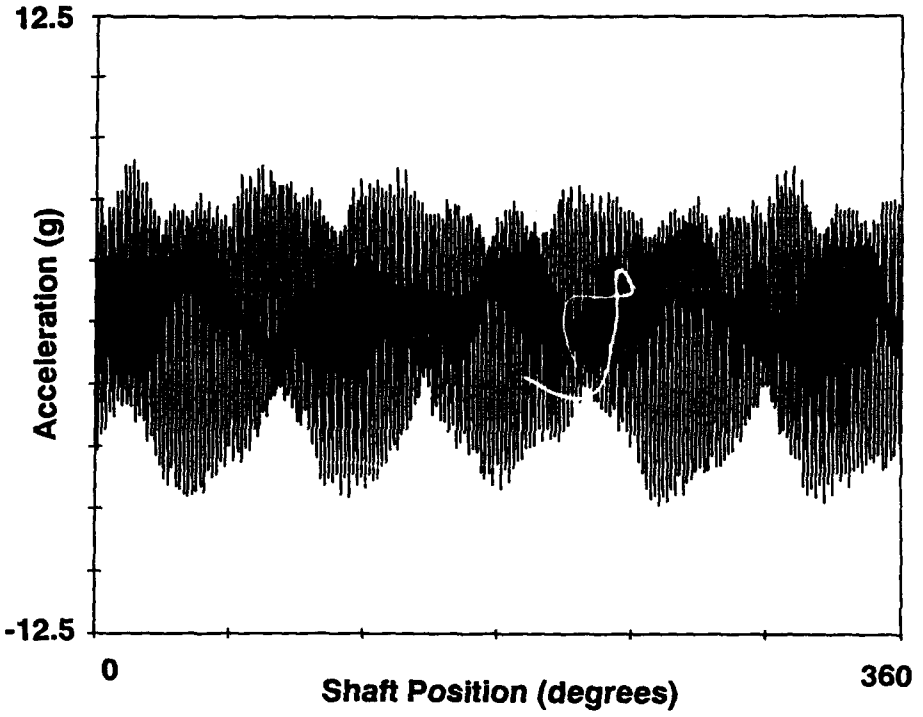

Figure 1. Carrier arm signal average from a Sea King transmission.

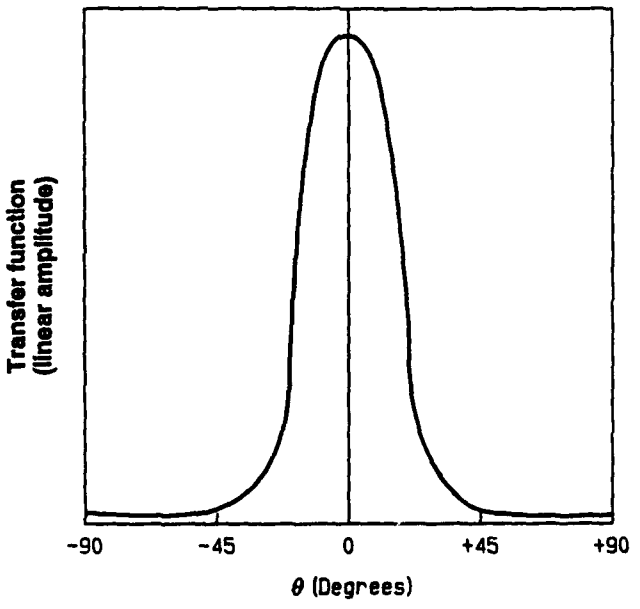

Planet angular position with respect to transducer

Figure 2. Annulus gear transfer function.

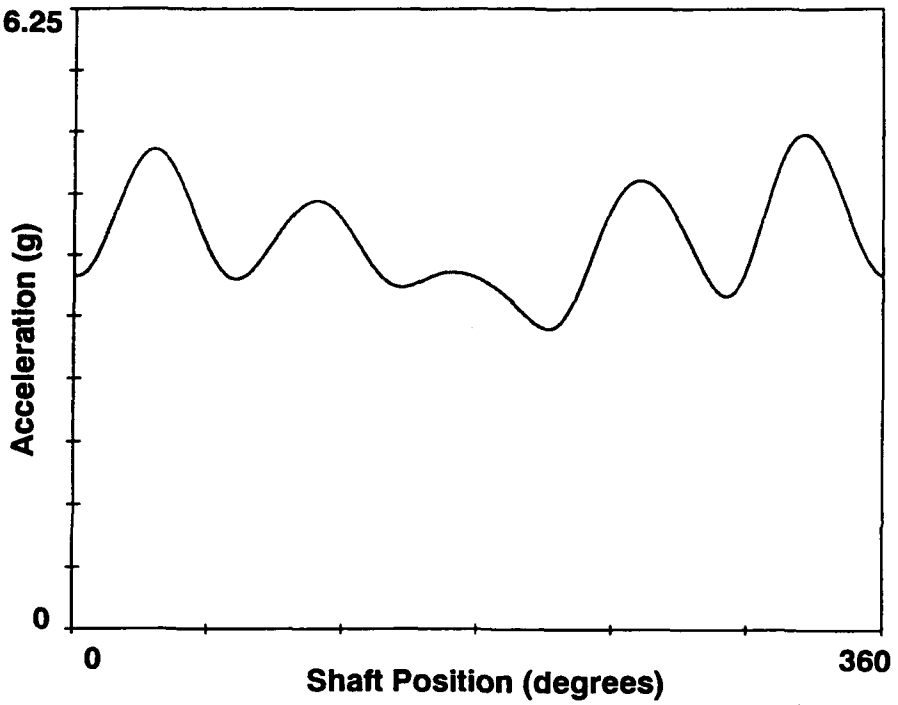

Figure 3. Amplitude modulation of carrier arm signal average.

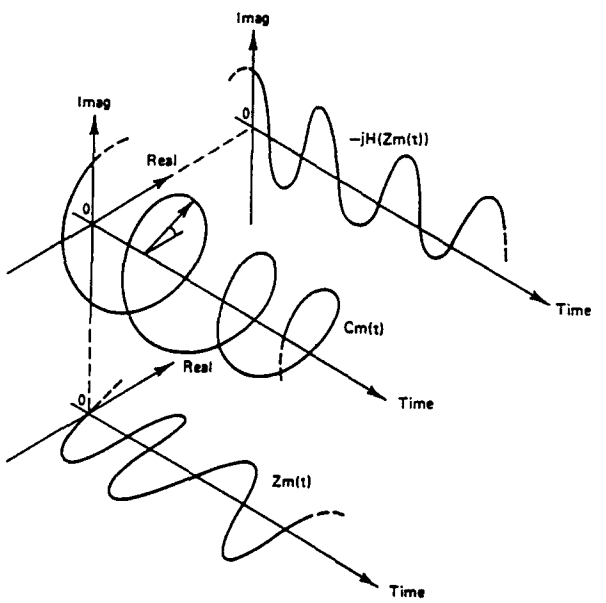

Figure 4. Complex rotating vector and its projections.

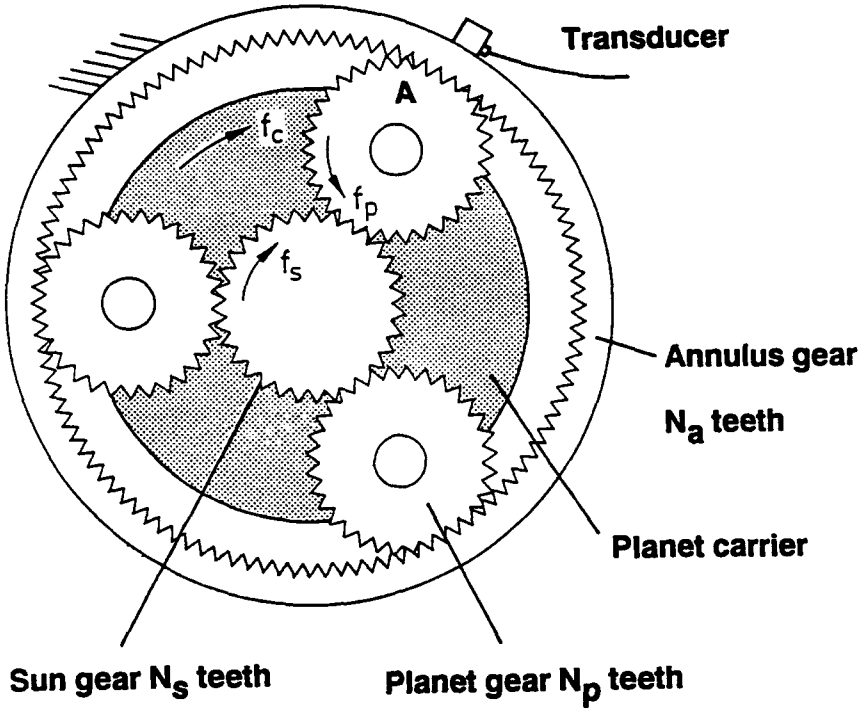

Figure 5. Simple epicyclic gear system.

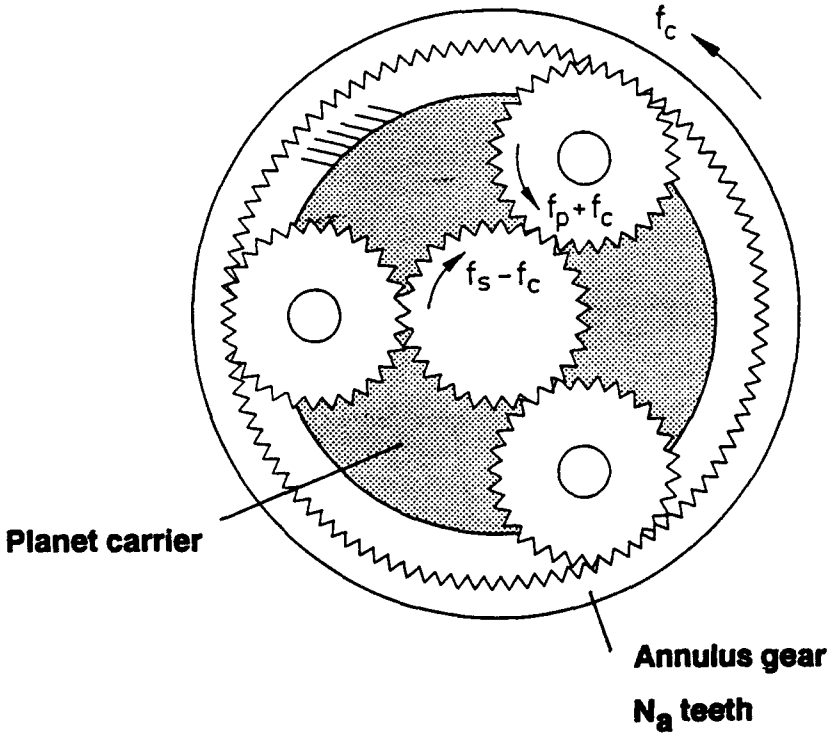

Figure 6. Relative motion of epicyclic gears.

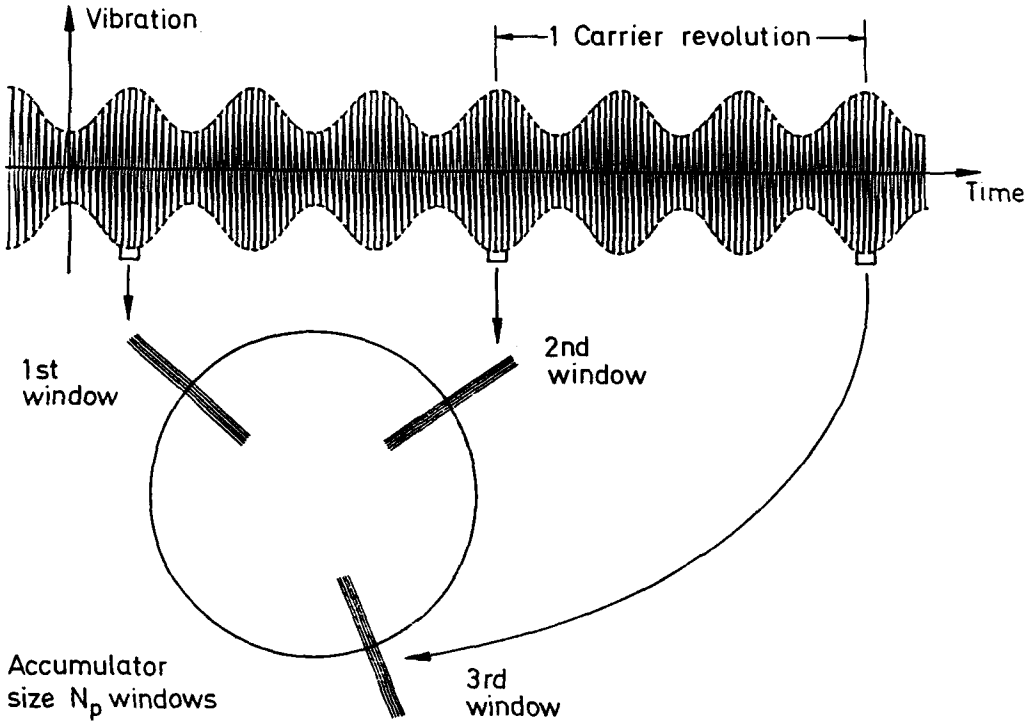

Figure 7. Placing data windows in accumulator.

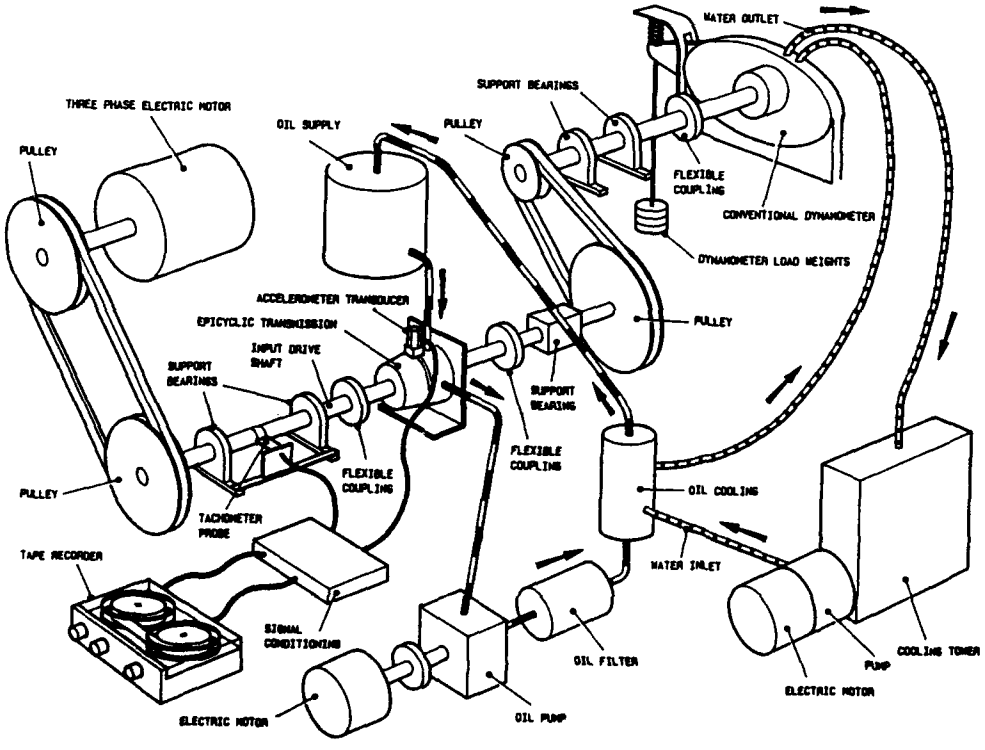

Figure 8. Epicyclic gearbox test facility.

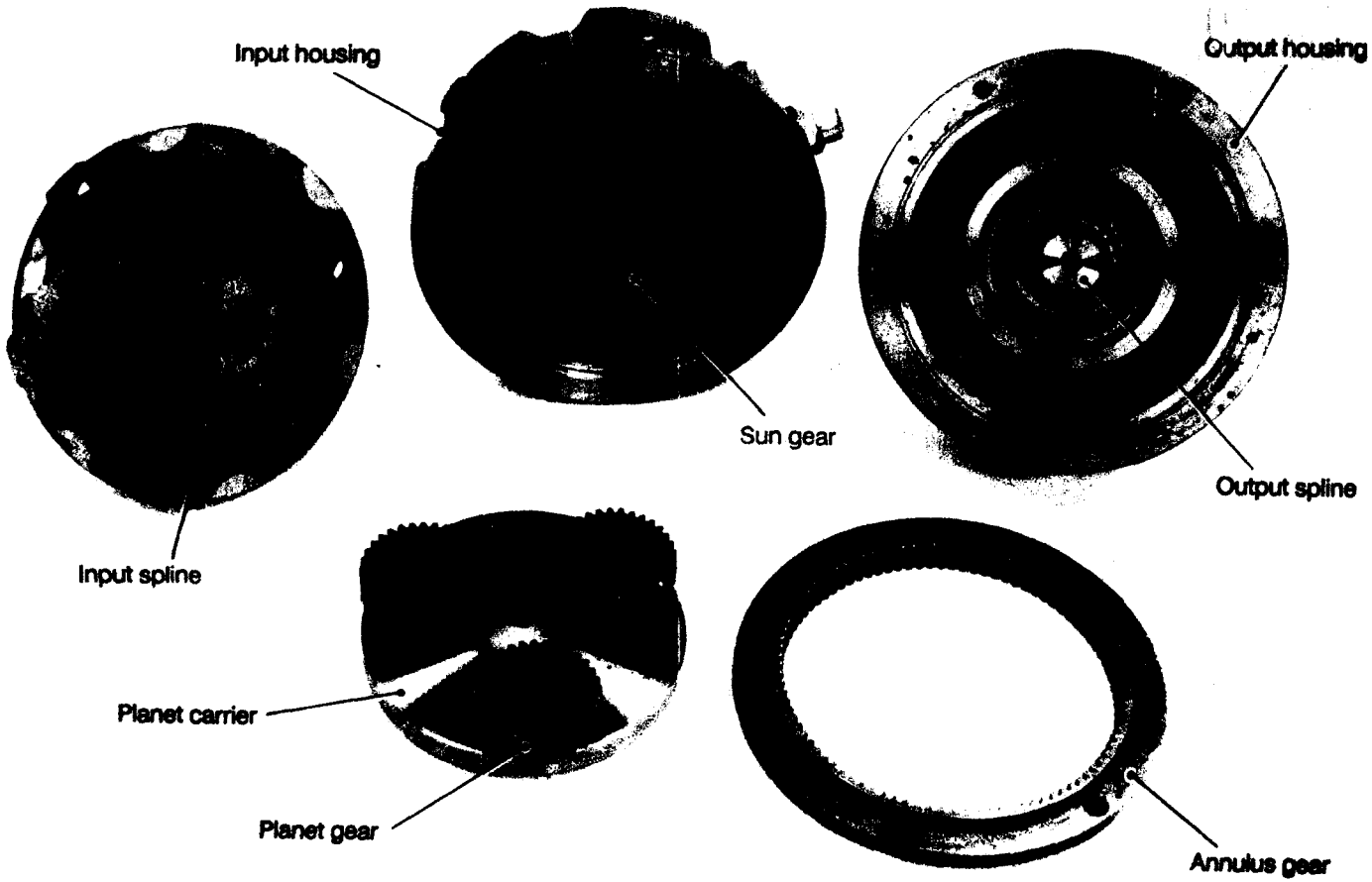

FIGURE 9. EXPLODED VIEW OF THE EPICYCLIC GEARBOX

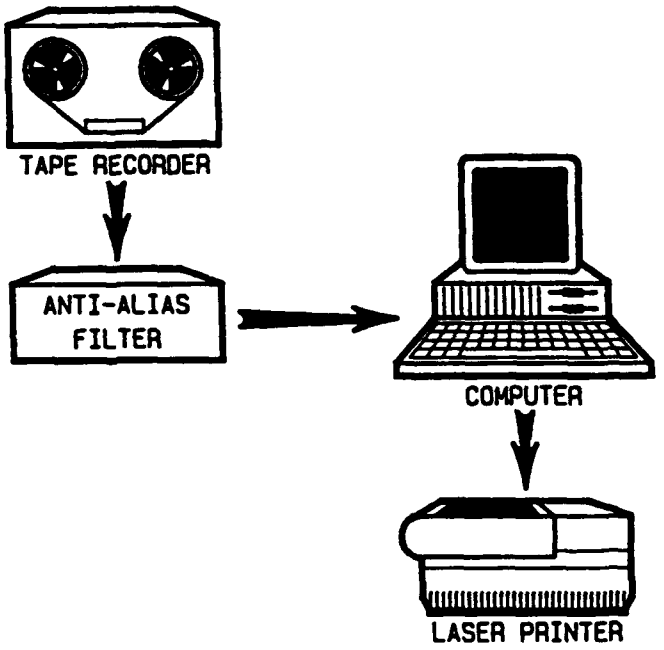

Figure 10. Computer hardware.

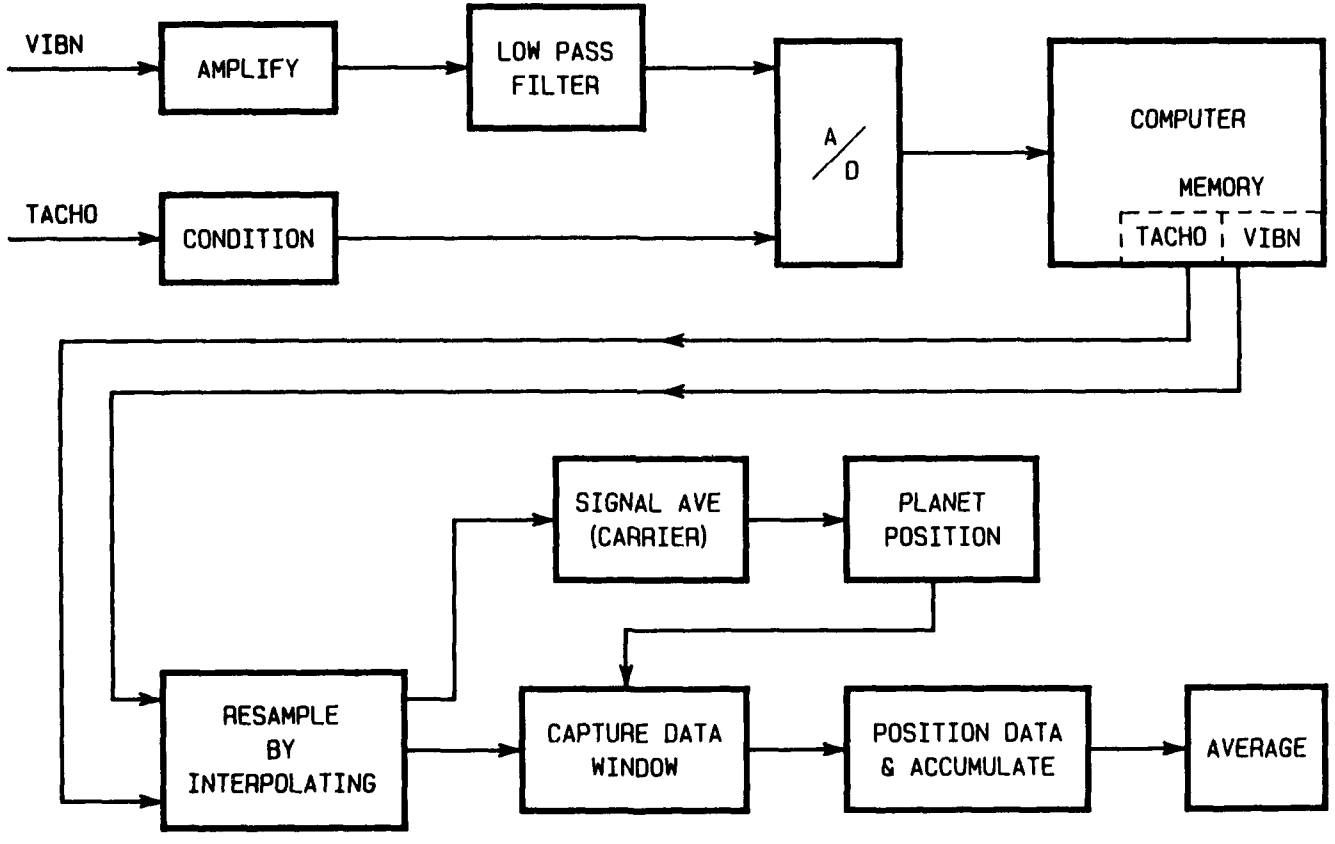

FIGURE 11. EPICYCLIC COMPONENT SIGNAL AVERAGING PROCEDURE

FIGURE 12. DAMAGED PLANET WITH 60% OF THE WIDTH OF ONE TOOTH REMOVED

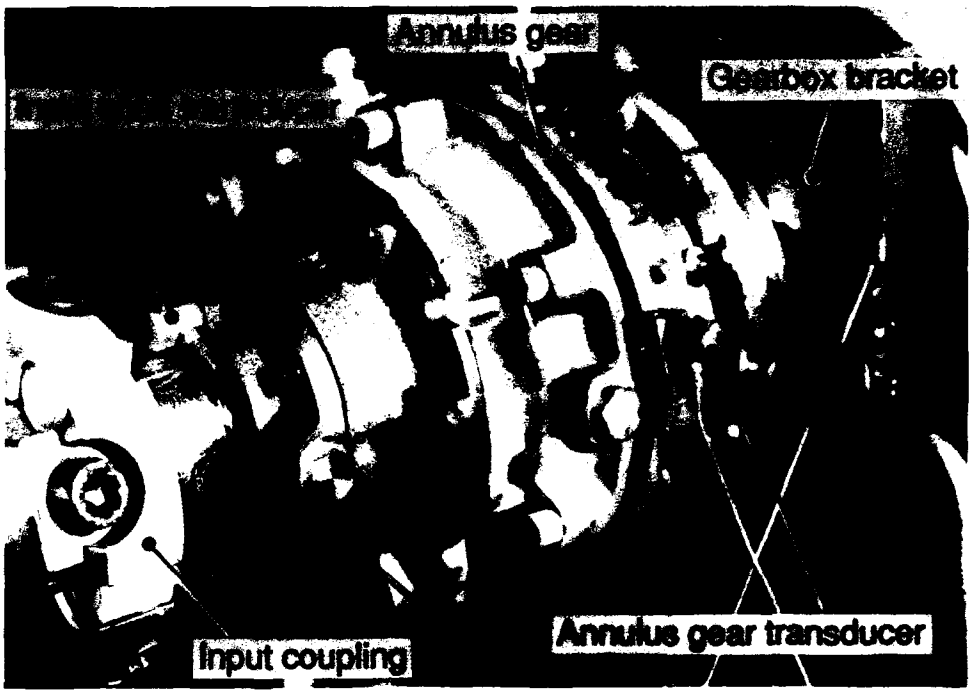

(a)

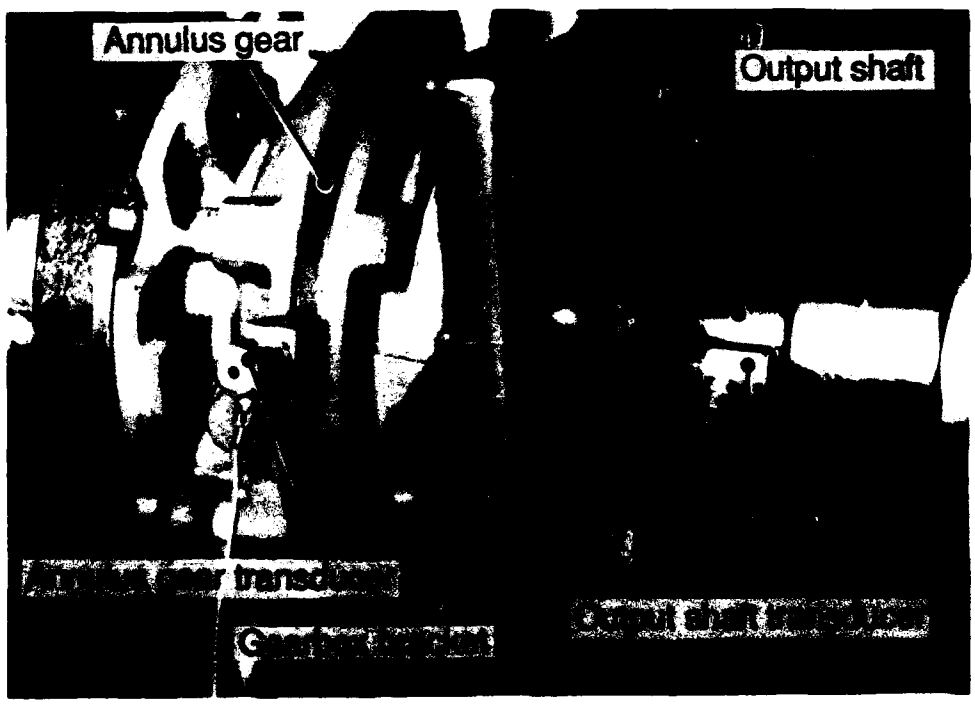

(b)

FIGURE 13. PHOTOS OF THE TRANSDUCER MOUNTED ON THE GEAR CASE. (a) INPUT SIDE (b) OUTPUT SIDE

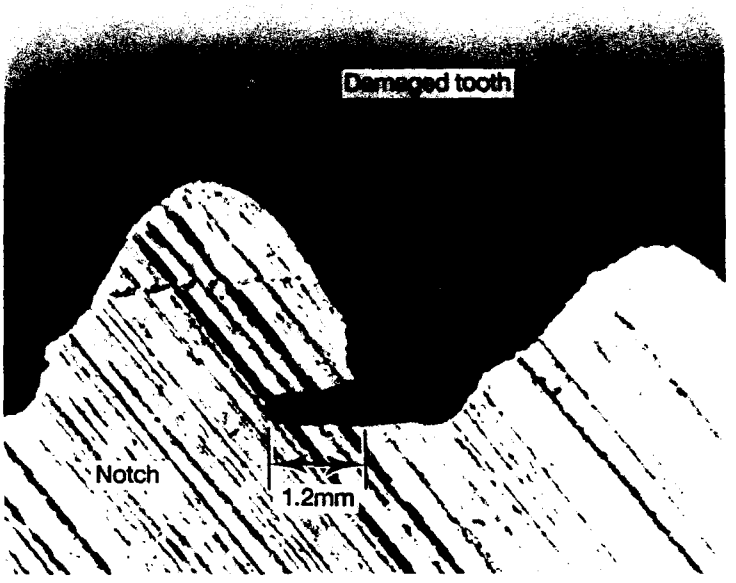

Figure 14. Damaged planet gear tooth with implanted notch.

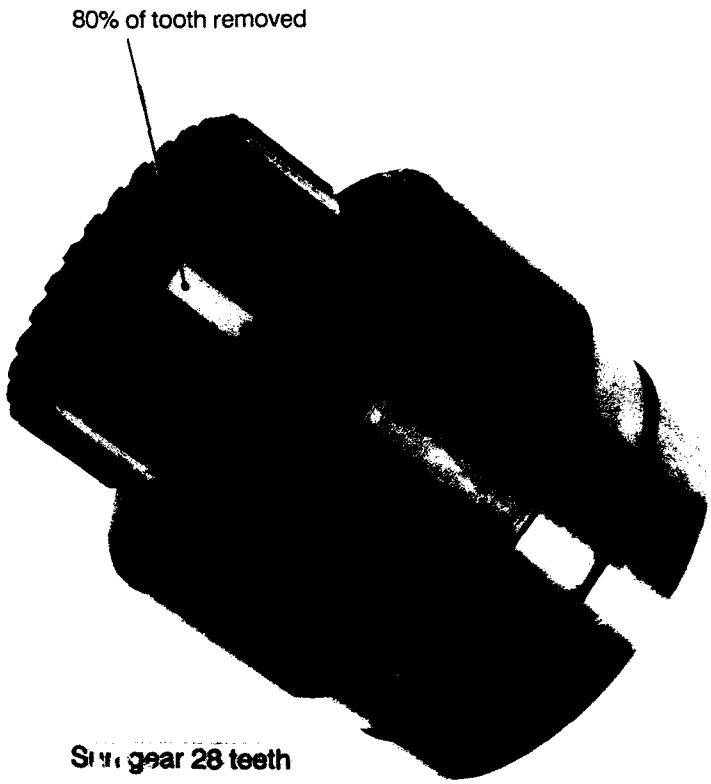

Figure 15. Damaged sun gear with 80% of tooth removed.

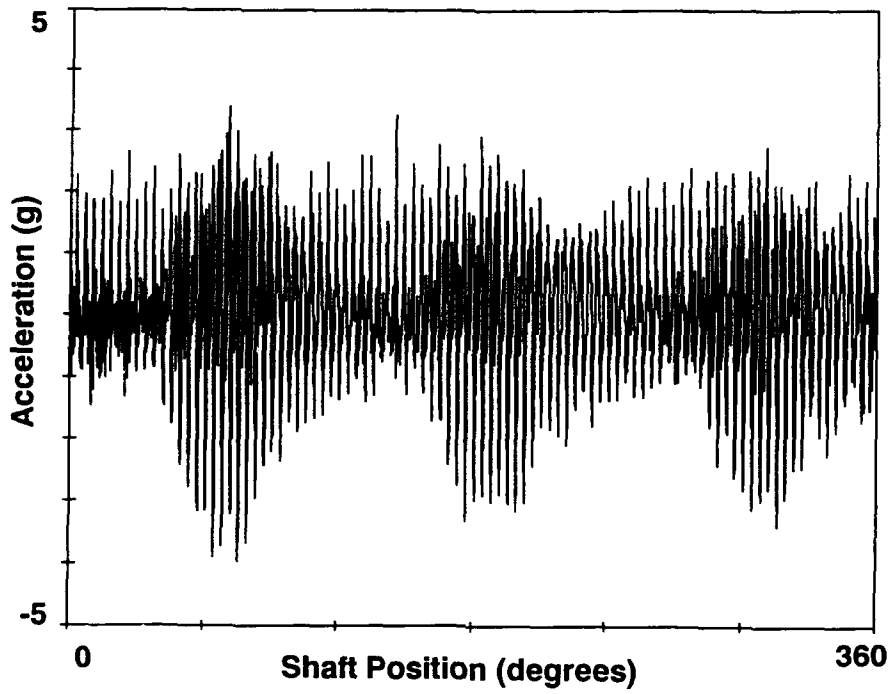

Figure 16a. Carrier arm signal average.

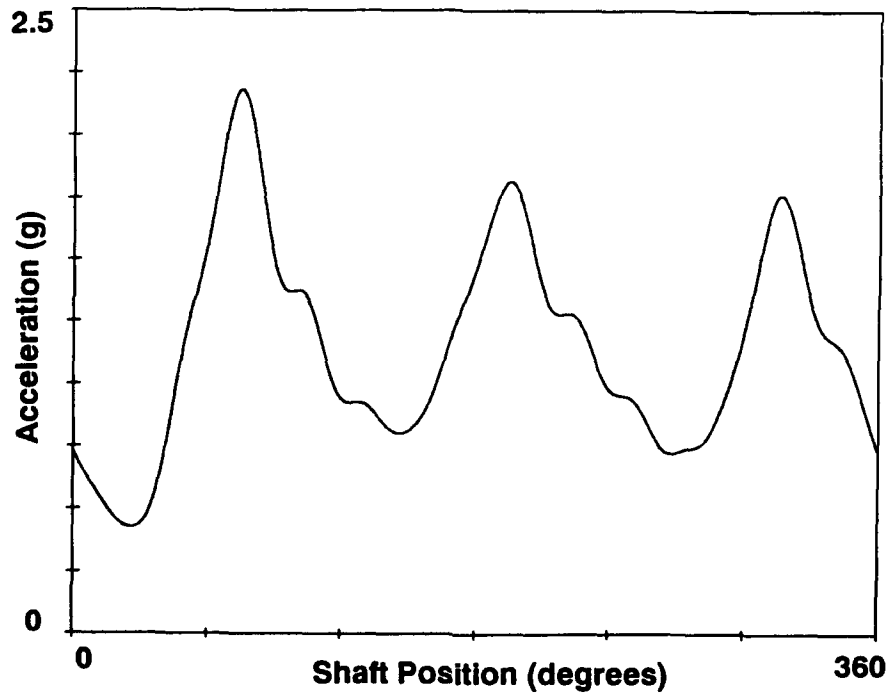

Figure 16b. Amplitude modulation of carrier arm signal average.

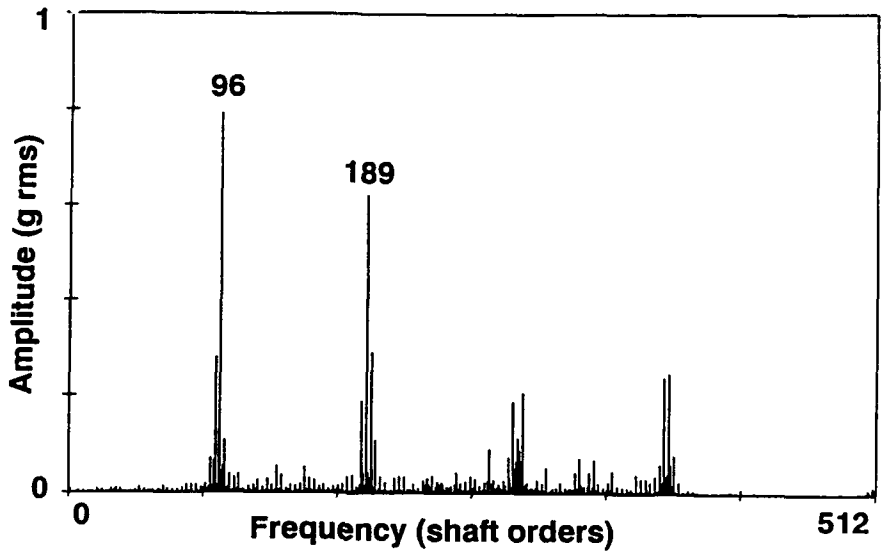

Figure 16c. Frequency spectrum of the carrier arm signal average.

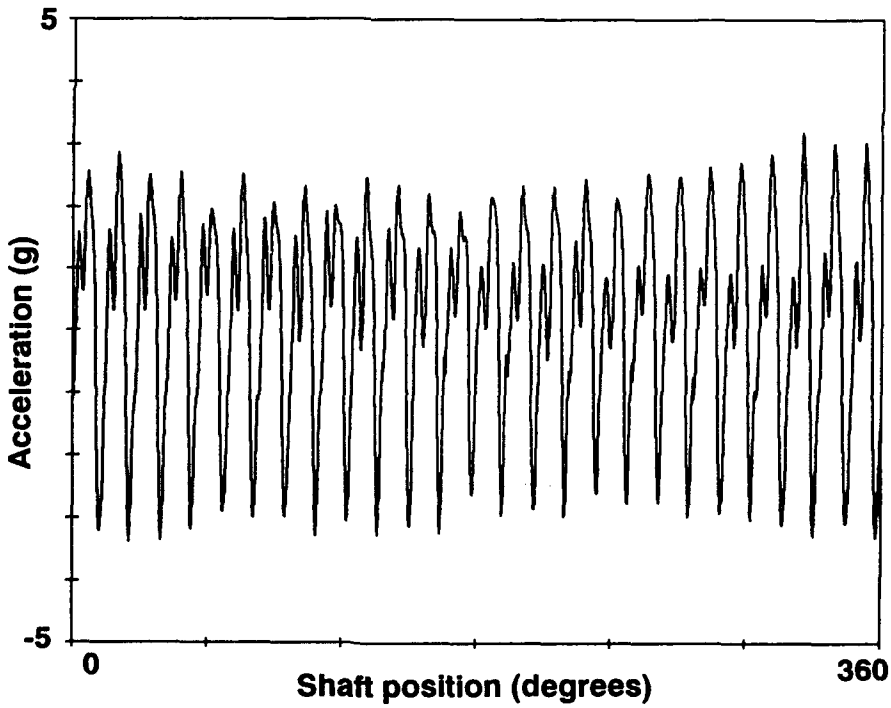

Figure 17a. Undamaged planet gear signal average.

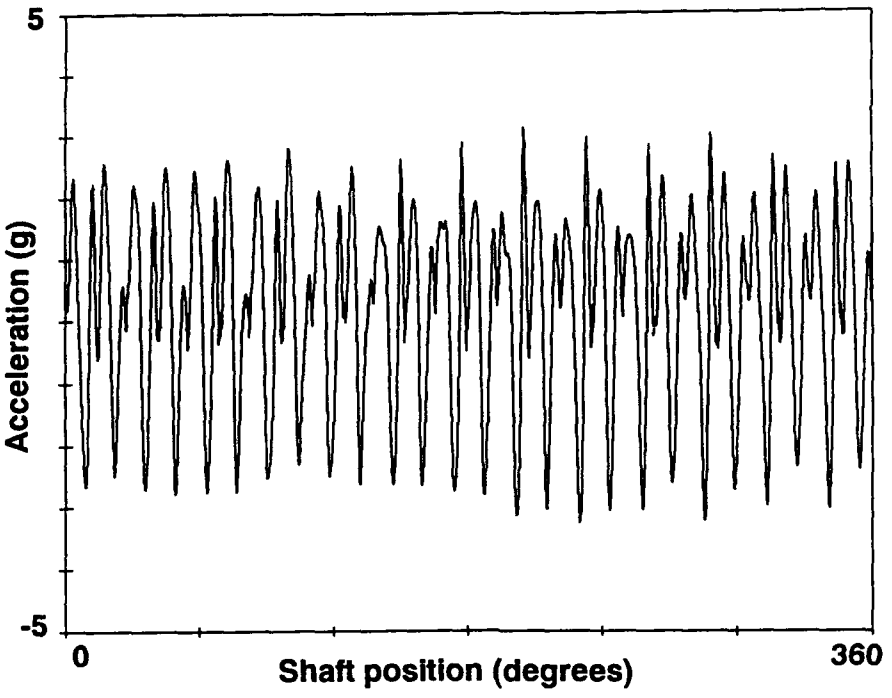

Figure 17b. Planet gear signal average. 20% of one tooth removed.

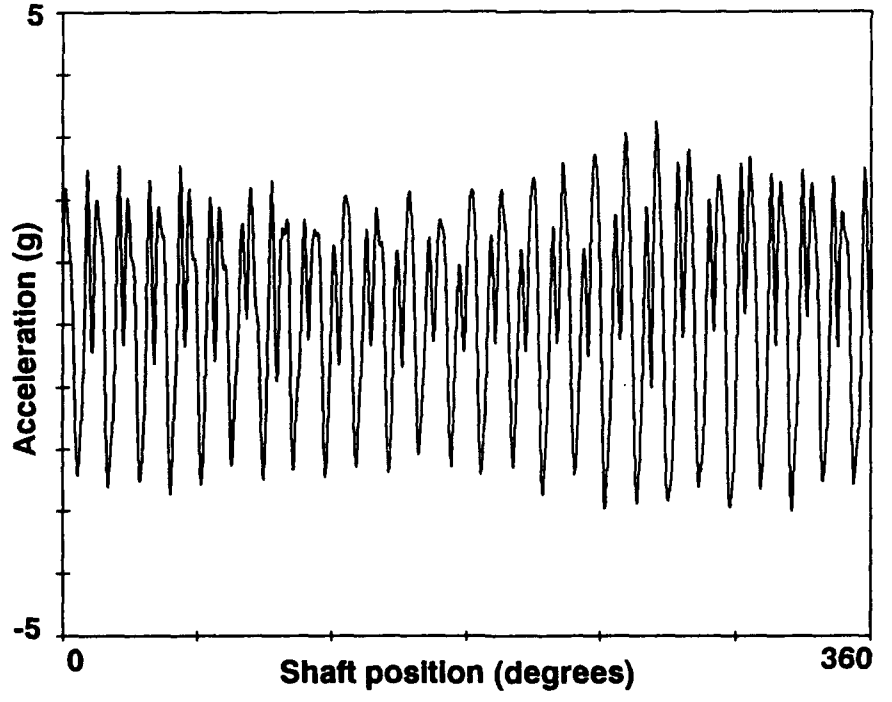

Figure 17c. Planet gear signal average. 40% of one tooth removed.

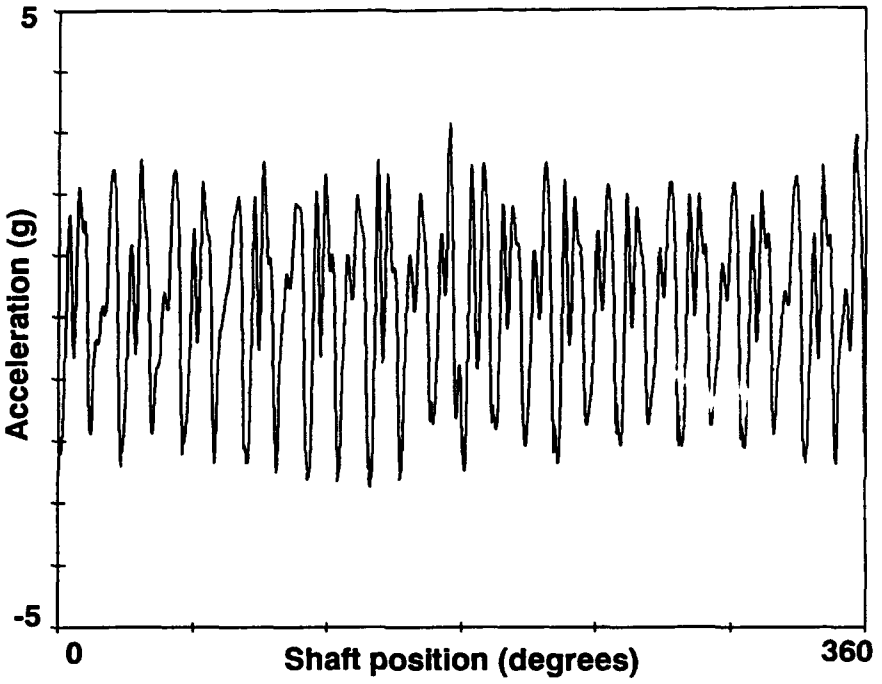

Figure 17d. Planet gear signal average. 60% of one tooth removed.

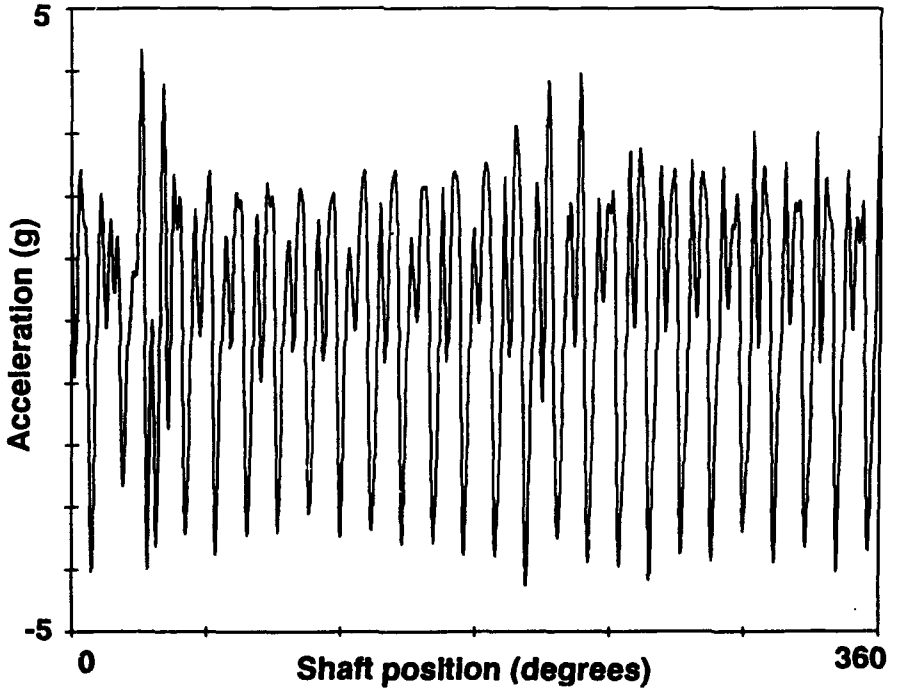

Figure 17e. Planet gear signal average. 80% of one tooth removed.

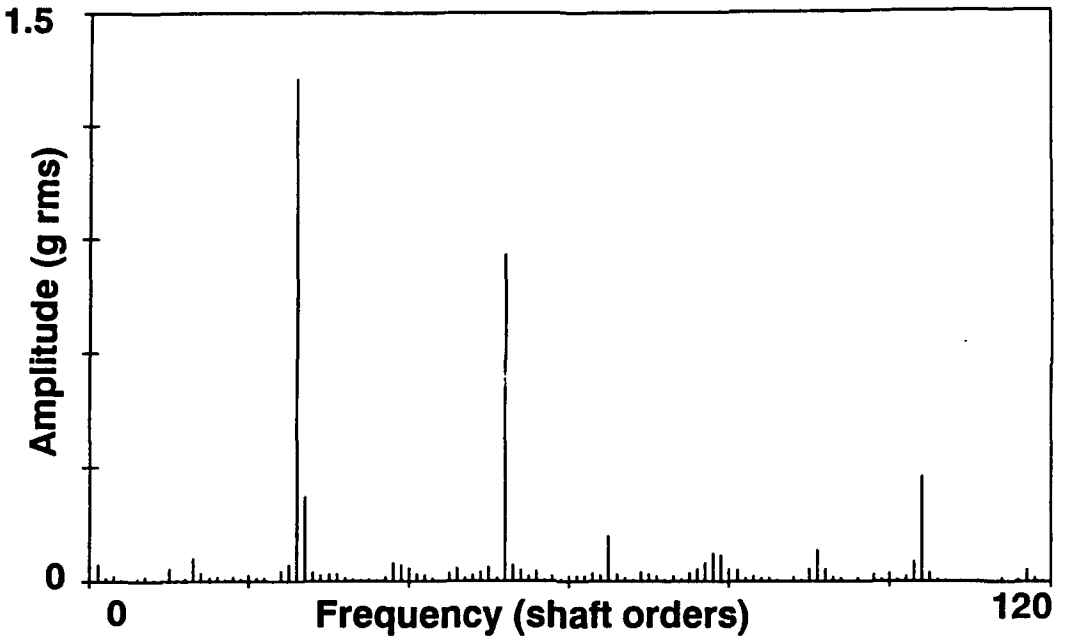

Figure 18a. Frequency spectrum of planet gear signal average.

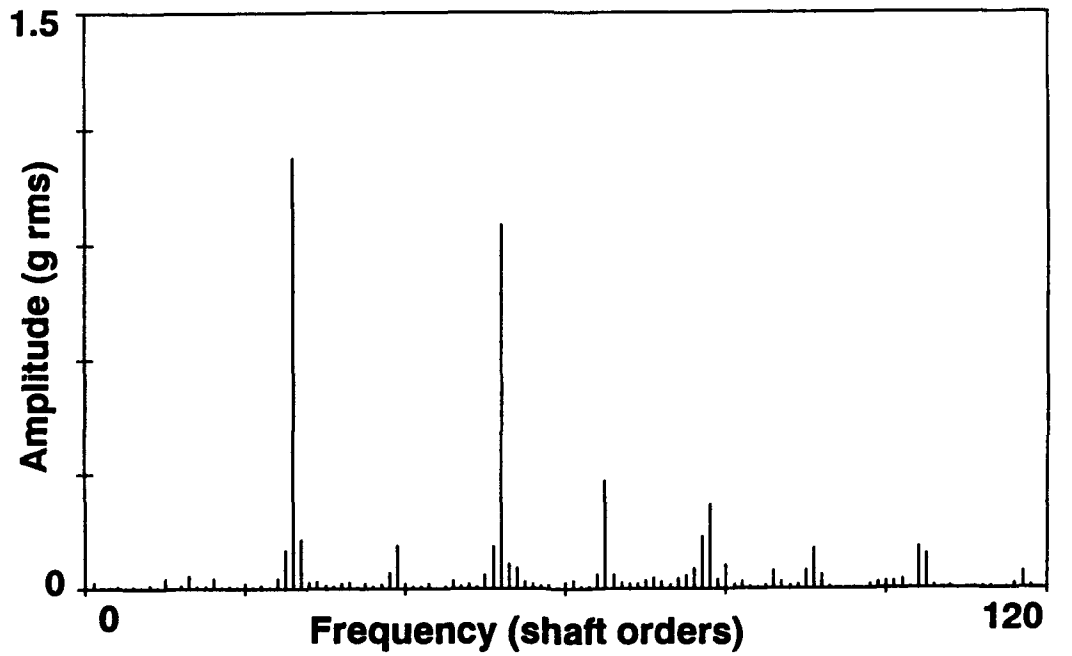

Figure 18b. Frequency spectrum with 20% of one tooth removed.

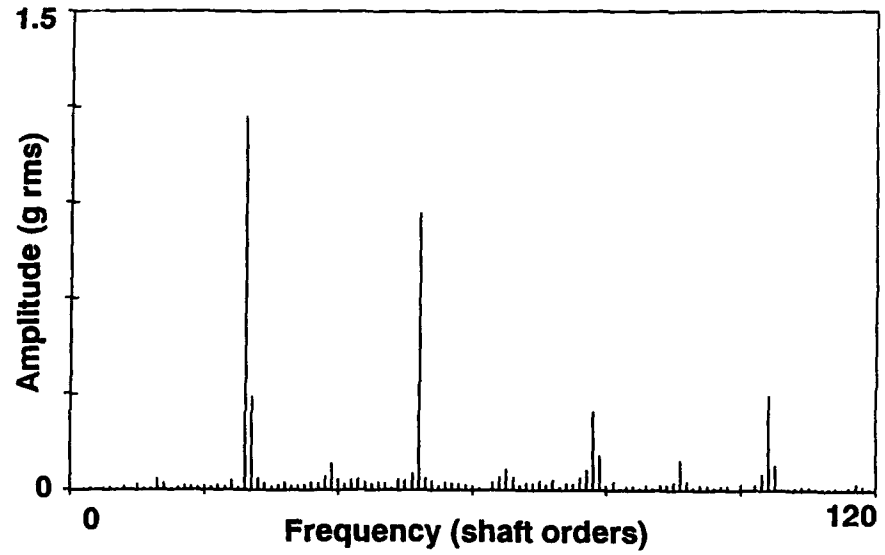

Figure 18c. Frequency spectrum with 40% of one tooth removed.

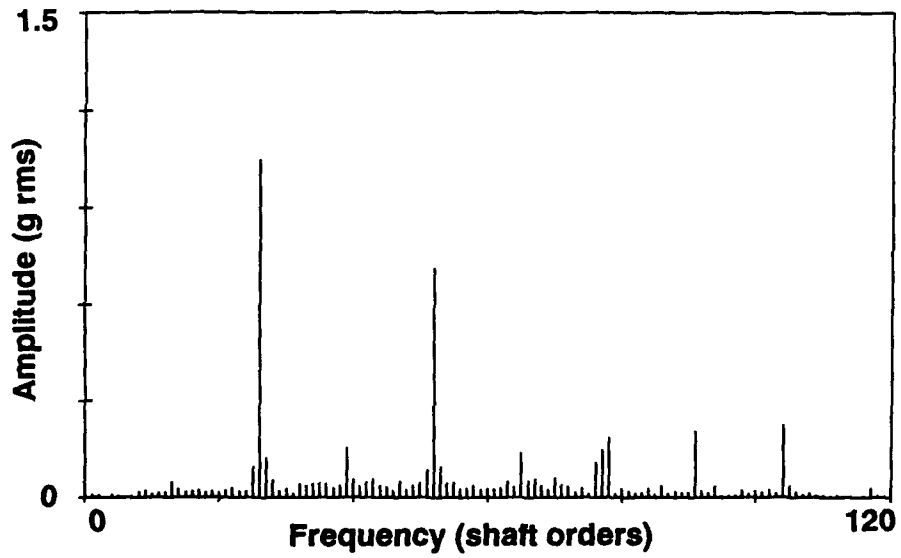

Figure 18d. Frequency spectrum with 60% of one tooth removed.

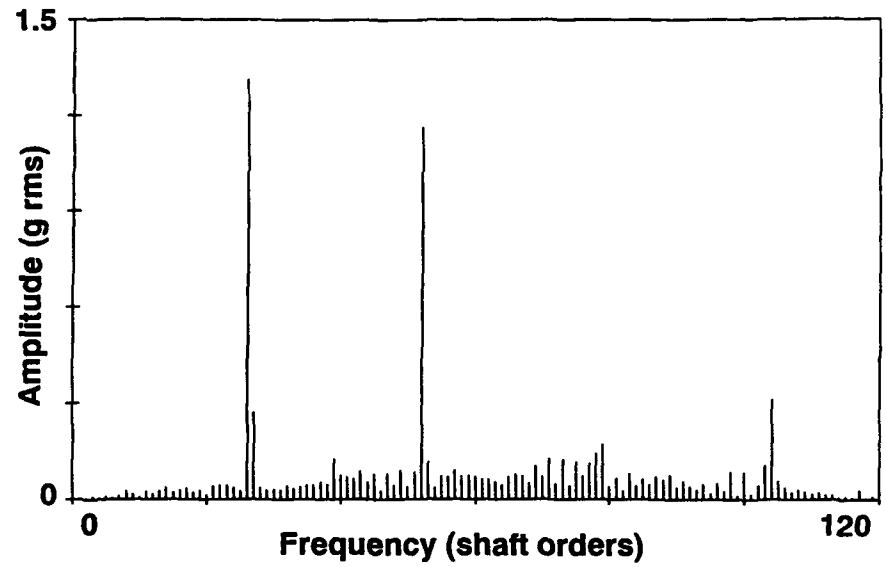

Figure 18e. Frequency spectrum with 80% of one tooth removed.

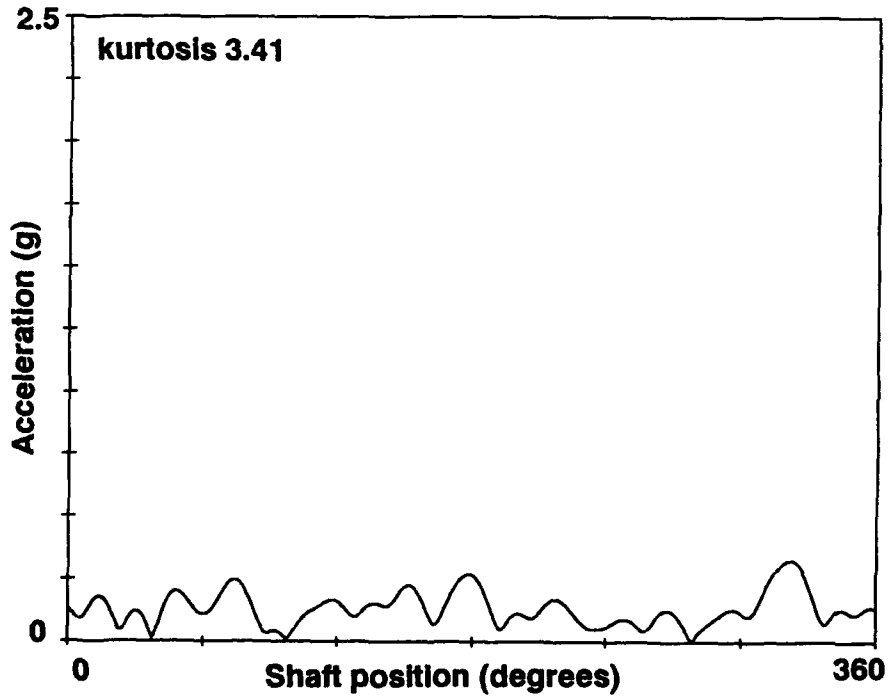

Figure 19a. Narrow band envelope of undamaged planet gear.

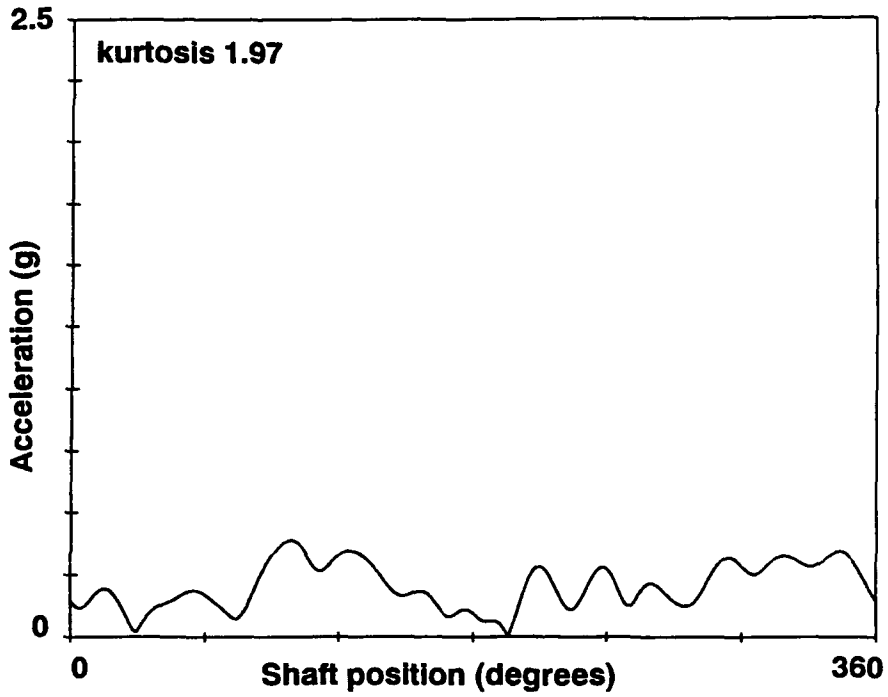

Figure 19b. Narrow band envelope with 20% of one tooth removed.

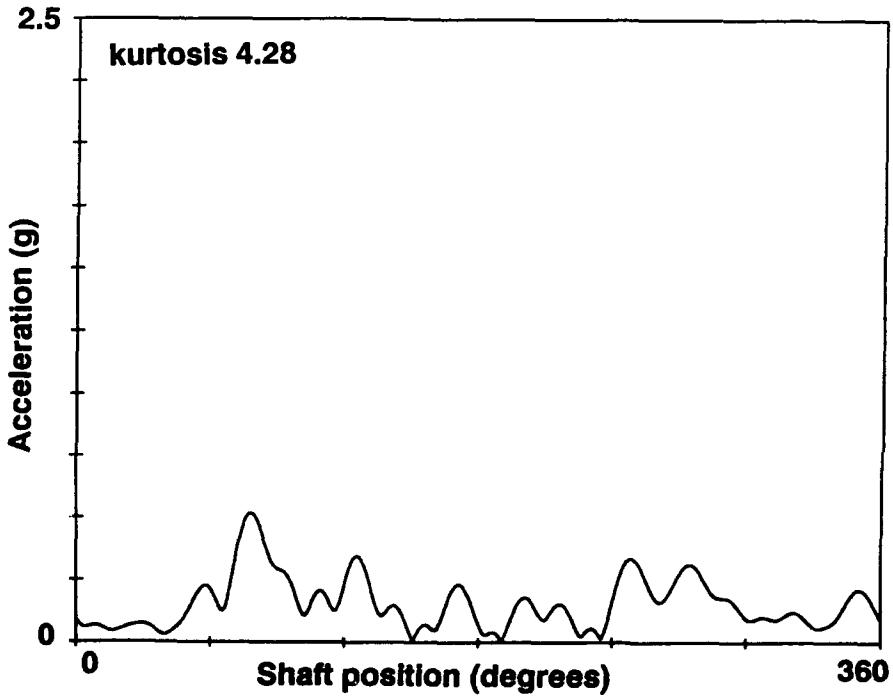

Figure 19c. Narrow band envelope with 40% of one tooth removed.

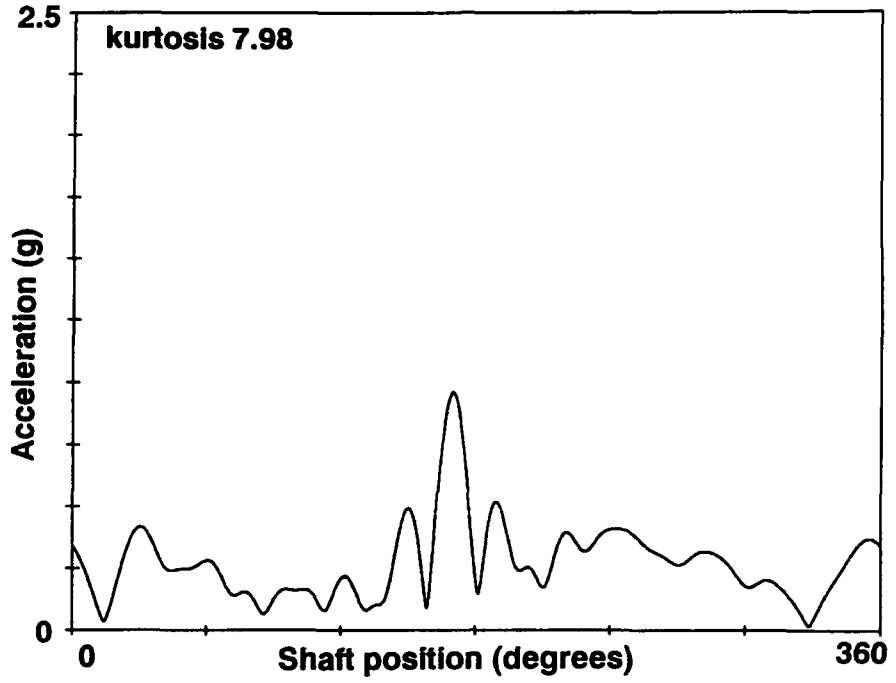

Figure 19d. Narrow band envelope with 60% of one tooth removed.

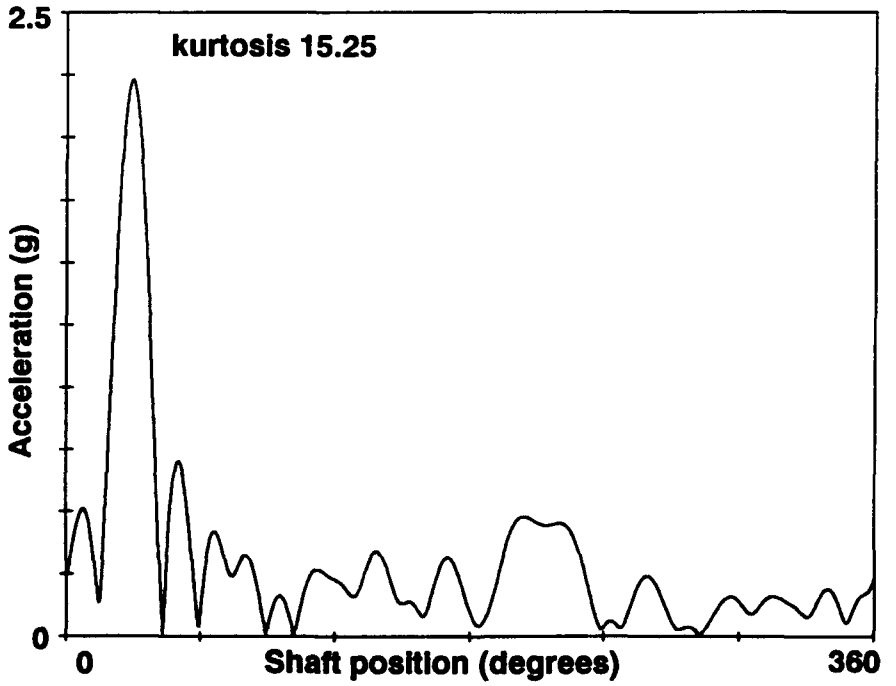

Figure 19e. Narrow band envelope with 80% of one tooth removed.

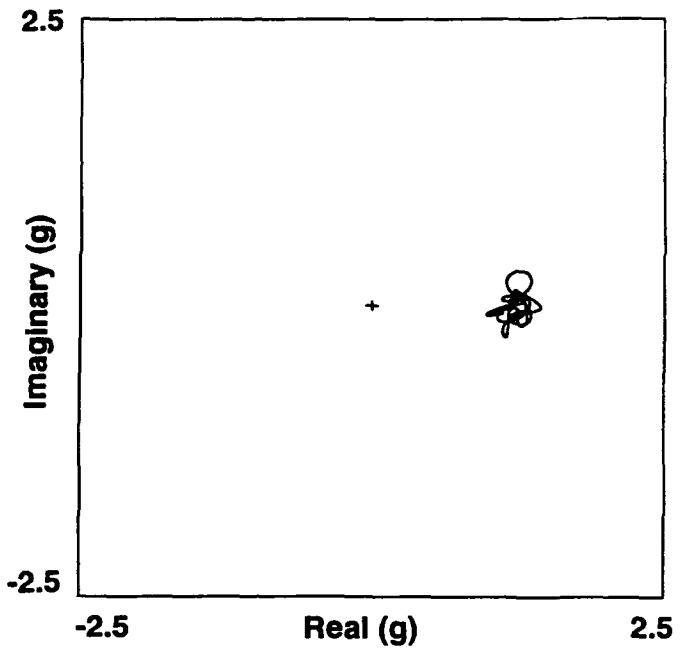

Figure 20a. Polar plot of the undamaged planet gear average.

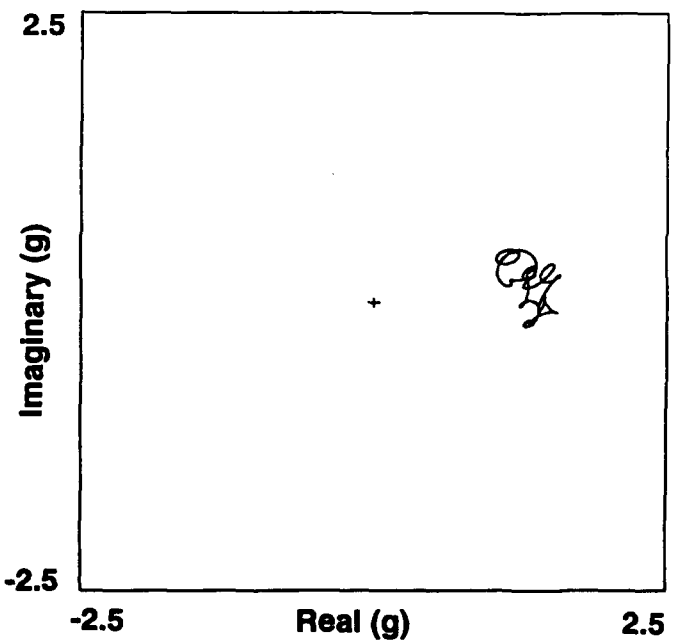

Figure 20b. Polar plot with 20% of one tooth removed.

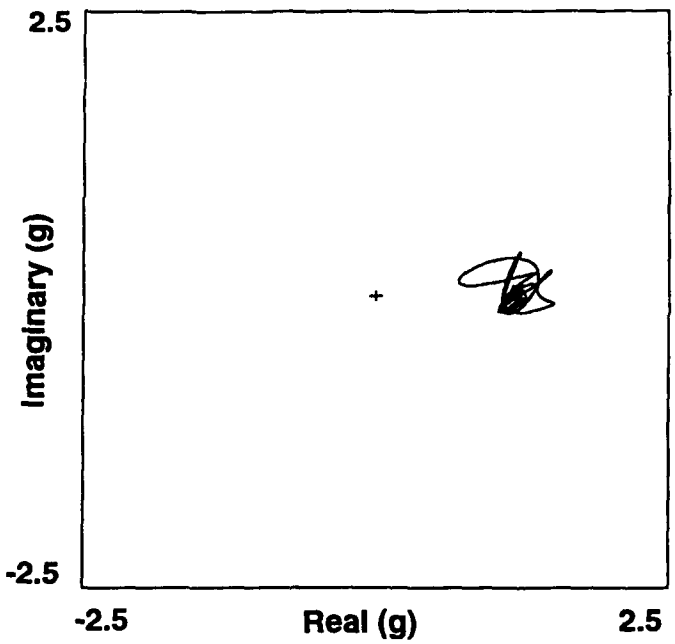

Figure 20c. Polar plot with 40% of one tooth removed.

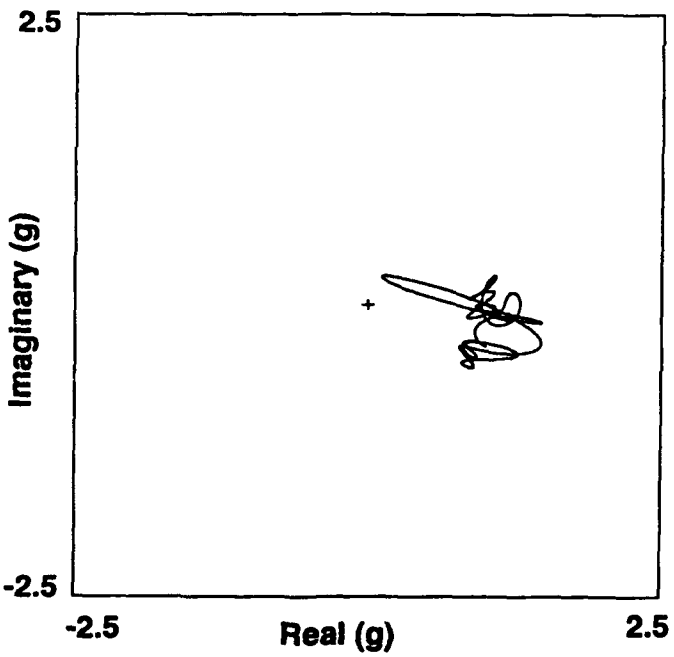

Figure 20d. Polar plot with 60% of one tooth removed.

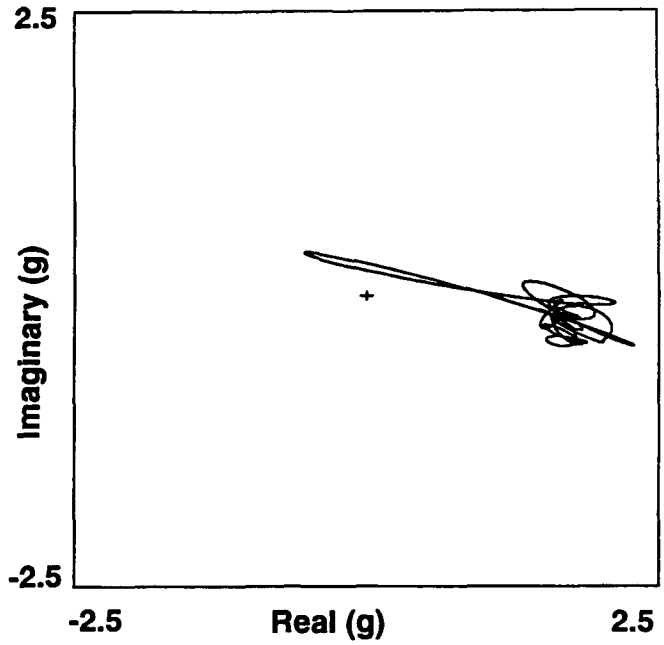

Figure 20e. Polar plot with 80% of one tooth removed.

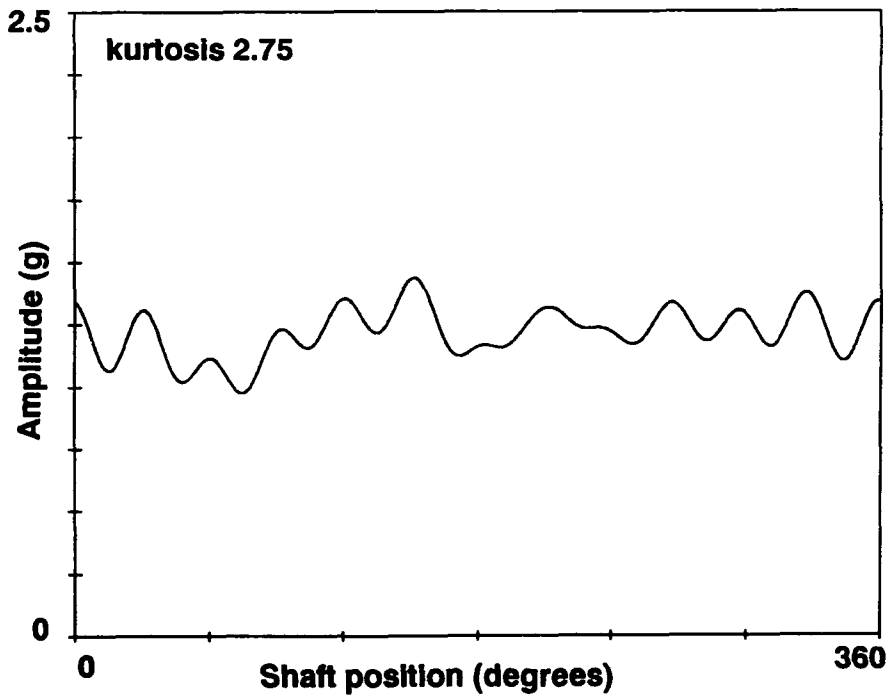

Figure 21a. Amplitude of the undamaged planet gear average.

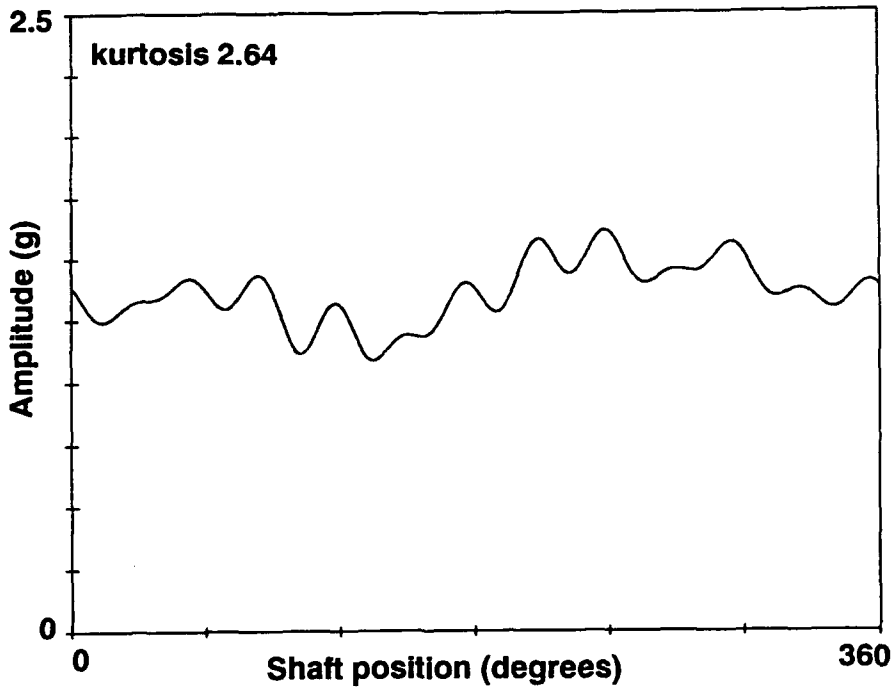

Figure 21b. Amplitude with 20% of one tooth removed.

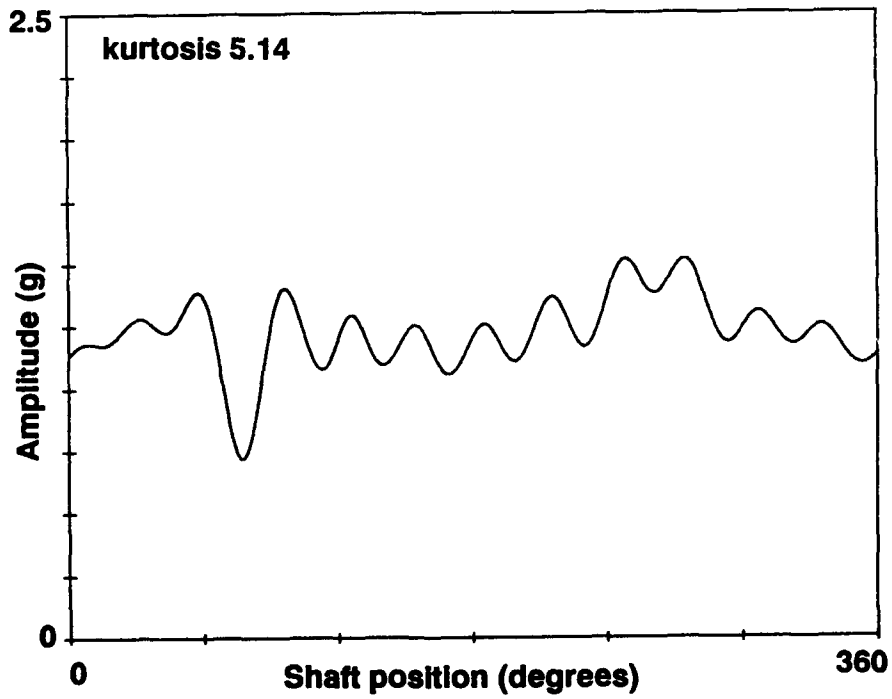

Figure 21c. Amplitude with 40% of one tooth removed.

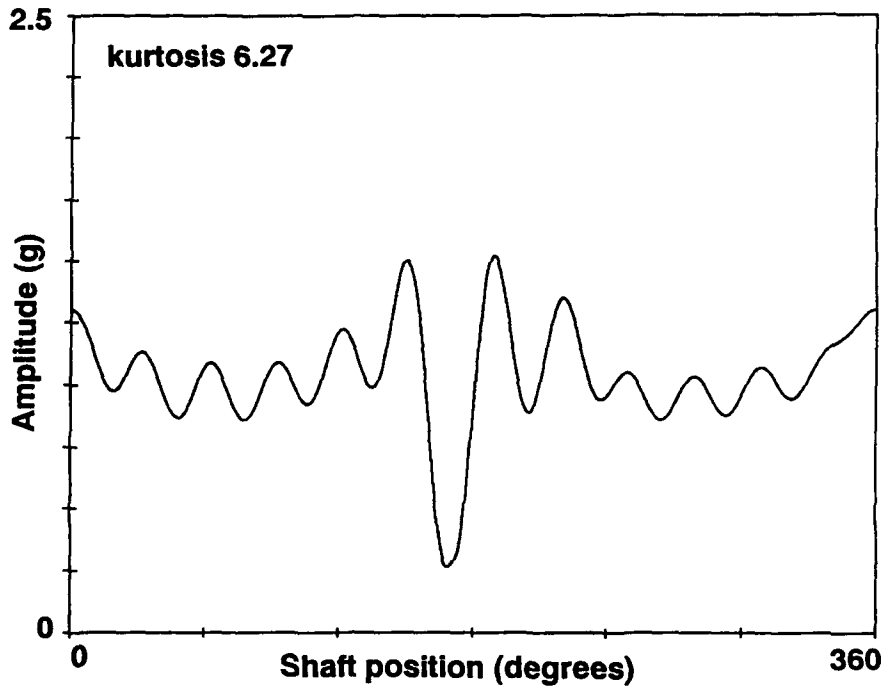

Figure 21d. Amplitude with 60% of one tooth removed.

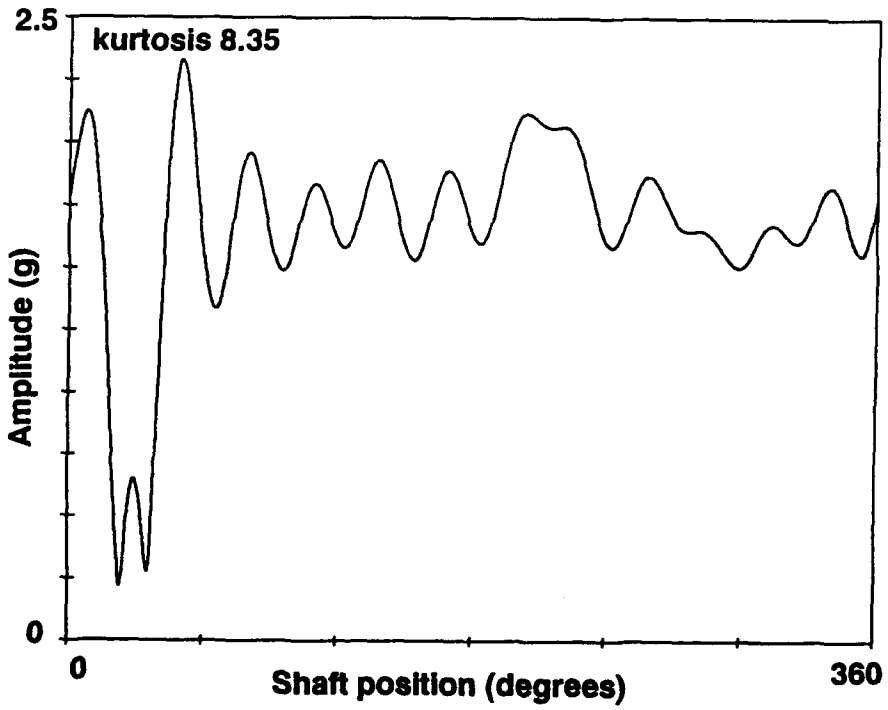

Figure 21e. Amplitude with 80% of one tooth removed.

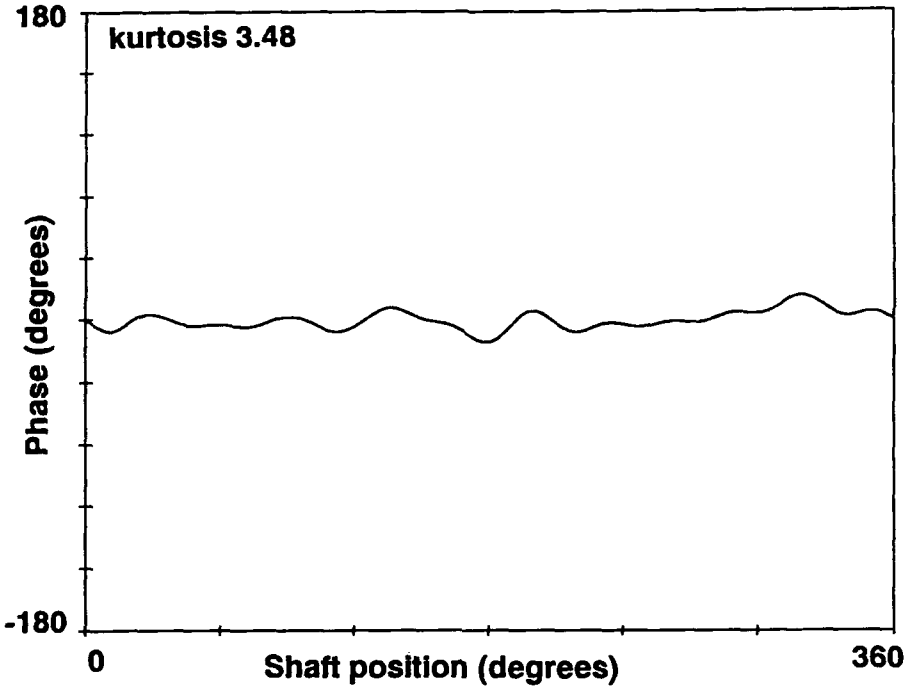

Figure 22a. Phase of the undamaged planet gear signal average.

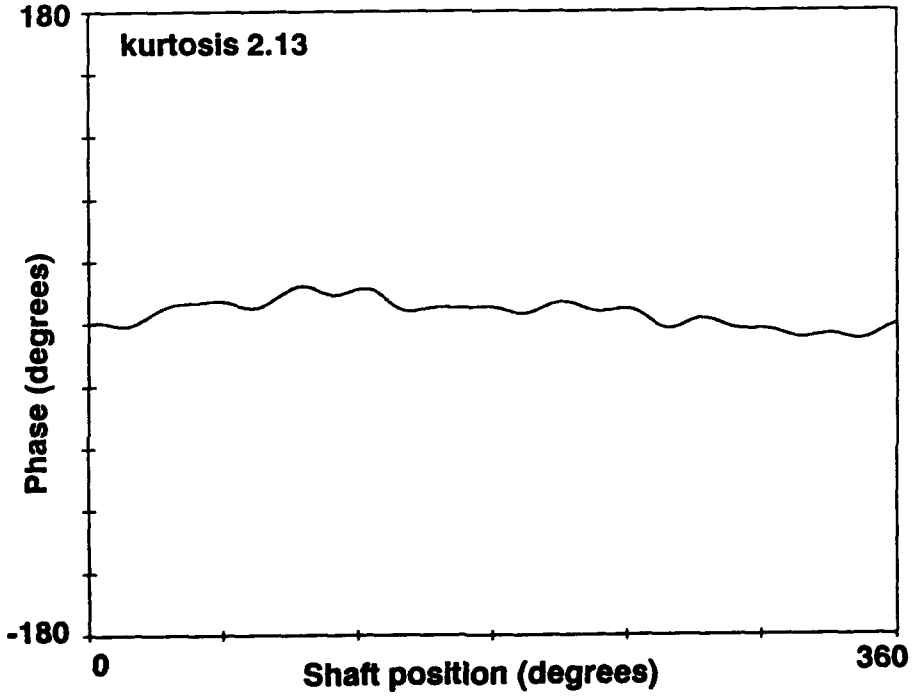

Figure 22b. Phase with 20% of one tooth removed.

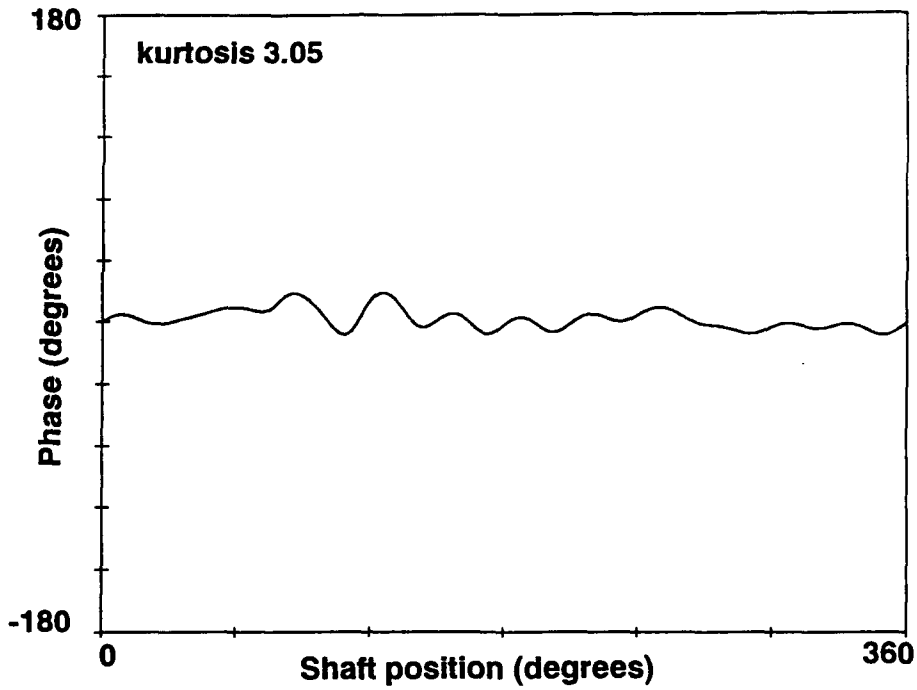

Figure 22c. Phase with 40% of one tooth removed.

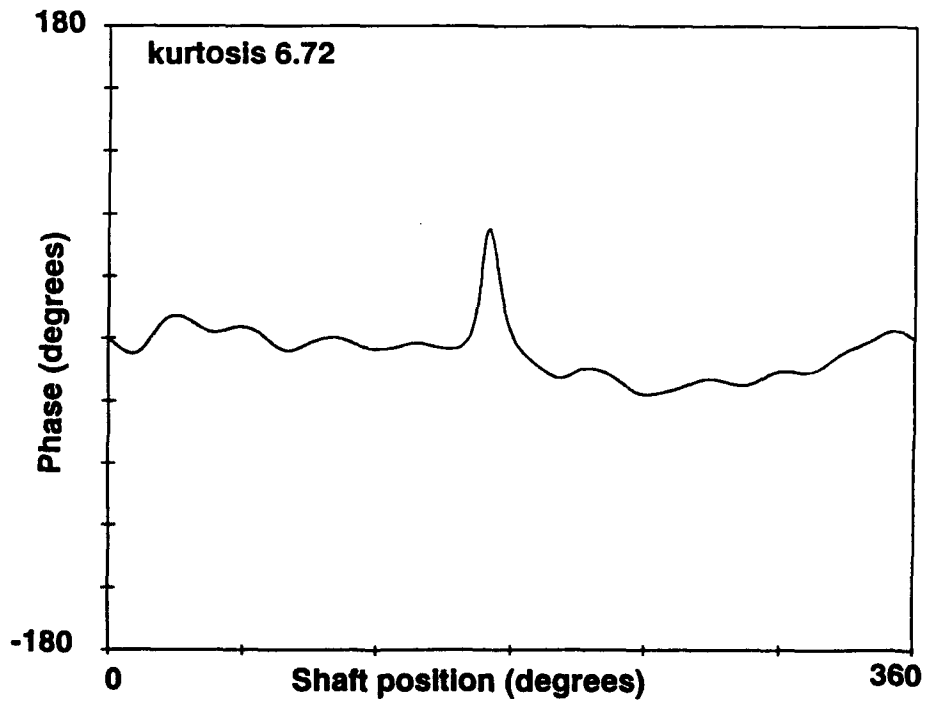

Figure 22d. Phase with 60% of one tooth removed.

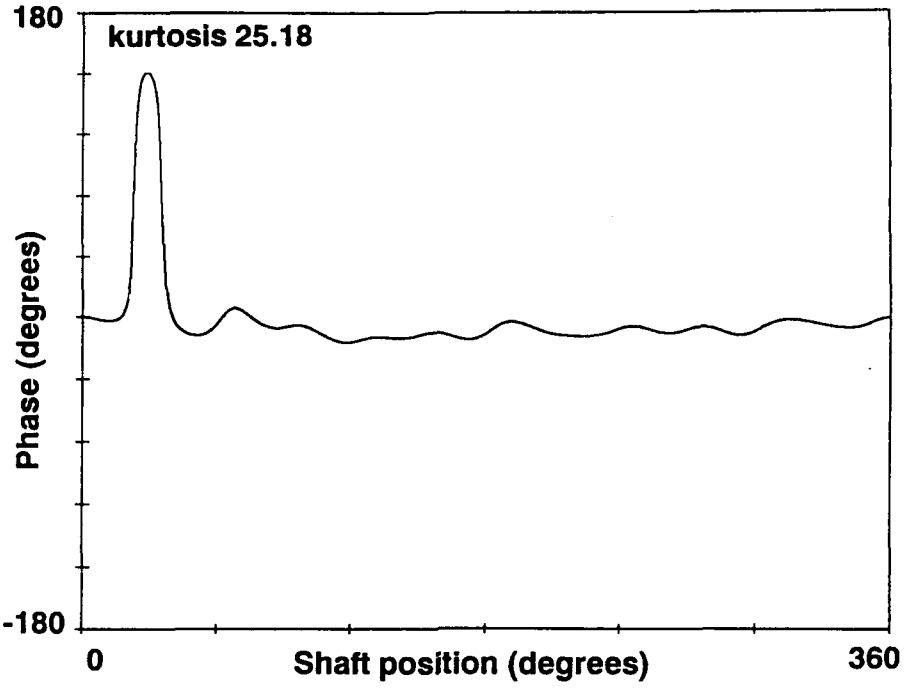

Figure 22e. Phase with 80% of one tooth removed.

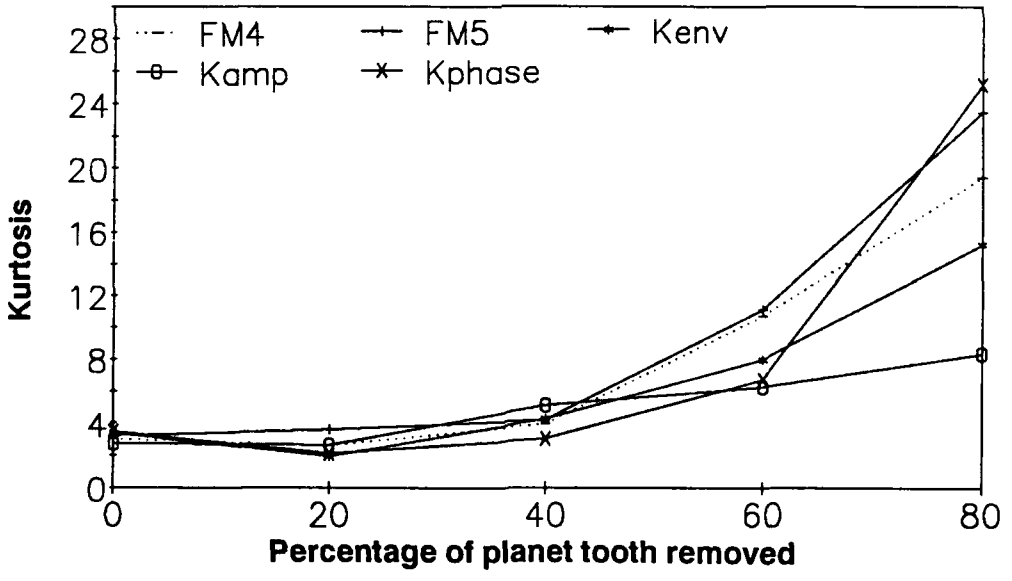

Figure 23. Trend of five condition indexes.

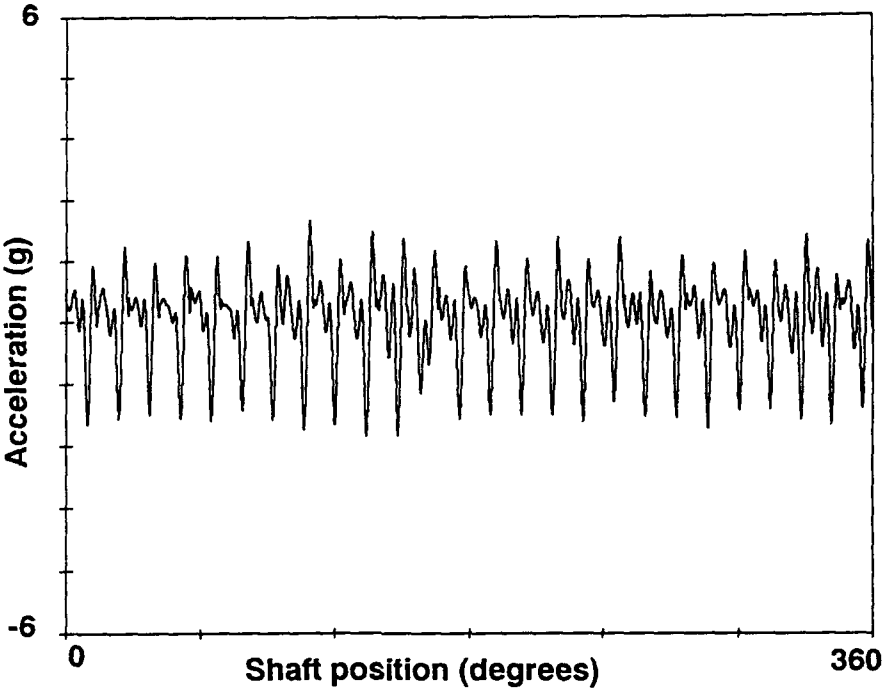

Figure 24a. Planet gear signal average with 1.4mm notch.

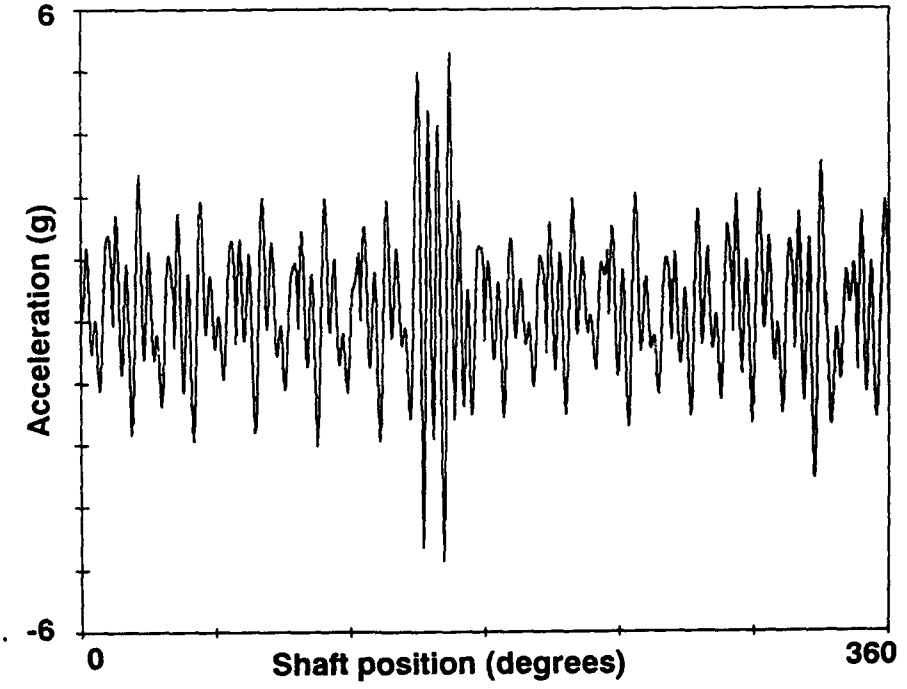

Figure 24b. Planet gear signal average with tooth removed.

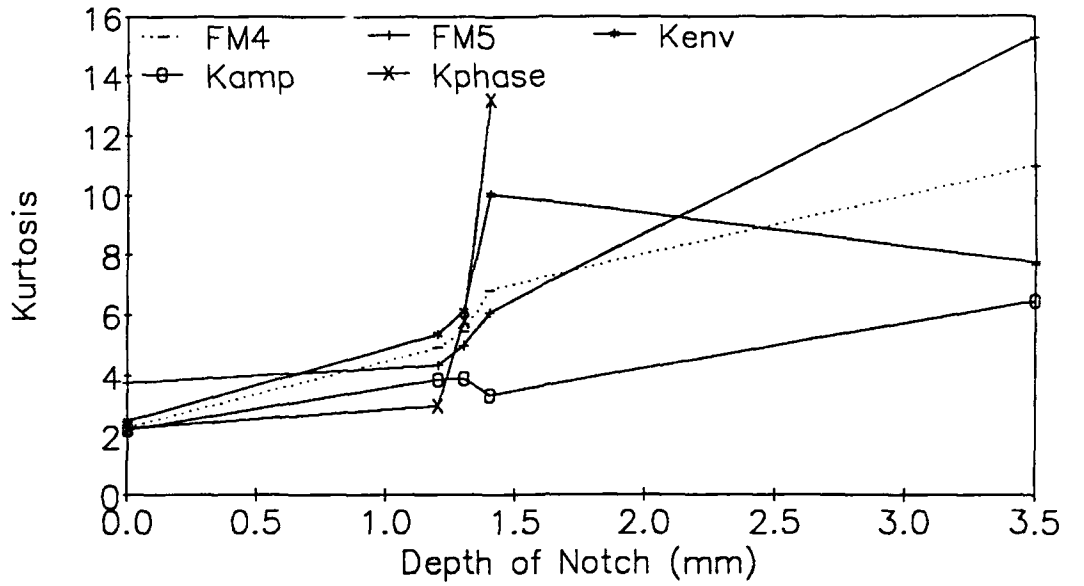

Figure 25. Condition indexes as a function of notch depth.

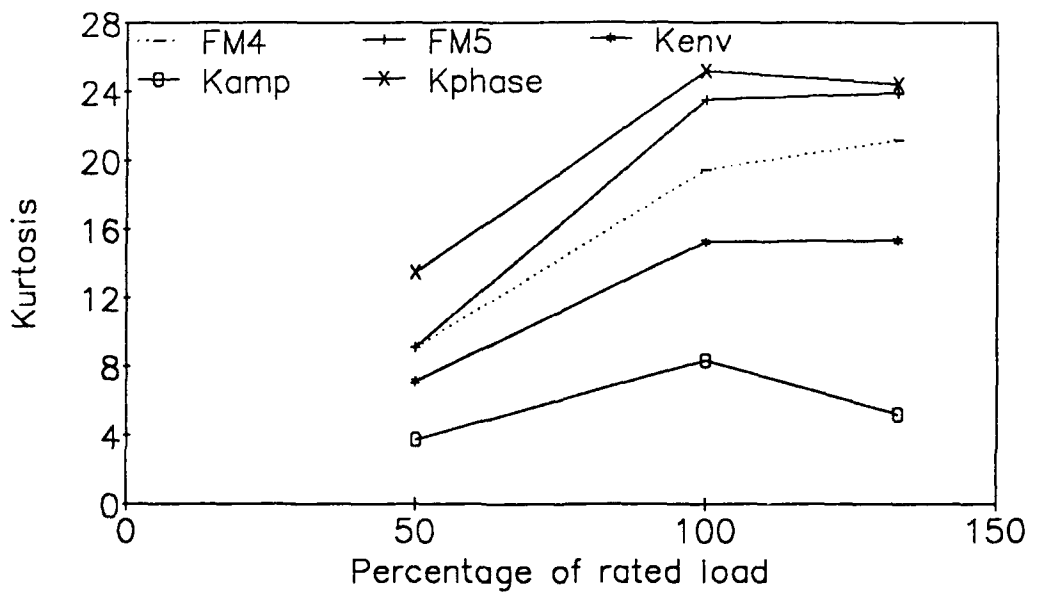

Figure 26. Effect of load with 80% of one tooth removed.

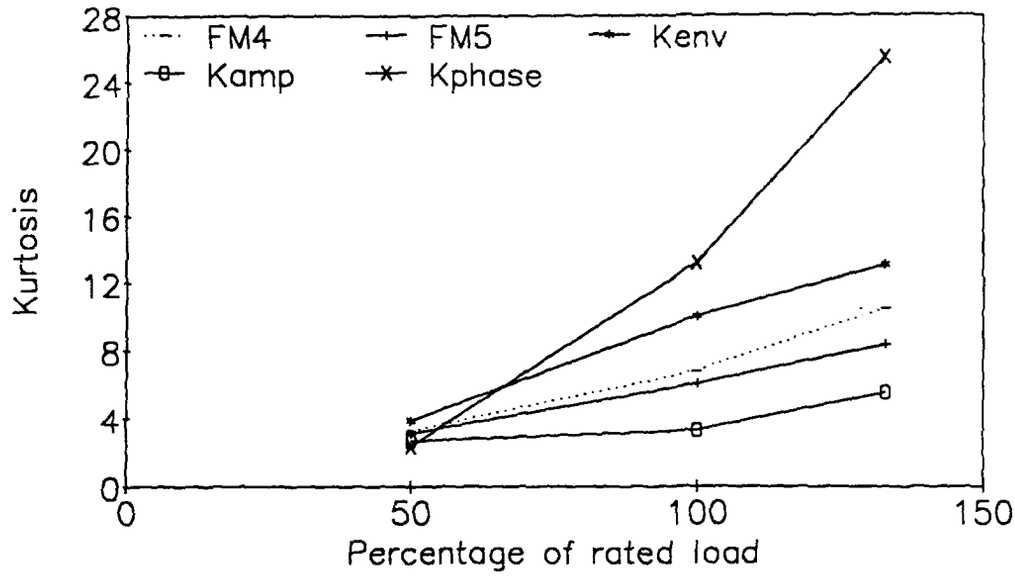

Figure 26b. Effect of load with 1.4mm notch.

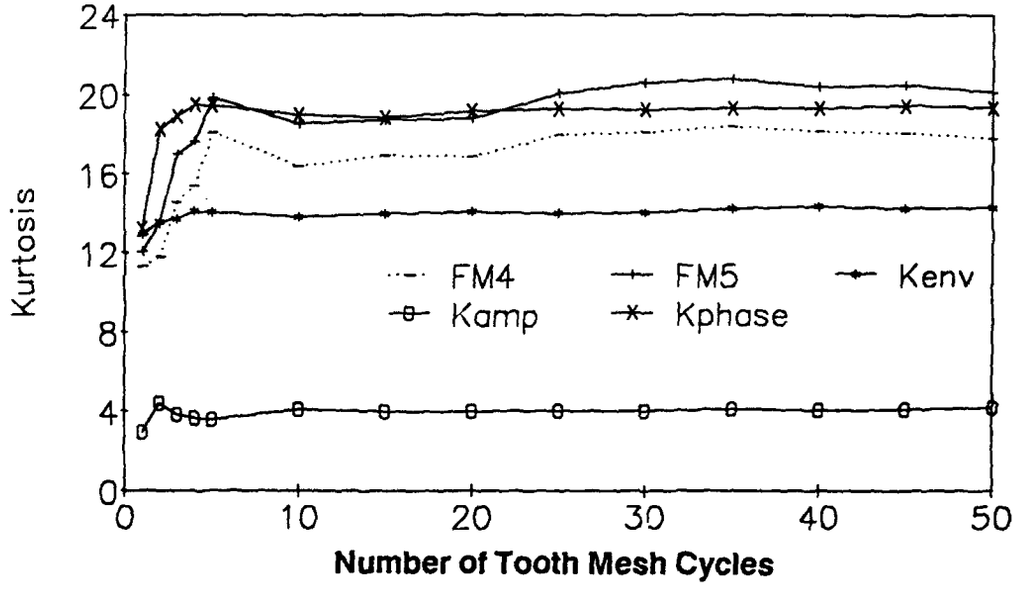

Figure 27a. Effect of number of tooth mesh cycles.

80% of one tooth removed.

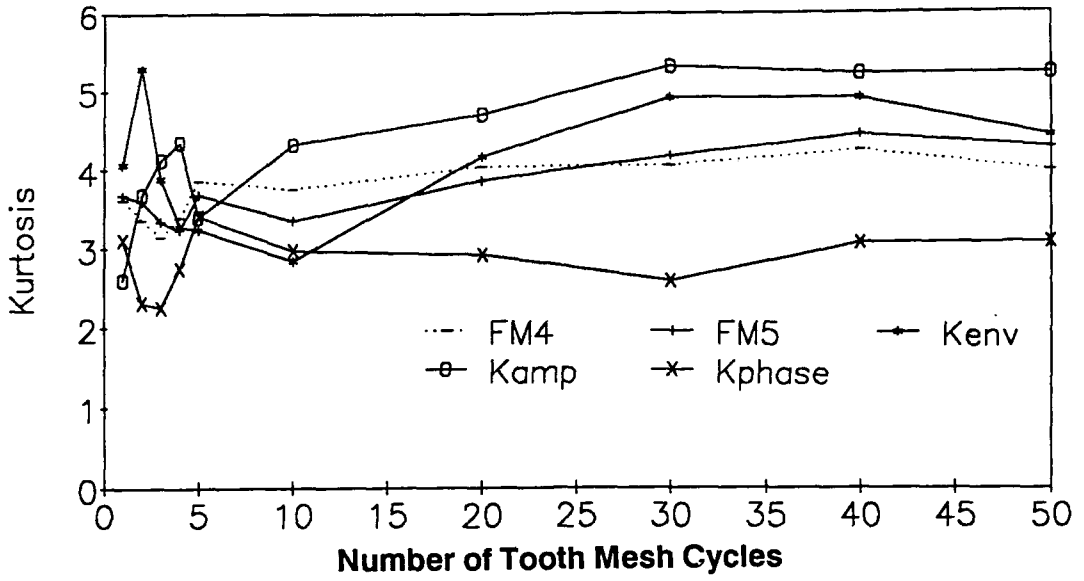

Figure 27b. Effect of the number of tooth mesh cycles.

40% of one tooth removed.

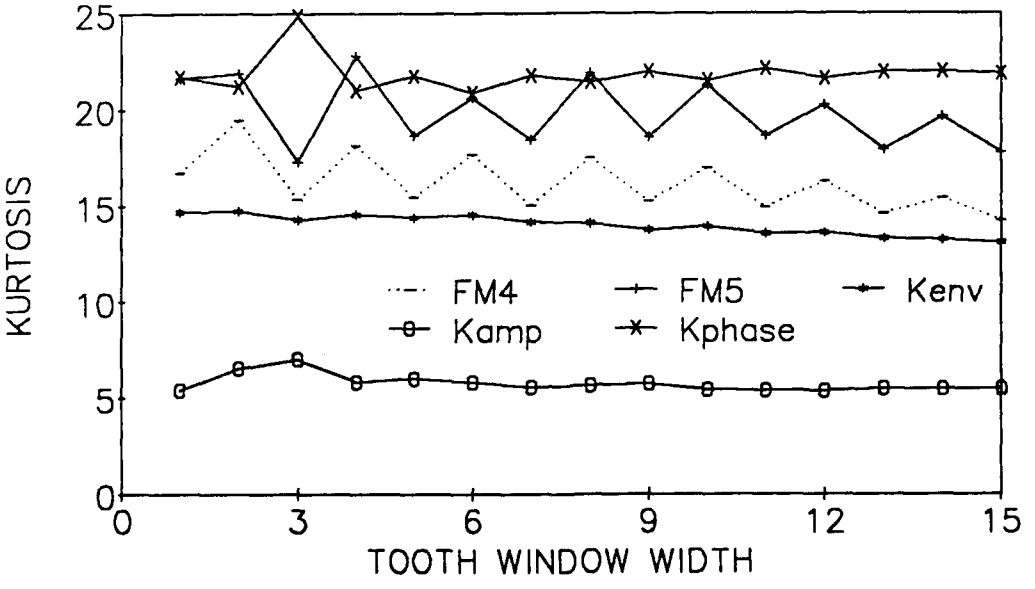

Figure 28. Effect of window width.

80% of one tooth removed.

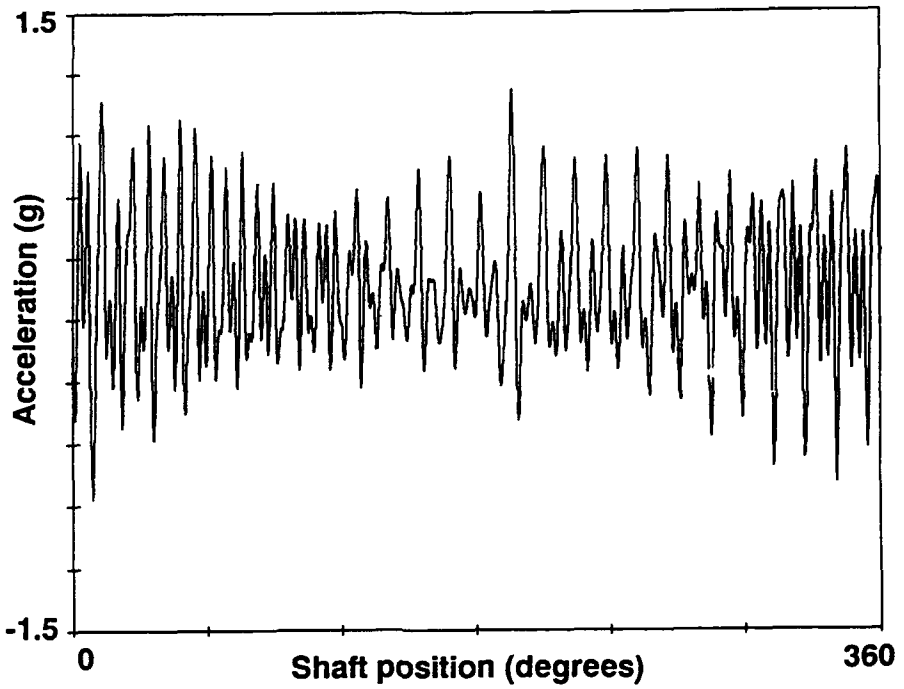

Figure 29a. Composite planet average.

80% of one tooth removed.

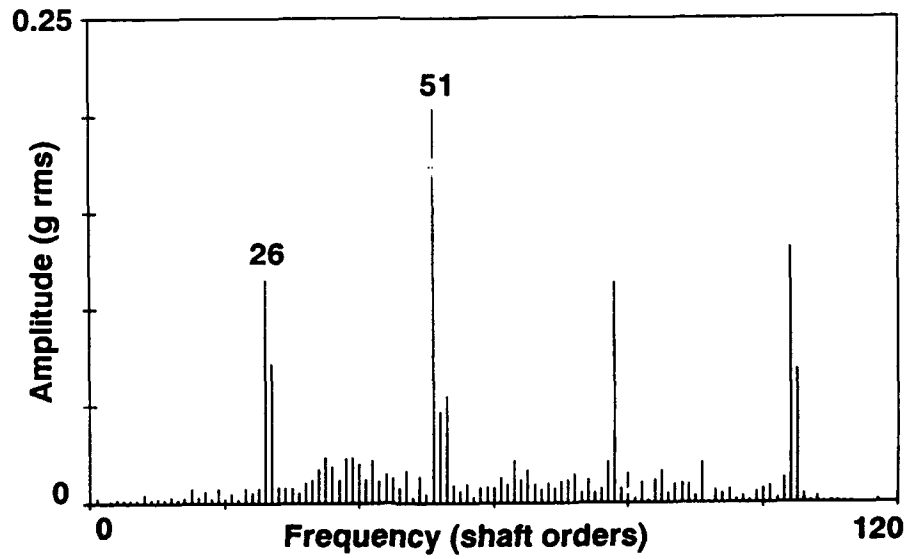

Figure 29b. Frequency spectrum of composite planet average.

80% of one tooth removed.

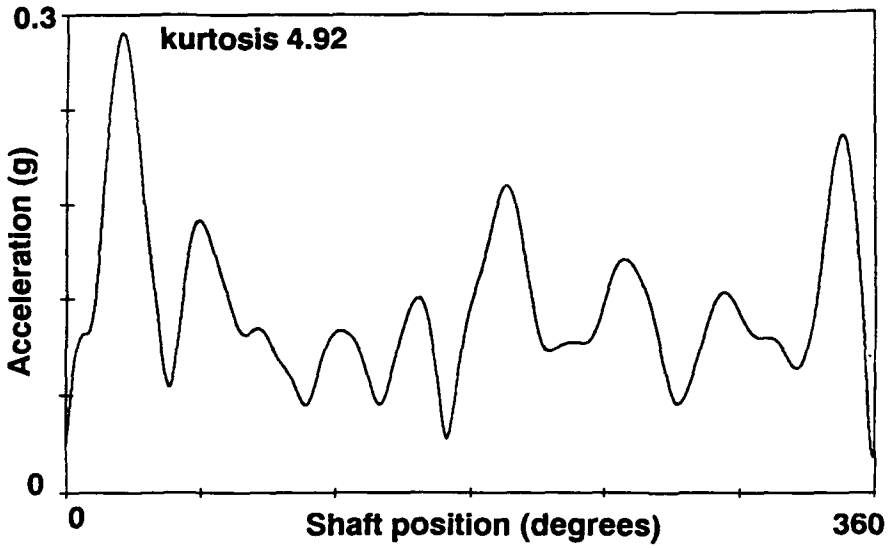

Figure 30a. Envelope of the composite planet average.

80% of one tooth removed.

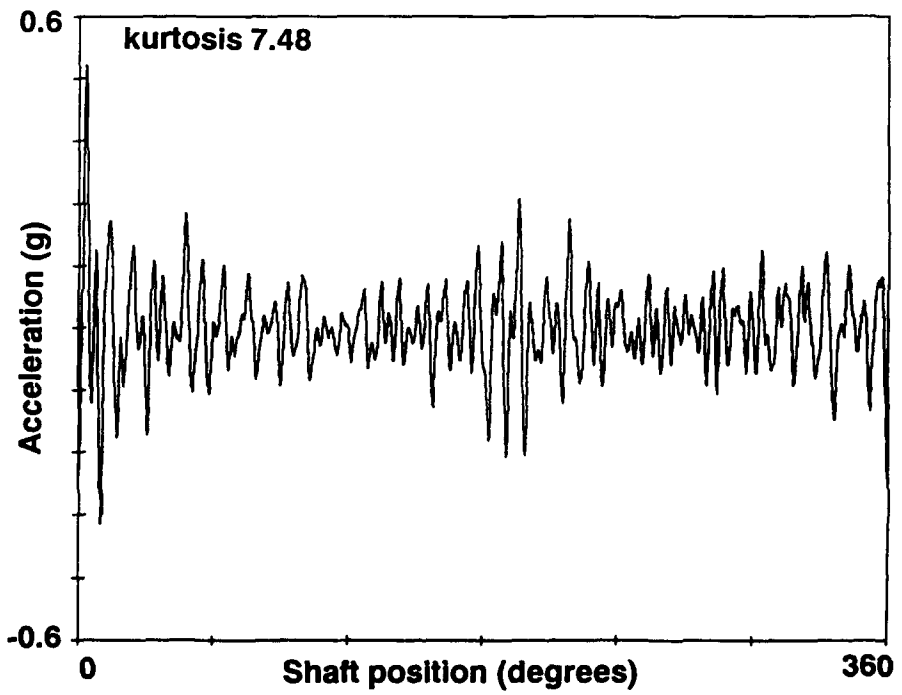

Figure 30b. Figure of merit FM4 of the composite planet average.

80% of one tooth removed.

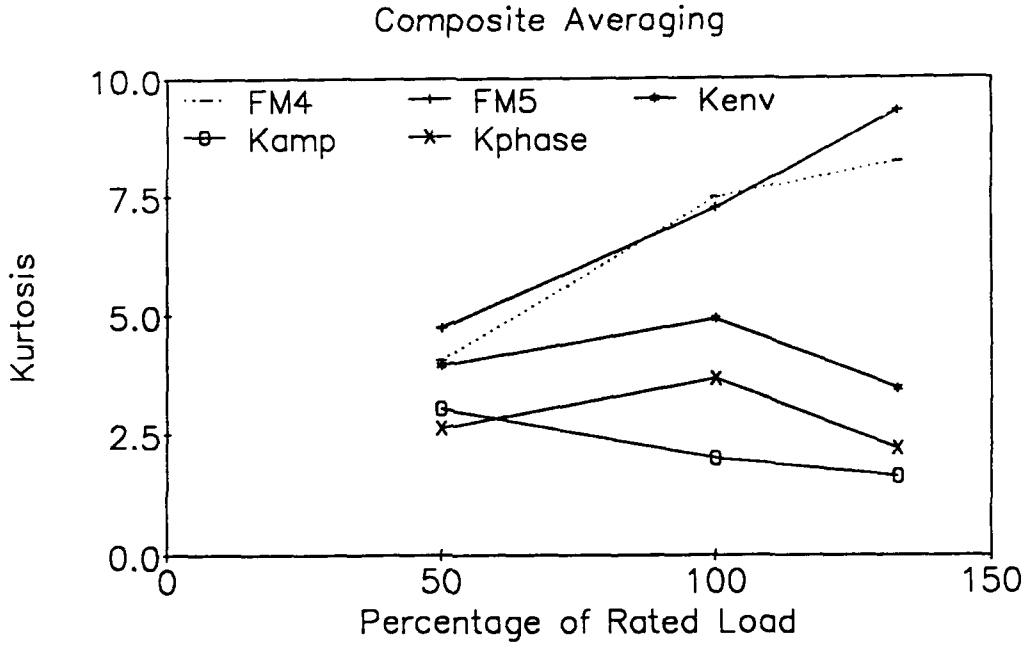

Figure 31. Effect of load upon the composite planet average.

80% of one tooth removed.

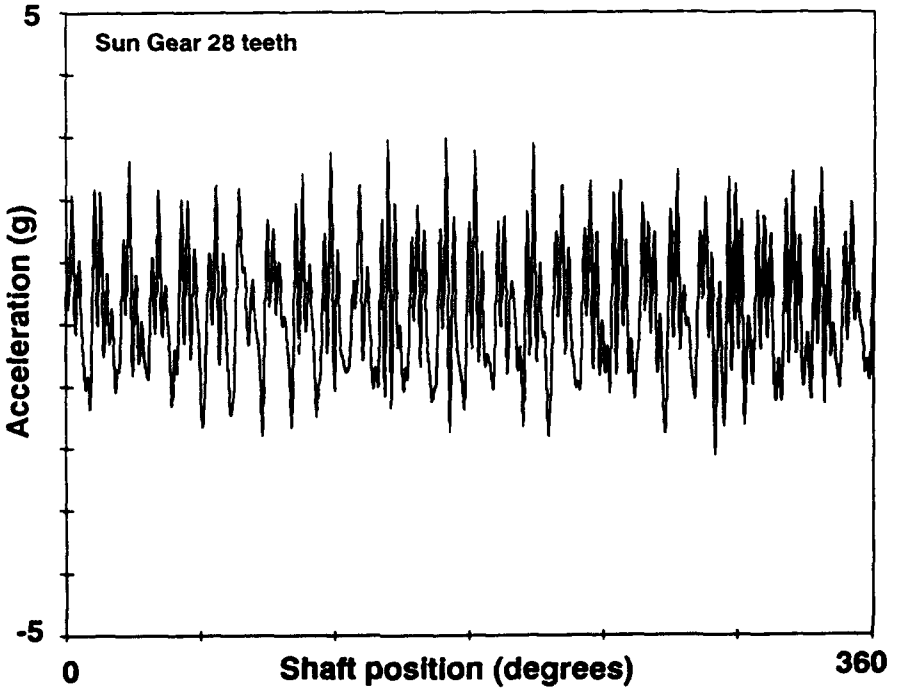

Figure 32a. Undamaged sun gear signal average.

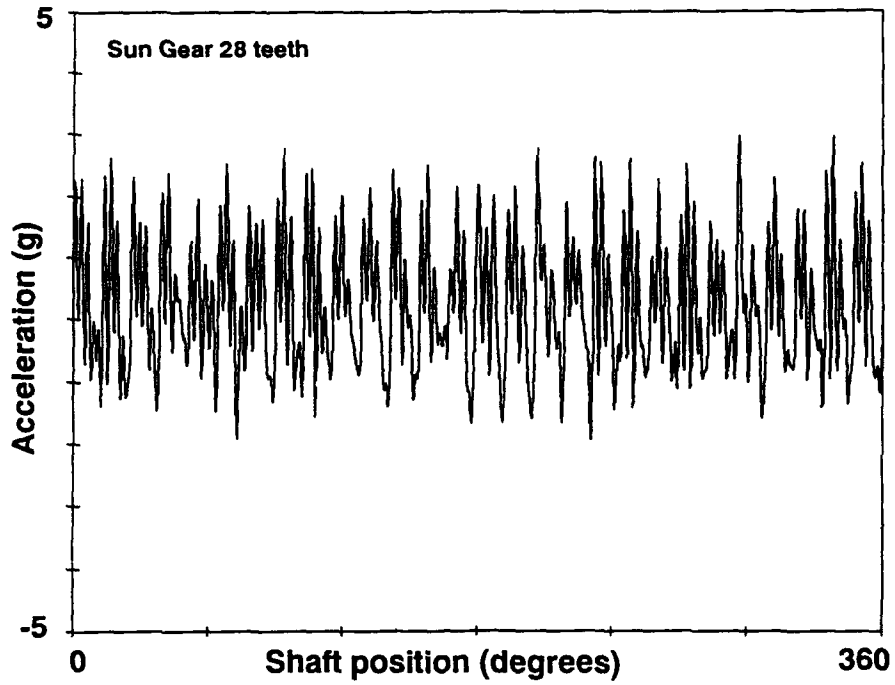

Figure 32b. Sun gear signal average.

80% of one tooth removed.

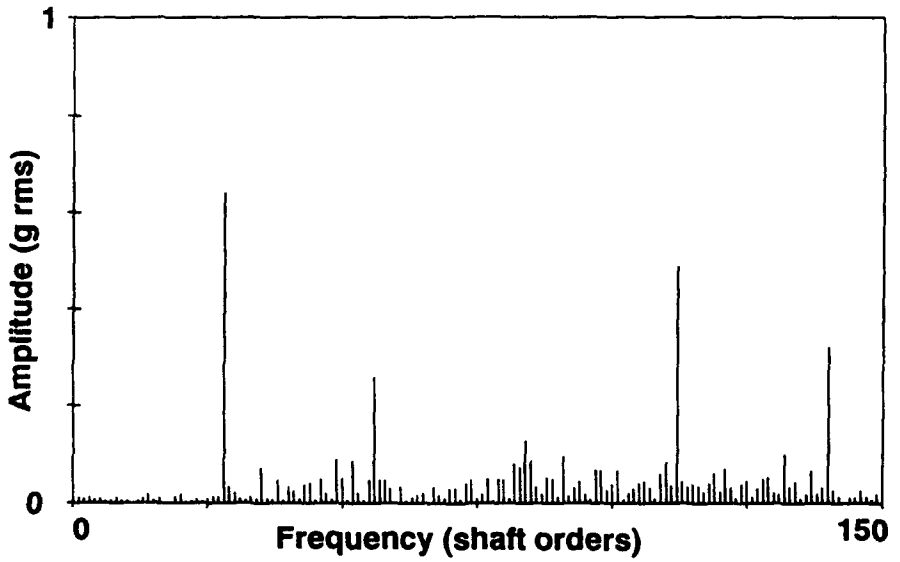

Figure 33a. Frequency spectrum of undamaged sun gear average.

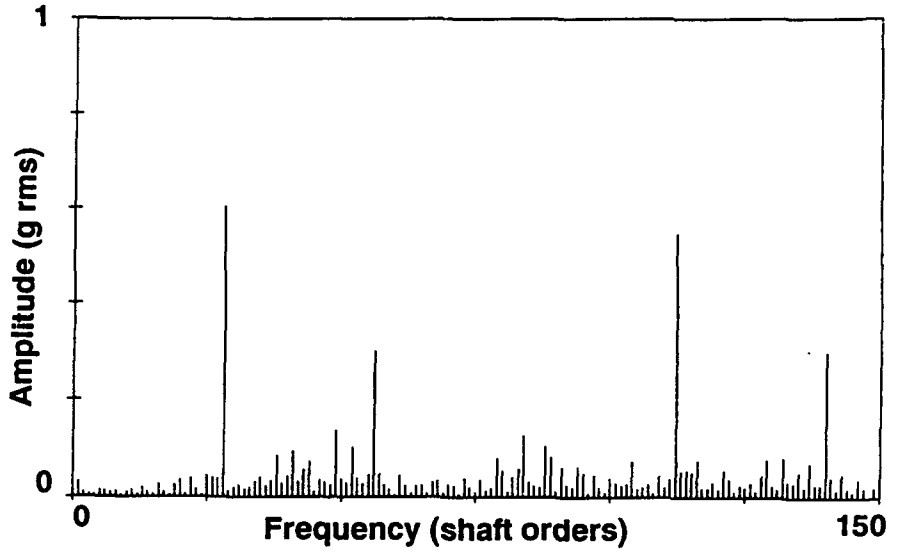

Figure 33b. Frequency spectrum of the sun gear.

80% of one tooth removed.

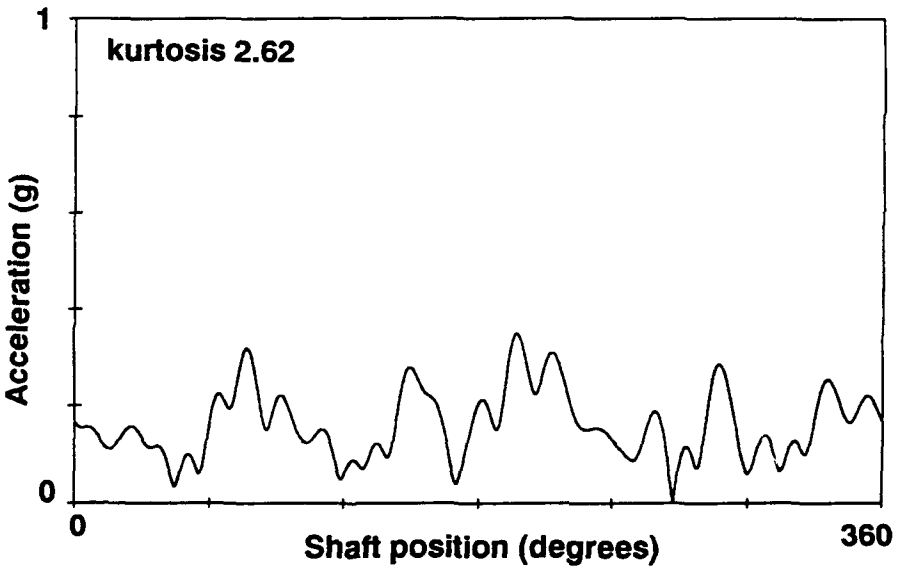

Figure 34a. Envelope of the undamaged sun gear average.

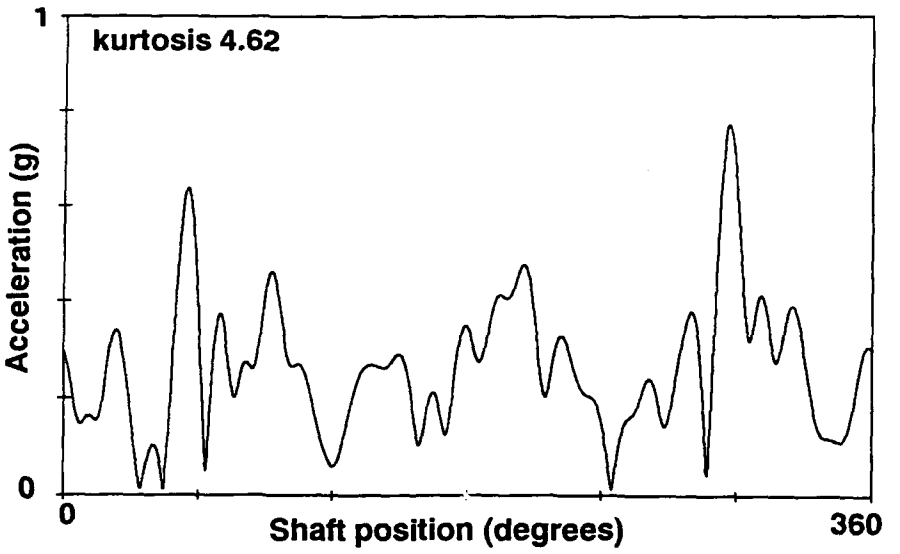

Figure 34b. Narrow band envelope with 80% of one tooth removed.

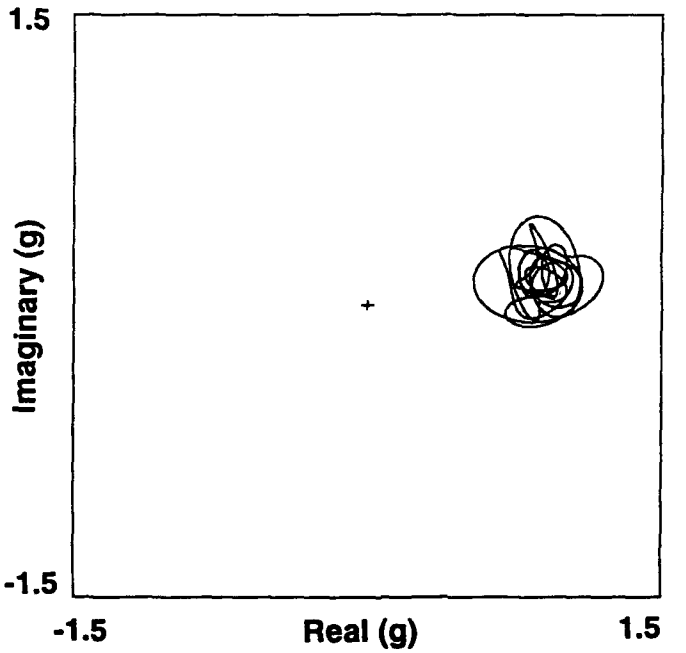

Figure 35a. Polar plot of the undamaged sun gear signal average.

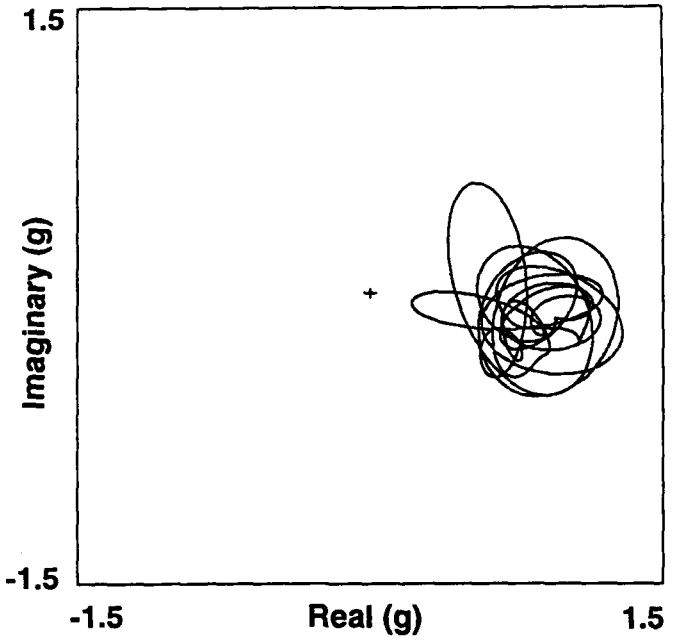

Figure 35b. Polar plot with 80% of one tooth removed.

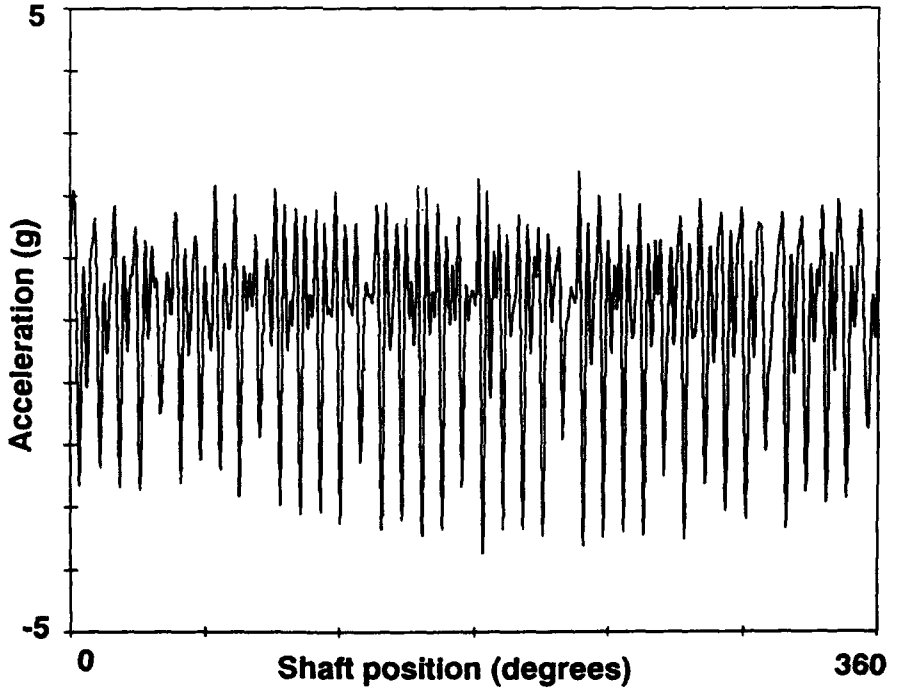

Figure 36a. Undamaged sun gear signal average with 40 teeth.

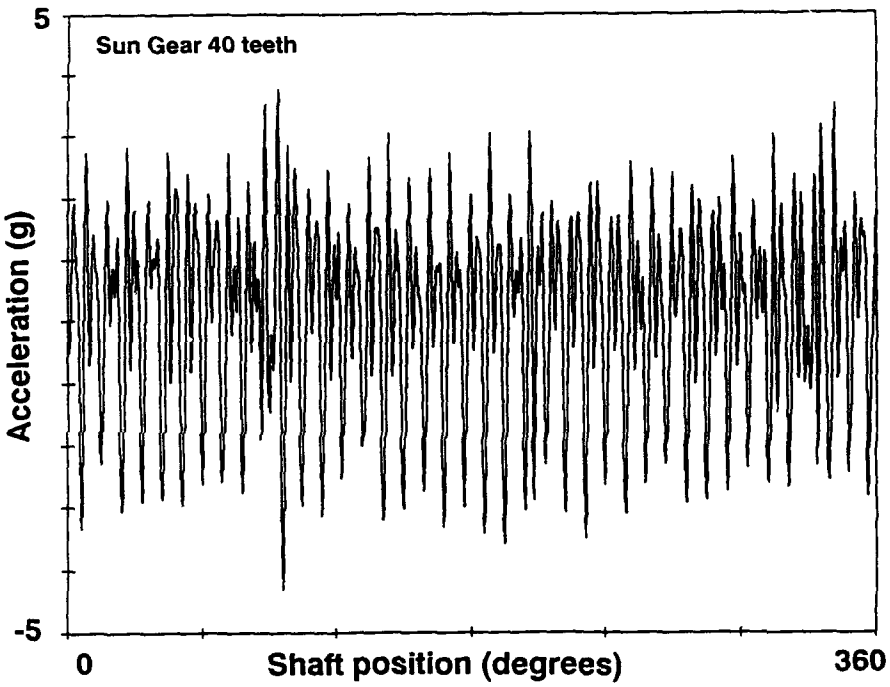

Figure 36b. Sun gear signal average.

80% of one tooth removed.

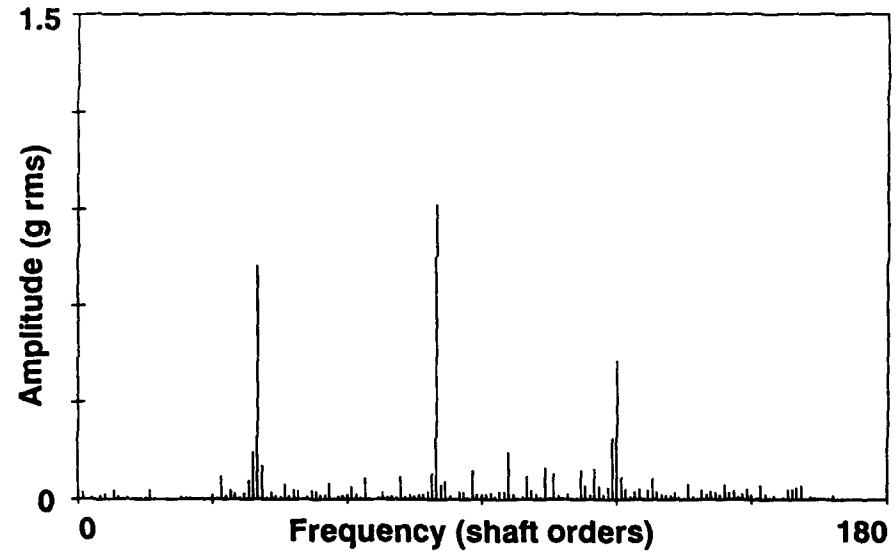

Figure 37a. Frequency spectrum of undamaged sun gear average.

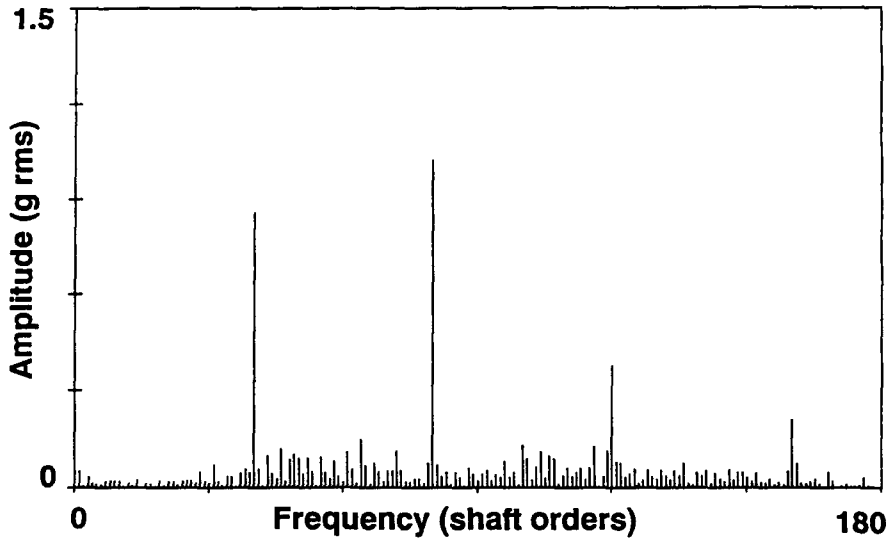

Figure 37b. Frequency spectrum with 80% of one tooth removed.

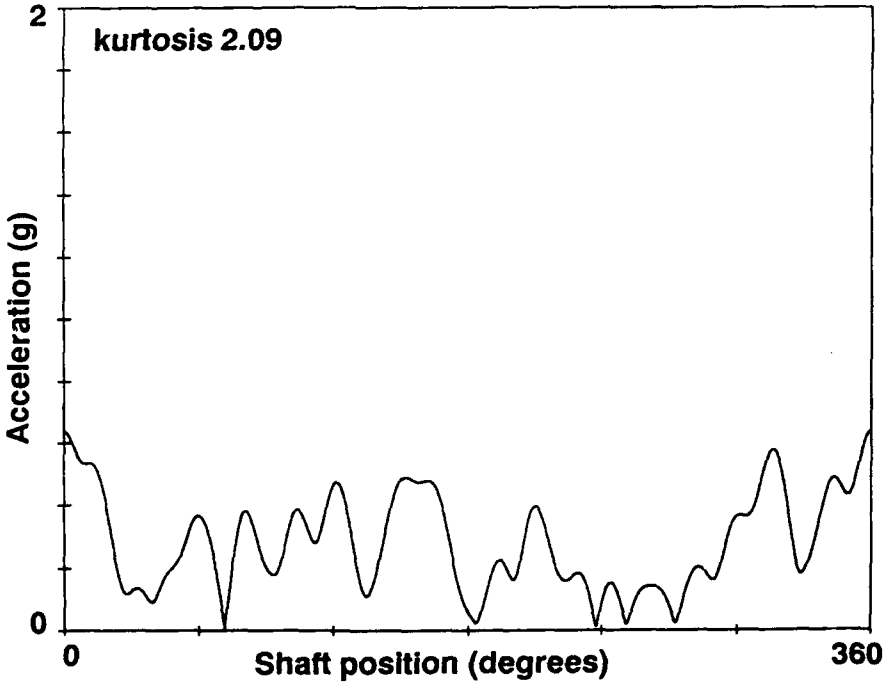

Figure 38a. Envelope of the undamaged sun gear signal average.

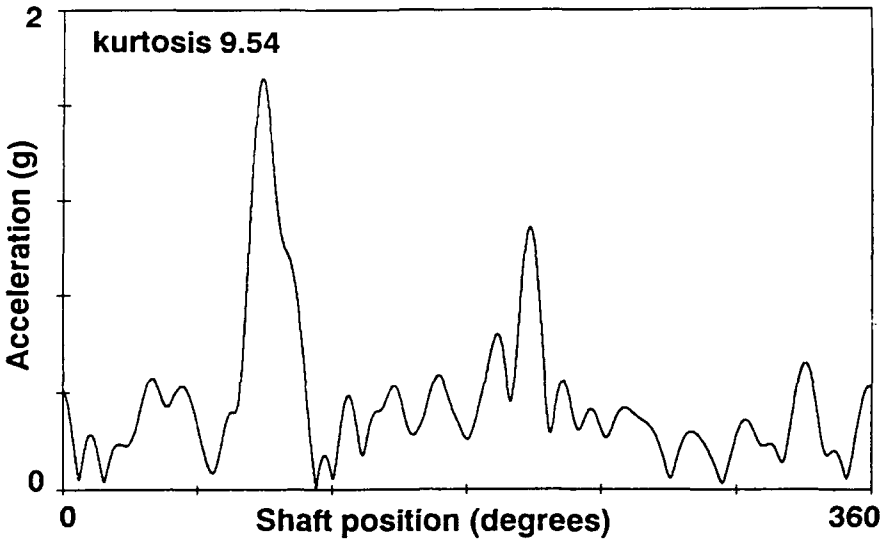

Figure 38b. Narrow band envelope with 80% of one tooth removed.

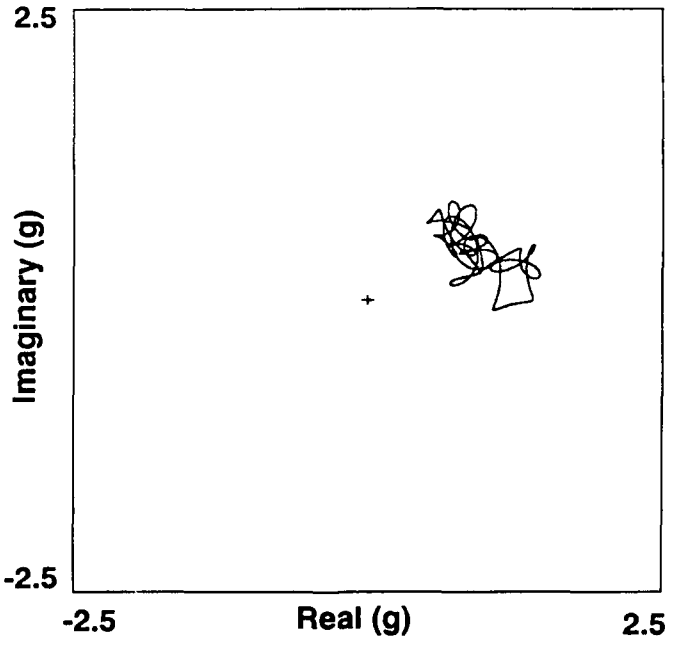

Figure 39a. Polar plot of the undamaged sun gear signal average.

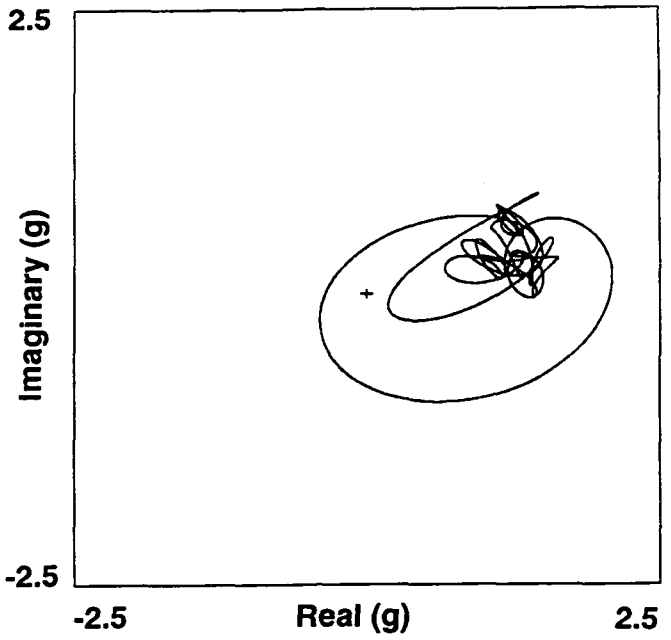

Figure 39b. Polar plot with 80% of one tooth removed.

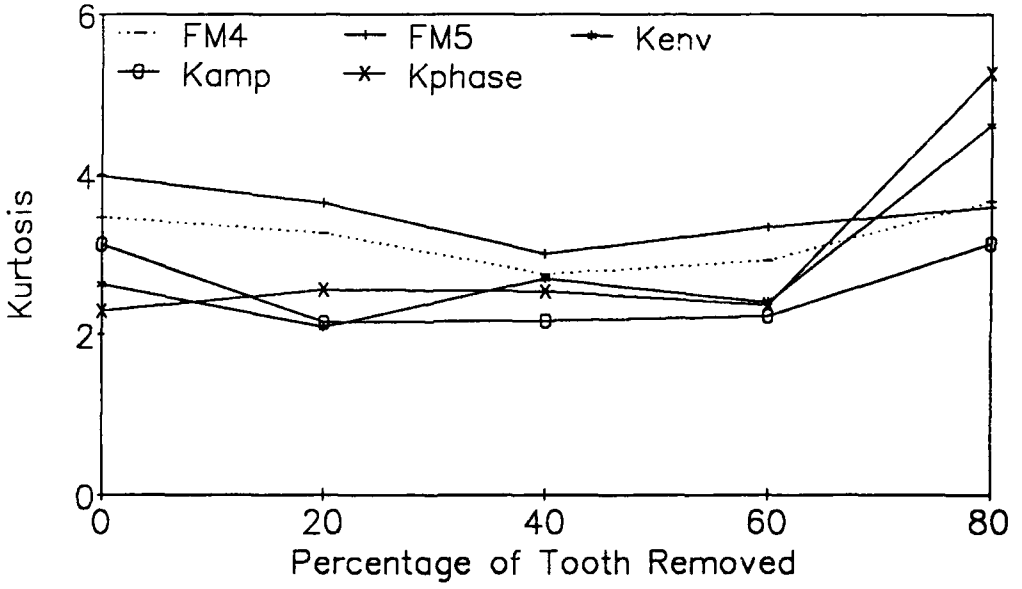

Figure 40a. Condition indexes as a function of tooth removal.

28 tooth sun gear.

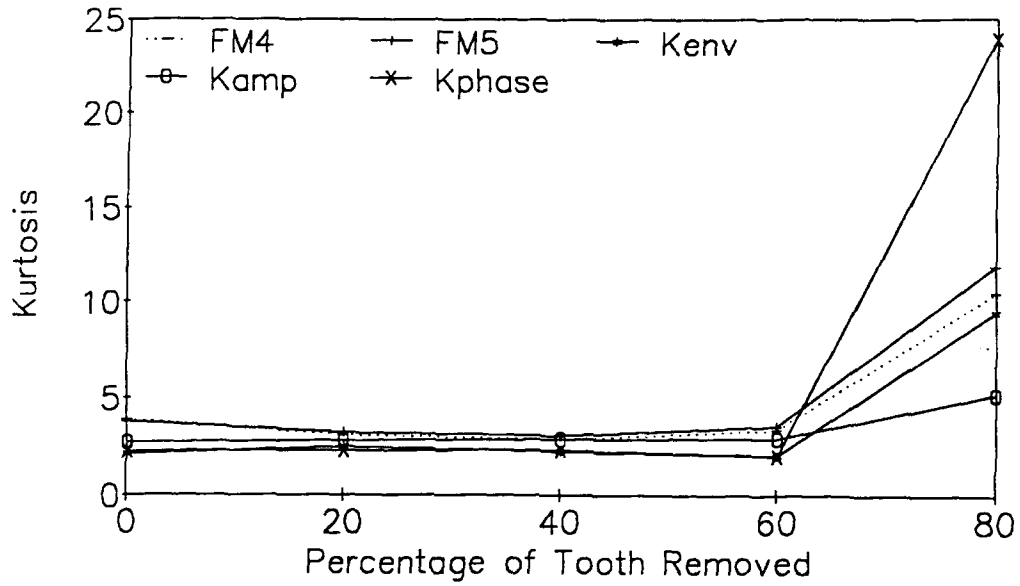

Figure 40b. Condition indexes as a function of tooth removal.

40 tooth sun gear.

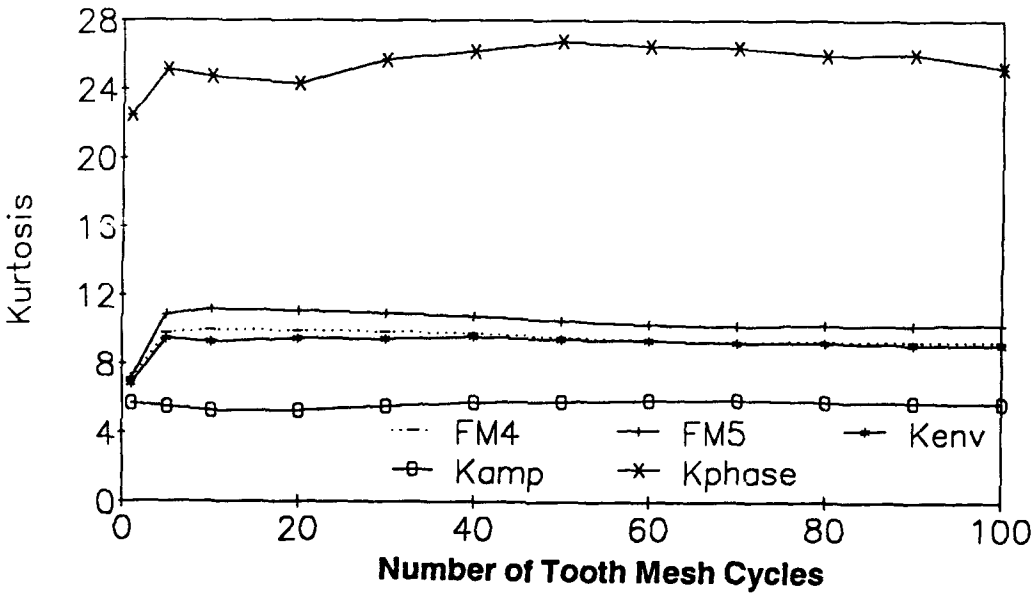

Figure 41. Effect of the number of tooth mesh cycles.

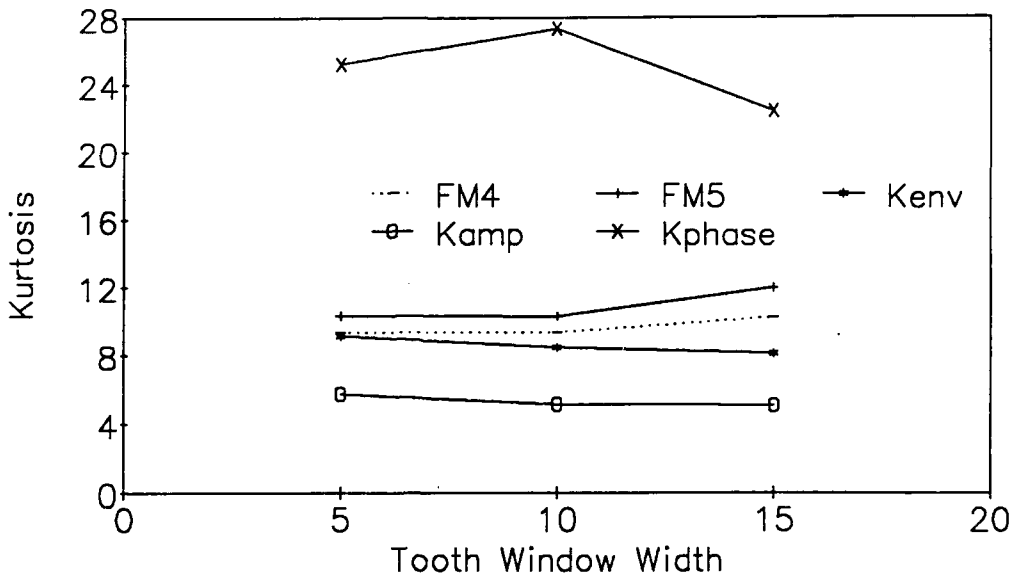

Figure 42. Effect of the vibration window width.

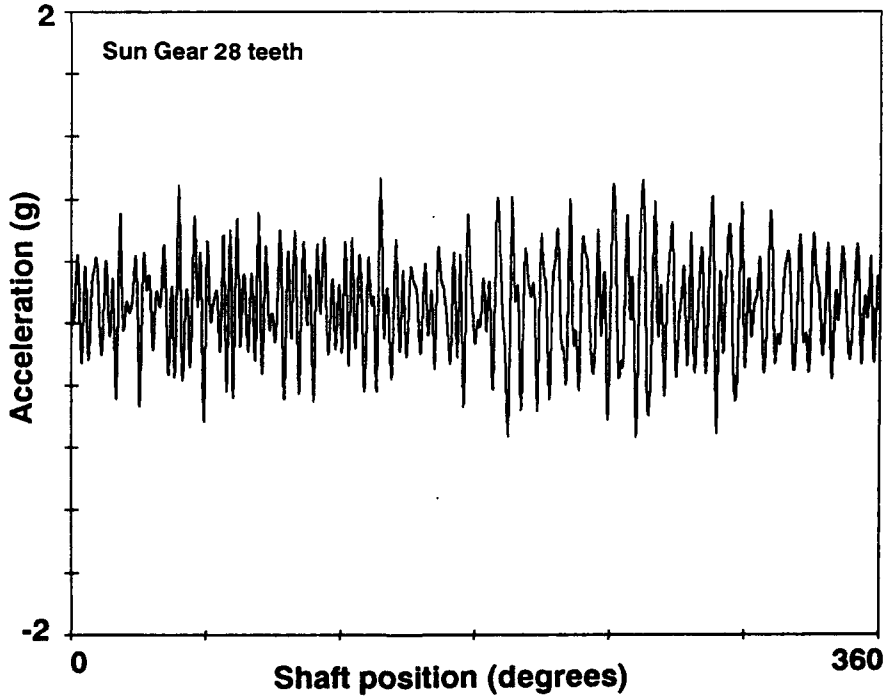

Figure 43a. Composite undamaged sun gear signal average.

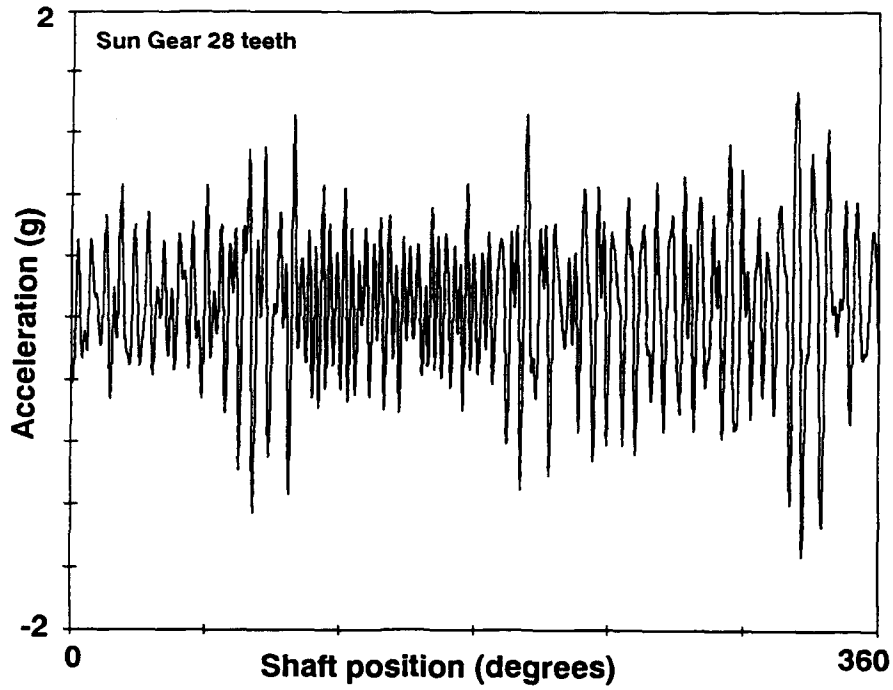

Figure 43b. Composite sun gear average.

80% of one tooth removed.

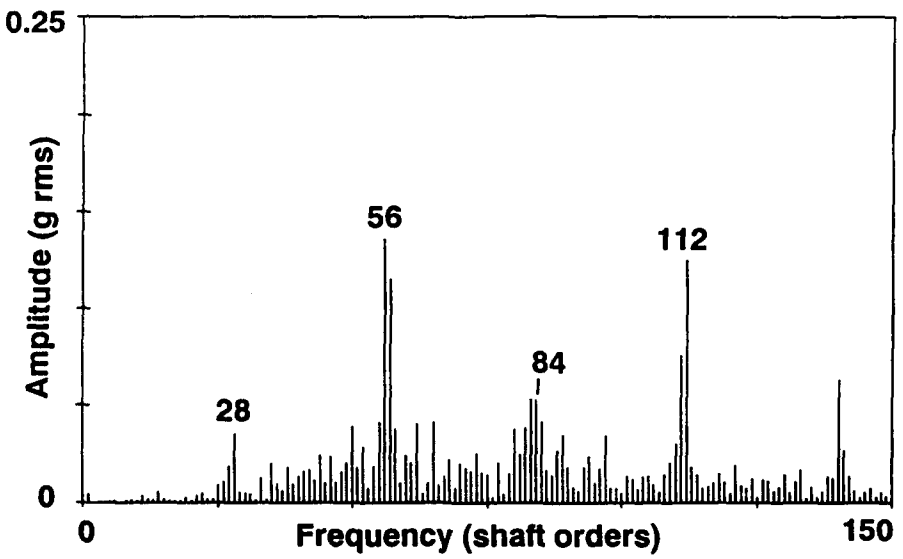

Figure 44a. Frequency spectrum of the composite signal average.

Undamaged 28 tooth sun gear.

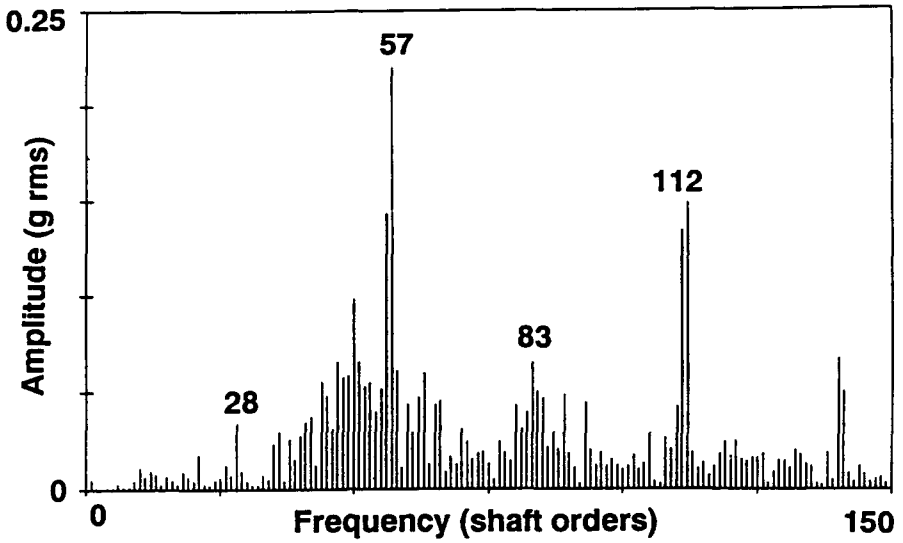

Figure 44b. Frequency spectrum of the composite signal average.

80% of one tooth removed.

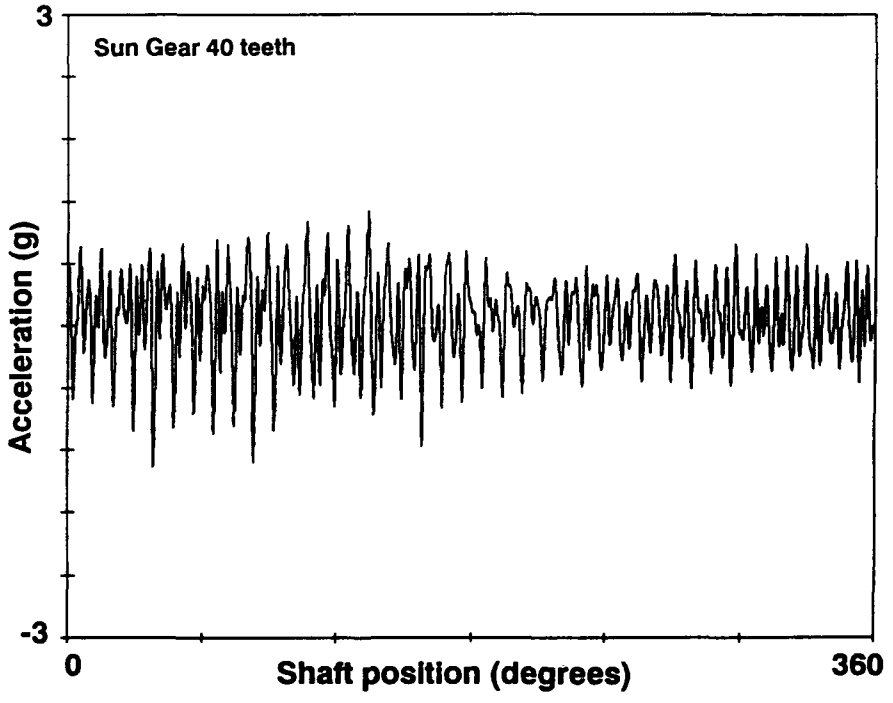

Figure 45a. Composite sun gear average.

40% of one tooth removed.

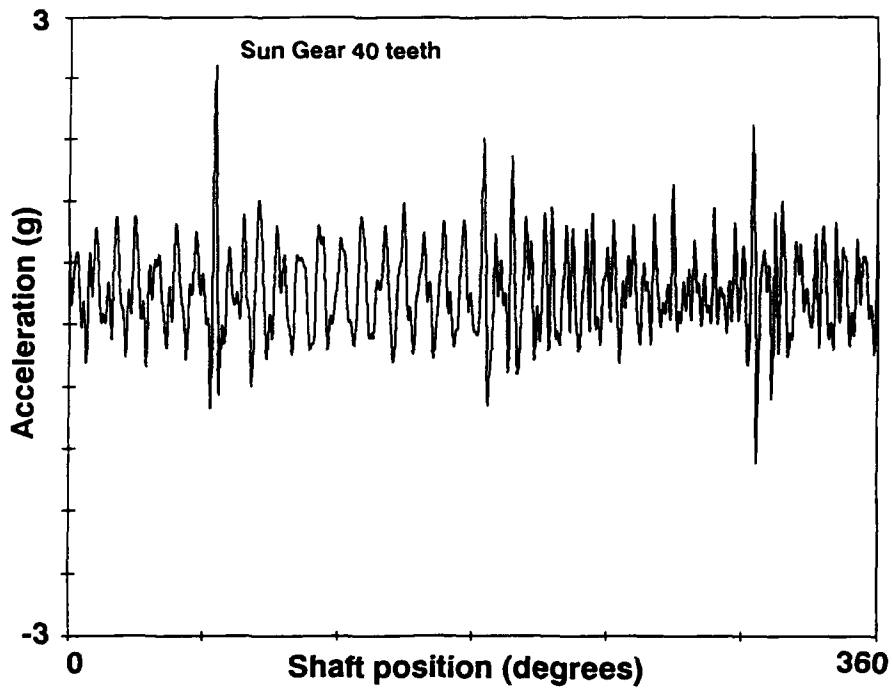

Figure 45b. Composite sun gear average.

80% of one tooth removed.

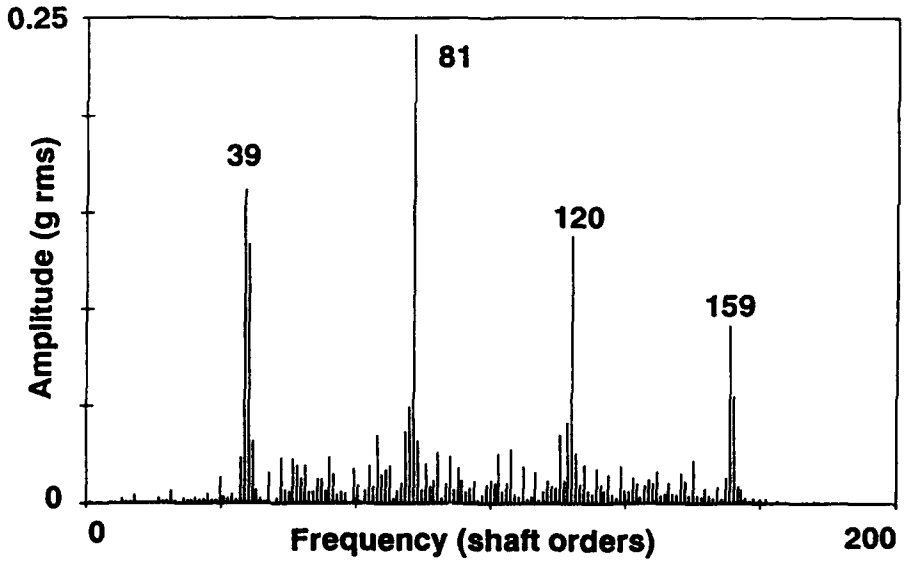

Figure 46a. Frequency spectrum with 40% of one tooth removed.

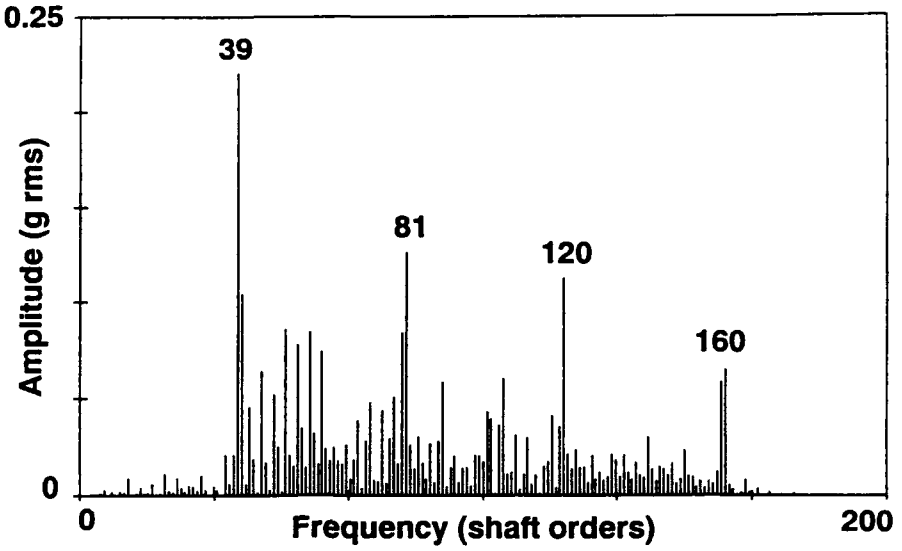

Figure 46b. Frequency spectrum with 80% of one tooth removed.

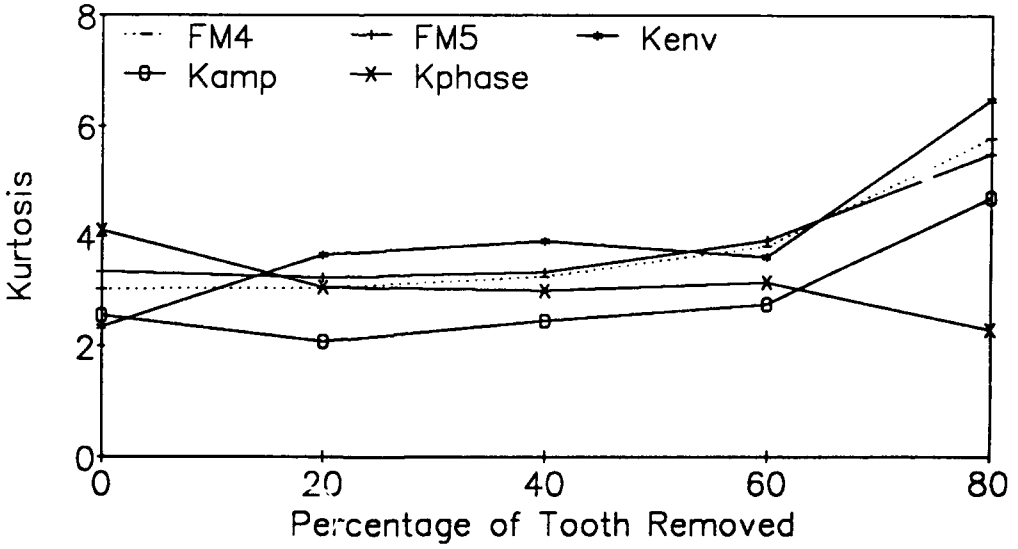

Figure 47. Condition indexes as a function of tooth removal.

28 tooth sun gear.

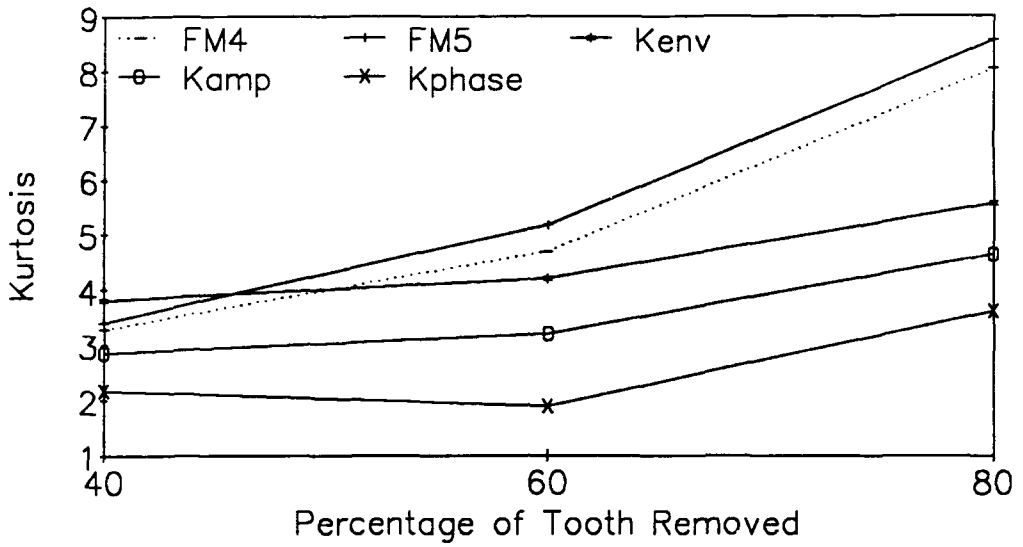

Figure 48. Condition indexes as a function of tooth removal.

40 tooth sun gear.

DISTRIBUTION

AUSTRALIA

Department of Defence

Defence Central
- Chief Defence Scientist
- AS, Science Corporate Management (shared copy)
- FAS Science Policy (shared copy)
- Director, Departmental Publications
- Counsellor, Defence Science, London (Doc Data Sheet Only)
- Counsellor, Defence Science, Washington (Doc Data Sheet Only)
- S.A. to Thailand MRD (Doc Data Sheet Only)
- S.A. to the DRC (Kuala Lumpur) (Doc Data Sheet Only)
- OIC TRS, Defence Central Library
- Document Exchange Centre, DSTIC (8 copies)
- Defence Intelligence Organisation
- Librarian H Block, Victoria Barracks, Melbourne
- Director General - Army Development (NSO) (4 copies)
- Defence Industry and Materiel Policy, FAS

Aeronautical Research Laboratory
- Director
- Library
- Chief Flight Mechanics & Propulsion Division
- Divisional File - Propulsion Branch
- Author: I.M. Howard
- B. Rebbechi
- B.D. Forrester
- N.S. Swansson
- K.F. Fraser

Materials Research Laboratory
- Director/Library

Defence Science & Technology Organisation - Salisbury
- Library

WSRL
- Maritime Systems Division (Sydney)

Navy Office
- Navy Scientific Adviser
- Aircraft Maintenance and Flight Trials Unit
- RAN Tactical School, Library
- Director Naval Engineering Requirements - Aviation Systems
- Director Aviation Systems Engineering - Navy
- Director of Naval Air Warfare
- Naval Support Command
  - Superintendent, Naval Aircraft Logistics
- Director of Naval Architecture

Army Office
- Scientific Adviser - Army (Doc Data Sheet Only)
- Engineering Development Establishment Library
- US Army Research, Development and Standardisation Group

Air Force Office
Air Force Scientific Adviser (Doc Data Sheet Only)
Aircraft Research and Development Unit
Scientific Flight Group
Library
Engineering Branch Library
Director General Engineering - Air Force
Director General Air Warfare Plans & Policy
Director Air Warfare
AHQ (SMAINTSO)
HQ Logistics Command (DGELS)

HQ ADF
Director General Force Development (Air)

Statutory and State Authorities and Industry
Aero-Space Technologies Australia, Manager/Librarian
Ansett Airlines of Australia, Library

Universities and Colleges
Adelaide
Barr Smith Library
Professor Mechanical Engineering

Melbourne
Engineering Library

Monash
Hargrave Library
Head, Mechanical Engineering
Dr J. Mathew, Centre for Machine Condition Monitoring

Newcastle
Library
Professor R. Telfer, Institute of Aviation

Sydney
Engineering Library

NSW
Physical Sciences Library
Mr R.B. Randall, Mechanical & Manufacturing Engineering
Library, Australian Defence Force Academy

Queensland
Library

Tasmania
Engineering Library

Western Australia
Physical Sciences Library
Assoc Prof M.P. Norton, Mechanical Engineering

RMIT
Library
Dr L. Wood, Dept of Transport & Resource Eng
Mr M.L. Scott, Aerospace Engineering

CANADA

NRC, Ottawa
Division of Mechanical Engineering, Mr J. Ploeg
Engine Laboratory, Dr G. Krishnappa
NRC, Vancouver
Tribology & Mechanics Laboratory, Dr P. Kim

ISRAEL
Technion-Israel Institute of Technology
Prof S. Braun, Engineering Department

NEW ZEALAND
Defence Scientific Establishment, Library
Transport Ministry, Airworthiness Branch, Library

Universities
Canterbury
Head, Mechanical Engineering

UNITED KINGDOM

Ministry of Defence, Research, Materials and Collaboration
Defence Research Agency (Aerospace)
Head Airworthiness Division
Defence Research Agency (Naval)
Holton Heath, Dr N.J. Wadsorth
St Leonard's Hill, Superintendent
Naval Aircraft Material Laboratory
Mr P. Gadd
British Aerospace
Kingston-upon-Thames, Library
Hatfield-Chester Division, Library
Civil Aviation Authority, Safety Regulation Group,
Mr S.L. James
Mr A.G. Sayce

Universities and Colleges
Bristol
Engineering Library

Cambridge
Library, Engineering Department

Cranfield Inst. of Technology
Library
Dr R.H. Bannister, School of Mechanical Engineering

Imperial College
Aeronautics Library

Manchester
Professor, Applied Mathematics
Head, Dept of Engineering (Aeronautical)

Oxford
Library
Dept of Engineering Science, Dr P.D. McFadden

Southampton
Library
Professor J. Hammond Institute of Sound & Vibration Research

UNITED STATES OF AMERICA
NASA Scientific and Technical Information Facility
United Technologies Corporation
Library
Mr M. Hawman, Research Center
Nondestructive Testing Information Analysis Center
Naval Aircraft Test Center (Patuxent River)
Dr L. Mertaugh
United Technologies Sikorsky Aircraft
Dr Ray Carlson
Bell Helicopter Company
McDonnell Douglas Helicopter Company
Boeing Helicopter Company
Mr J. Cronkhite
NASA Lewis Research Center
Dr J. Coy
Naval Air Propulsion Center
Mr D. Rawlinson
US Army Aviation Technology Directorate

Universities and Colleges

Chicago
John Crerar Library

Florida
Aero Engineering Department
Head, Engineering Sciences

Johns Hopkins
Head, Engineering Department

Iowa State
Head, Mechanical Engineering

Purdue
Library

Princeton
Head, Mechanics Department

Massachusetts Inst. of Technology
MIT Libraries

SPARES (10 COPIES)
TOTAL (127 COPIES)

AL 149 DEPARTMENT OF DEFENCE

DOCUMENT CONTROL DATA

PAGE CLASSIFICATION
UNCLASSIFIED

PRIVACY MARKING

1a. AR NUMBER	1b. ESTABLISHMENT NUMBER	2. DOCUMENT DATE	3. TASK NUMBER
AR-006-147	ARL-PROP-R-185	JUNE 1991	NAV89/089

4. TITLE
AN INVESTIGATION OF VIBRATION SIGNAL AVERAGING OF INDIVIDUAL COMPONENTS IN AN EPICYCLIC GEARBOX

5. SECURITY CLASSIFICATION (PLACE APPROPRIATE CLASSIFICATION IN BOX(S) IE. SECRET (S), CONF. (C) RESTRICTED (R), UNCLASSIFIED (U)).

DOCUMENT	TITLE	ABSTRACT
U	U	U

6. NO. PAGES
75

7. NO. REFS.
33

8. AUTHOR(S)
I.M. HOWARD

9. DOWNGRADING/DELIMITING INSTRUCTIONS
Not applicable

10. CORPORATE AUTHOR AND ADDRESS
AERONAUTICAL RESEARCH LABORATORY
506 LORIMER STREET
FISHERMENS BEND VIC 3207

11. OFFICE/POSITION RESPONSIBLE FOR:
SPONSOR NAVY
SECURITY -
DOWNGRADING -
APPROVAL DARL

12. SECONDARY DISTRIBUTION (OF THIS DOCUMENT)
Approved for public release

OVERSEAS ENQUIRIES OUTSIDE STATED LIMITATIONS SHOULD BE REFERRED THROUGH DSTIC, ADMINISTRATIVE SERVICES BRANCH, DEPARTMENT OF DEFENCE, ANZAC PARK WEST OFFICES, ACT 2601

13a. THIS DOCUMENT MAY BE ANNOUNCED IN CATALOGUES AND AWARENESS SERVICES AVAILABLE TO ....
No limitations

13b. CITATION FOR OTHER PURPOSES (IE. CASUAL ANNOUNCEMENT) MAY BE [X] UNRESTRICTED OR [ ] AS FOR 13a.

14. DESCRIPTORS
Gear boxes
Vibration measurement
Planetary gears

15. DISCAT SUBJECT CATEGORIES
1309

16. ABSTRACT

An investigation of vibration signal averaging for individual components in an epicyclic gearbox has been conducted. A new signal averaging technique was developed specifically for analysing planetary gears within epicyclic transmissions using the vibration measured on the annulus gear casing. It enables the acquisition of signal averages for individual planetary gears whereas previous methods gave a composite vibration pattern from all the planet gears. The new technique is outlined and its implementation is described. Results of tests on an epicyclic gearbox showed the advantages of separating individual planetary gear averages, compared with previous methods. Other conclusions include the effects of transducer location, number of tooth mesh cycles averaged, window width and the use and difficulties with the composite sun gear signal average.

PAGE CLASSIFICATION
UNCLASSIFIED
PRIVACY MARKING

THIS PAGE IS TO BE USED TO RECORD INFORMATION WHICH IS REQUIRED BY THE ESTABLISHMENT FOR ITS OWN USE BUT WHICH WILL NOT BE ADDED TO THE DISTIS DATA UNLESS SPECIFICALLY REQUESTED.

16. ABSTRACT (CONT).

17. IMPRINT

AERONAUTICAL RESEARCH LABORATORY, MELBOURNE

18. DOCUMENT SERIES AND NUMBER	19. COST CODE	20. TYPE OF REPORT AND PERIOD COVERED
Propulsion Report 185	41 4140	

21. COMPUTER PROGRAMS USED

22. ESTABLISHMENT FILE REF.(S)

23. ADDITIONAL INFORMATION (AS REQUIRED)